TESIS DOCTORAL

RECONSTRUCCIÓN 3D A TRAVÉS DE UN SISTEMA VIDEOGRAMÉTRICO BASADO EN LA UTILIZACIÓN DE VISUALSLAM Y UN PROCEDIMIENTO ESPECÍFICO DE SELECCIÓN DE IMÁGENES.

Pedro Ortiz Coder

Programa de Doctorado en Ciencia y Tecnología de los Sistemas Agroforestales

Año 2020

UNIVERSIDAD DE EXTREMADURA

TESIS DOCTORAL

RECONSTRUCCIÓN 3D A TRAVÉS DE UN SISTEMA VIDEOGRAMÉTRICO BASADO EN LA UTILIZACIÓN DE VISUALSLAM Y UN PROCEDIMIENTO ESPECÍFICO DE SELECCIÓN DE IMÁGENES.

Autor: Pedro Ortiz Coder

Director de la Tesis Doctoral: Dr. Alonso Sánchez Ríos.

Año de lectura: 2020

Programa de Doctorado en Ciencia y Tecnología de los Sistemas Agroforestales

Conformidad del Director de esta Tesis Doctoral.

La conformidad del director de la tesis consta en el original en papel de esta Tesis Doctoral

Fdo. Dr.Alonso Sánchez Ríos

Pedro Ortiz Coder email: portizcoder@gmail.com

Informe del director de tesis:

La Tesis Doctoral titulada: "Reconstrucción 3d a través de un sistema videogramétrico basado en la utilización de visual SLAM y un procedimiento específico de selección de imágenes", presentada por D. Pedro Ortiz Coder reúne los requisitos exigidos a una Tesis Doctoral y que se pasan a detallar a continuación:

El tema presentado por el doctorando en su Tesis Doctoral se enmarca en el campo de la reconstrucción 3D, la videogrametría, la fotogrametría y la programación de algoritmos de filtrado para la selección de imágenes, alineándose adecuadamente con el Programa de Doctorado. La metodología propuesta y el conjunto de algoritmos de cálculo desarrollados en la Tesis Doctoral presentan aspectos muy novedosos en estos campos, permitiendo abordar los objetivos propuestos en la investigación de forma exitosa. En este sentido, hay que destacar la producción científica derivada de este trabajo de Tesis Doctoral, que avalan la calidad y relevancia de la misma y que consiste en la publicación de 2 artículos publicados en revistas científicas de calidad reconocida indexadas en bases de datos internacionales, como Journal Citation Report (JCR) o Scimago Journal & Country Rank (SJR); ambas publicaciones ocupan posiciones destacadas en los listados de esta bases de datos con un índice de impacto elevado y siendo contribuciones relevantes en su campo científico según los criterios publicados por la Comisión Nacional Evaluadora de la Actividad Investigadora (BOE nº 284, de 26 de noviembre de 2019, subcampo 6.3, apartado 3b). Además, un tercer artículo ha sido presentado en otra revista científica de idénticas características a las anteriores, en el que se explora la aplicación de las técnicas y procedimientos resultantes de la investigación en la mejora de las técnicas de cirugía mínimamente invasiva, en el contexto de la cirugía oral y maxilofacial. Para dar respuesta al Artículo 46, apartado 2 de la Normativa de los estudios de Doctorado de la Universidad de Extremadura, se relaciona el factor de impacto y la categorización de las publicaciones incluidas en la Tesis Doctoral, así como la participación del doctorando en cada artículo, declarando expresamente que su utilización, por parte del doctorando, de los trabajos relacionados son procedentes para la elaboración de esta Tesis Doctoral:

Artículo 1:

Ortiz-Coder, P.; Sánchez-Ríos, A. A Self-Assembly Portable Mobile Mapping System for Archeological Reconstruction Based on VSLAM-Photogrammetric Algorithm. *Sensors* 2019, *19*, 3952. https://doi.org/10.3390/s19183952

Revista: Sensors, Special Issue "Visual and Camera Sensors". ISSN: 1424-8220 Impact Factor: 3.031 (2018), JCR category rank: 15/61 (Q1) in 'Instruments and Instrumentation'

Fecha de publicación: 12 de septiembre de 2019

Participación del doctorando: Diseño de prototipo para captura de datos, programación del software de adquisición y procesado de datos y valoración de resultados.

Artículo 2:

Ortiz-Coder, P.; Sánchez-Ríos, A. An Integrated Solution for 3D Heritage Modeling Based on Videogrammetry and V-SLAM Technology. *Remote Sens.* 2020, *12*, 1529. https://doi.org/10.3390/rs12091529

Revista: Remote Sensing, Special Issue " Photogrammetry and Image Analysis in Remote Sensing". ISSN: 2072-4292. SJR: 1.422 (2019), SJR Quartil (Q1) in 'Earth and Planetary Sciences'

Fecha de publicación: 11 de mayo de 2020

Participación del doctorando: Diseño de filtros de procesamiento y selección de imágenes, toma de datos y valoración de resultados.

Artículo 3:

Ortiz-Coder, P.; Monje Gil, F.; Sánchez-Ríos, A. Automatic 3d dense reconstruction using VSLAM and photogrammetric algorithms: approach in the temporomandibular arthroscopy case. *Measurement.*

Revista: Measurement. ISSN: 0263-2241 Impact Factor: 2.791 (2018), JCR category rank: (Q2) in 'Instruments and Instrumentation'

Fecha de publicación: Sin publicar. Entregado para su valoración por parte de los editores de la revista.

Participación del doctorando: Diseño de la estructura de la investigación, desarrollo de experimentos y casos prácticos y validación de resultados.

Otro aspecto a destacar de este trabajo de Tesis Doctoral es el de la posible transferencia de tecnología derivada en forma del desarrollo de softwares y patentes, puesto que se ha desarrollado un sistema de captura y procesado de datos para la reconstrucción 3D (materializado en forma de prototipo experimental) que puede competir directamente con la amplia variedad de productos existentes en el mercado para este fin, (con un coste económico y de formación menores que la mayoría de éstos) con idénticos resultados de calidad métrica. Los diversos informes emitidos por expertos de empresas dedicadas al diseño y fabricación de este tipo de productos, procedentes de países como Alemania, Reino Unido y China, así como los emitidos por otros profesionales que usan estas tecnologías, manifiestan un elevado interés por los resultados de las investigaciones llevadas a cabo en la realización de esta Tesis Doctoral.

El apartado de Conclusiones y Perspectivas Futuras merece una mención especial en este informe, pues en el mismo se especifican las principales aportaciones de la investigación realizada, para que puedan ser objeto de crítica y discusión; asimismo, se plantea el desarrollo de futuros trabajos enmarcados en esta línea de investigación.

Por todo lo anteriormente reseñado, emito un informe con todos mis pronunciamientos favorables y autorizo su presentación como Tesis Doctoral en el Programa de Doctorado en Ciencia y Tecnología de los Sistemas Agroforestales, de la Escuela Internacional de Posgrado (Universidad de Extremadura).

Mérida, 23 de junio de 2020

EL DIRECTOR DE LA TESIS DOCTORAL

La firma del director de la tesis consta en el original en papel de esta Tesis Doctoral

Dr. Alonso Sánchez Ríos

Mérida, 23 de junio de 2020

Menciones sobre esta Tesis Doctoral

Informes de diferentes expertos sobre la Tesis Doctoral aquí expuesta y sobre los avances que de ésta se pueden desprender. Los expertos que contribuyen a continuación, lo son en áreas relacionadas con esta Tesis Doctoral (Diseño, fabricación y venta de instrumental topográfico, fotogrametría o arquitectura).

Dr. Thomas Fischer

CEO (Chief Executive Officer) de la empresa familiar NEDO (Dornstetten, Alemania), con una historia de 119 años diseñando, fabricando y vendiendo instrumental topográfico. La empresa vende productos en más de 100 países de todo el mundo y tiene en plantilla de más de 140 empleados. Productos suyos son utilizados en CERN y fabrica productos para Leica Geosystem.

Daniel Frisch

CEO (Chief Executive Officer) de la empresa FlexiJet (Bad Oeynhausen, Alemania) fundada en 2011. Diseñador y fabricante del innovador sistema de medición de interiores Flexijet3D (premiado con el prestigioso Red Dot Design Award 2018) los cuales han vendido más de 2000 instrumentos y 4500 softwares por todo el mundo.

Dornstetten, Alemania, 11 Junio 2020.

Image-based measurements are a growing methodology, which are being used by more and more instruments to complement their tools and sensors. This PhD project presents an interesting new instrument based solely on images (videogrammetric camera) and is consisting of three phases:

i. the user has a guide in real time on a tablet, which indicates whether to continue or go back, in case a trajectory was interrupted.

ii. the system automatically chooses best images from a high resolution video camera.

iii. these images are automatically processed to generate a point cloud and a textured mesh.

These three steps together create an innovative measurement system and open the door for a new generation of photogrammetric / videogrammetric 3D scanners which can be complemented with other sensors.

On the other hand, the technology to select automatically best images or frames from a video camera to perform photogrammertry also open new research lines in other applications like Mobile Mapping Systems (MMS) to integrate photogrammetry with Lidar technology, or Unnamed Aerial Vehicles (UAV) to do photogrammetry without previous flight planning. This can be very interesting in emergencies where the user has not enough time to select way points, overlaps, and others flight parameters. This includes those cases, where the user may change the flight direction in the field without previous planning, depending on events like a fire.

Dr. Rubén Cabecera Soriano.

Doctor Arquitecto y director de aiuEstudio, slp. Es profesor de la Universidad de Extremadura en el Centro Universitario Santa Ana e Investigador en GICA (Grupo de Investigación de Construcciones Arquitectónicas) de la Universidad de Extremadura. Tiene una fabulosa experiencia en construcción de edificios y restauración de patrimonio histórico.

Mérida, a 11 de Junio de 2020.

La fotogrametría, como ciencia que posibilita la toma de medidas de objetos con precisión gracias a la utilización de imágenes, introdujo en el mundo de la arquitectura y demás artes vinculadas a ella, como la arqueología, el urbanismo, o el propio proceso constructivo —aunque resulta obvio que no solo es aplicable a estos sectores—, un abanico de posibilidades prácticamente inagotable que va directamente asociado a la evolución tecnológica de la propia ciencia fotogramétrica.

La información que ofrece un estudio fotogramétrico de un entorno concreto facilita de forma singular el proceso de diseño gracias a la caracterización y delimitación del espacio permitiendo la toma de decisiones y reduciendo considerablemente el margen de error en las mismas tras su análisis. Esta información, convenientemente procesada, es hoy en día de un interés extremo en cualquier proceso arquitectónico desde la introducción de la tecnología BIM que, a grandes rasgos, supone una novedosa metodología de trabajo fundamentada en la modelización en una base de datos, más o menos compleja, de cualquier objeto. Parte de la información contenida en dicha base de datos es la fotogramétrica.

Como quiera que la evolución que se está produciendo en los últimos tiempos orienta todos los procesos de diseño arquitectónico, de análisis arqueológico, de planificación urbanística, etc. hacia la metodología BIM y demostrada la vinculación directa entre esta y la fotogrametría, podemos inferir un vínculo indisoluble entre ellas que augura una continuada y próspera relación. La demanda de esta información por parte de aquellos que nos dedicamos al diseño arquitectónico, especialmente a las intervenciones en patrimonio tanto para su rehabilitación como para su restauración o para su reutilización, solo puede ser satisfecha por la fotogrametría en sus distintas vertientes, y dicha información objetualizada y transformada a un formato compatible con la tecnología BIM se convierte, hoy por hoy, en indispensable.

Sin embargo, el patrimonio susceptible de ser intervenido, aunque solo sea a los efectos documentales, es inmenso y los procesos de conversión fotogramétrica, a pesar de haber evolucionado profundamente desde mi primer contacto con la fotogrametría, allá por 1996 en los Cursos de Verano de la Escuela Universitaria Politécnica de Mérida, suponen un gran esfuerzo humano y tecnológico, en ocasiones incompatible con la obsesiva rentabilidad económica demandada por nuestra sociedad. En este sentido, la evolución tecnológica que ofrece la videogrametría supone un antes y un después en el binomio arquitectura-fotogrametría ya que garantiza resultados precisos con tiempos de procesado razonables a costes asumibles, lo que hace que esta tecnología, con el hardware y el software apropiados, se convierta en indispensable en cualquier intervención arquitectónica en nuestro patrimonio.

Este es el escenario en el que se desarrolla la investigación de Pedro Ortiz-Coder, aunque resulta evidente que su trabajo no encuentra límites en el ámbito arquitectónico, sino que ofrece un potencial desarrollo que abarca sectores sumamente dispares, pero necesitados de la información que su investigación tecnológica puede ofrecer cubriendo expectativas que actualmente el mercado no ofrece.

Marcel Goyvaerts.

Actualmente es Channel Manager en Oriente Medio, norte de África, Iberia, Benelux e India para la multinacional GeoSLAM (Nottingham), y además tiene una larga y riquísima experiencia en ventas internacionales de instrumental topográfico en multinacionales como Geomax (Director regional de ventas), Carlson (Director de Ventas y Marketing), Topcon (Manager de ventas Africa y Oriente medio) y Sokkia (Director de ventas y jefe de oficina europeo), entre otros.

Valencia, a 12 de Junio de 2020.

The trend in capturing reality in the recent years has shifted clearly and rapidly from classic 2/3D data acquisition as done by surveying engineers using their specialised single shot Total stations, GPS, levels etc. towards new, disruptive and easy-to-use mass capturing devices that combine new technologies like photogrammetry, (static & mobile) scanners, drones, HR digital cameras, IMU sensors, and highly advanced algorithms on extremely powerful processors etc to capture the same, but much more complete and easy-to do, and to be used by anyone who needs 3D information (thus no longer a specialised job!).

Pedro's unique developed camera as presented in this doctorate fits perfectly in this trend. It is an excellent result of a long journey of research that Pedro did over the last 10 years in this field.

His videogrammetric camera is based on highly advanced algorithms to find the best images from a video to perform photogrammetry, which guides the user in the scanning process and -fully automatically- results in a complete and accurate 3D reconstruction of the scene.

This combination of on-the-edge technology, mass data capture and easiness of use will find its way in the fast changing 3D industry without any doubt.

Clear applications will be found in architecture, urban mapping, archaeology, mining and construction, among others.In parallel the technology will be integrated in other measurement devices as well like in mobile mapping systems (cars, handheld scanners, trolleys or backpack) or UAV, thus adding to these devices a real extra dimension.

Congratulations Pedro and thanks a lot for having been able to follow part of your long scientific journey!

Dr. Prof. Bijun Li

El Doctor Li es profesor y especialista en fotogrametría y sensores remotos del laboratorio LIESMAR, en la Universidad de Wuhan (China). Este laboratorio de la información en ingeniería topográfica, cartografía y sensores remotos, es el primer laboratorio, en el campo de la medición de China y uno de los más importantes en el campo de la investigación en cartografía y teledetección del mundo.

Dr.Prof. Chen Changjun

El Dr.Chen comparte su tiempo como profesor en la escuela de Geodesia y Geomática de la Universidad de Wuhan, China.; y en Wuhan RG Space Co.,LTD, en la división de Mobile Mapping de la empresa CHC Navigation, donde diseña y trabaja con los Sistemas Mobile Mapping. La empresa CHC Navigation es una multinacional en pleno crecimiento y gran proyección, está presente en más de 100 países y tiene más de 1300 empleados.

Andrei Gorb

El ingeniero Andrei Gorb es el director del Segmento de Mobile Mapping Solution en CHC Nav (Shangai, China). Andrei tiene una gran experiencia con el diseño de instrumentos topográficos, ya que también trabajó durante años como director del Segmento de HDS – en la planta de procesos de medición (Survey Plant Processes) en Leica Geosystem (Heerbrugg, Suiza).

Budapest, Hungria y Wuhan,China. 14 Junio 2020

Shooting video is a common way to record information. Through this innovative method, a terrestrial handheld videogrammetric 3D scanner, researched in this PhD project, we can endow video with measurement and 3D reconstruction ability. We are very surprised that the high-density point cloud constructed by this technology, which it has the characteristics of good precision and realistic texture. We believe that Sr. Pedro Ortiz's work will open up a very interesting way for the research of close range photogrammetry and new easy to use and intuitive products which can be comparing with traditional scanners.

Dr. Florencio Monje Gil.

Actualmente es profesor en la facultad de Medicina de Badajoz, también ejerce la especialidad de cirujano maxilofacial en el Hospital Universitario de Badajoz y en su propia clínica denominada CICOM(Centro de Implantología, Cirugía Oral y Maxilofacial). El Dr.Florencio es, además, Presidente de la European Society of Temporomandibular and Surgery, fue Premio Nacional de Medicina S.XXI (2018) y es autor de varios libros y numerosos artículos científicos. Actualmente es considerado una de las figuras más relevantes de esta especialidad en la actualidad a nivel mundial.

Badajoz, a 17 de Junio de 2020.

En el siglo XXI la famosa globalización hace que personas, instituciones, empresas etc. tengan fácil relación. De igual modo, en la ciencia las distintas disciplinas deben buscar apoyo de forma mutua. Es obvio que todas las capacitaciones tienen una línea de desarrollo basado en la investigación continúa por los mismos equipos pero mejorando la tecnología. Pero es mucho mejor buscar sinergias entre distintas capacitaciones y profesiones. El mundo de la medicina en la actualidad está sustentado por una necesidad asistencial pero la clave del desarrollo es la investigación. Esta investigación debe ser una investigación aplicada, es decir, con el objetivo de la utilización clínica como destino final. Las ingenierías son un elemento de sinergia en el campo de la investigación y en especial en el campo de la investigación biomédica. Con la técnica que maneja Pedro Ortiz Coder, la fotogrametría o videogrametría seguro que pueden aplicarse a muchos aspectos de la tecnología y de la vida cotidiana. En nuestro caso la hemos desarrollado para mejorar el conocimiento de una articulación, la más activa del cuerpo humano, que es la articulación temporomandibular. Esta articulación puede ser afecta de numerosos procesos traumáticos, inflamatorios y neoplásicos. Pero la patología más frecuente se denomina síndrome de disfunción de la articulación temporomandibular. En algunos casos está indicada una técnica endoscópica para el diagnóstico y para la terapéutica. Mediante la fotogrametría podemos mejorar la visión y la imagen tridimensional de esta articulación, detectar morfológicamente cambios patológicos y cuantificar mediante distancias, áreas y volúmenes cuales son los factores pronósticos del resultado terapéutico de la artroscopia.

Ric Durrant.

Ingeniero experimentado en diseño y fabricación de instrumentos de medición de tipo móvil (Mobile Systems), actualmente es CTO (Chief Technology Officer) de la empresa GeoSLAM (Nottingham, Inglaterra), en la cual trabaja desde sus inicios como máximo responsable técnico donde desarrolla y evoluciona tecnológicamente sus innovadores productos, ya que fueron los primeros en comercializar los escáneres de mano basados en LIDAR y sistemas inerciales. Anteriormente estuvo trabajando más de 12 años en la empresa inglesa 3D Laser Mapping como Director de Ingeniería, donde desarrollaron sistemas mobile mapping (MMS), transportados en vehículos.

Nottingham, Inglaterra, a 18 de Junio de 2020.

This thesis introduces a novel approach to videogrammetry combining by visual SLAM with photogrammetry to enable a fast, accurate and reliable method for 3D reconstruction.

The addition of visual SLAM into the process enables smart frame selection and filtering methods to be applied to the photogrammetry stage whilst also potentially providing a guide to the operator if implemented in real time.

The dual camera system presented in the thesis provides an ingenious means of optimising the system for both VSLAM and photogrammetry.

The results presented are impressive both in terms of accuracy and scale of the project undertaken.

Overall ,the thesis opens up some very exciting potential for new developments in the field of 3D construction.

Lista de publicaciones:

La presente Tesis Doctoral está compuesta por un conjunto de tres artículos, en los dos primeros casos han sido previamente publicados en revistas científicas de calidad reconocida e indexadas en bases de datos internacionales, como Journal Citation Report (JCR) o SJR (Scimago Journal & Country Rank); ambas ocupan posiciones relevantes en los listados de esta bases de datos, con un índice de impacto elevado. En el caso del tercer artículo ha sido presentado en otra revista científica indexada en el JCR y en estos momentos, se encuentra en proceso de revisión. Los certificados de publicación (artículos I y II) y entrega (artículo III) se adjuntan en el Anexo II:

A Self-Assembly Portable Mobile Mapping System for Archeological Reconstruction Based on VSLAM-Photogrammetric Algorithm

Pedro Ortiz-Coder , and Alonso Sánchez-Ríos

Department of Graphic Expression, University Centre of Mérida, University of Extremadura, 06800 Mérida, Spain

Sensors 2019, 19(18), 3952; https://doi.org/10.3390/s19183952 (IF:3.031 JCR category rank: Q1)

Recibido: 19 Julio 2019 / Revisado: 29 Agosto 2019 / Aceptado: 9 Septiembre 2019 / Publicado: 12 Septiembre 2019

An Integrated Solution for 3D Heritage Modeling Based on Videogrammetry and V-SLAM Technology

Pedro Ortiz-Coder , and Alonso Sánchez-Ríos

Department of Graphic Expression, University Centre of Mérida, University of Extremadura, 06800 Mérida, Spain

Remote Sens. 2020, 12(9), 1529; https://doi.org/10.3390/rs12091529 SJR: 1.422 (2019), SJR Quartil (Q1)

Recibido: 12 Abril 2020 /Revisado: 5 Mayo 2020 / Aceptado: 8 Mayo 2020 / Publicado: 11 Mayo 2020

Automatic 3d dense reconstruction using VSLAM and photogrammetric algorithms: approach in the temporomandibular arthroscopy case.

Pedro Ortiz-Coder[1], Florencio Monje Gil[2] and Alonso Sánchez Ríos[1]

[1]Department of Graphic Expression, University Centre of Mérida, University of Extremadura, 06800 Mérida, Spain.

[2] Department of Oral and Maxillofacial Surgery, University Hospital of Badajoz, Badajoz 06001, Spain.

Measurements 2020. (IF:2.826 JCR category rank: Q2)

Recibido: 23 Junio 2020.

A mi Querida Gran Familia,
a mis hermanos, a mi padre y a mi madre,
a mi mujer Sara y a mi hijo Daniel,
por escucharme, por entenderme, por acompañarme, por animarme y
porque sin vuestro apoyo, esto no hubiese sucedido.
Muchas Gracias.

"En una línea el mundo se une, con una línea el mundo se divide, dibujar es hermoso y tremendo."
Eduardo Chillida.

Resumen

En un contexto de proliferación de instrumentos de medición en los campos de la ingeniería, la minería, forestales, la construcción, la arqueología y la arquitectura, asistimos a una imparable evolución de los sistemas de medición basados en imágenes, los cuales utilizan fundamentalmente procesos digitales de imágenes, técnicas de fotogrametría y visión computacional. Esta Tesis Doctoral estudia la interacción en éstos ámbitos, diseñando y experimentando diferentes tecnologías para la localización en tiempo real y para la reconstrucción 3D en postproceso de forma muy precisa, únicamente utilizando cámaras de video.

Este documento estudia distintos instrumentos existentes en el mercado atendiendo a la naturaleza de los sensores utilizados, velocidad de captura, alcance, resultados obtenidos y precio de mercado, entre otros parámetros. Se analizan productos actuales como los escáneres de mano basados en sensores LIDAR (Laser Imaging Detection and Ranging), sistemas de medición móvil transportados en carros o en mochilas, y también los sistemas móviles de medición transportados en vehículos (Mobile Mapping System -MMS-), además de los escáneres laser terrestres, sistemas de medición únicamente basados en imágenes y la fotogrametría actual.

El proyecto propone tres elementos que unidos conforman una nueva tecnología: 1. Sistema de guiado o asistencia al usuario en el proceso de escaneo. Para ello se utiliza la tecnología de localización simultánea a través de cámaras de video (Visual SLAM)[1] conectado a una Tablet o portátil. 2. Sistema refinado de selección de imágenes capturadas con una videocámara. En el texto se detalla el procedimiento para la selección de imágenes óptimas, extraídas de la videocámara, que garantiza una óptima y posterior reconstrucción 3D. Esta selección consta de imágenes clave o "*keyframes*" seleccionadas a partir de la tecnología VisualSLAM, y una posterior aplicación de diferentes filtros diseñados específicamente para éste fin. 3. Reconstrucción 3D a partir de las imágenes seleccionadas. En este punto se define un procedimiento específico para cada paso a través de los cuales, se genera la nube de puntos, se filtra, se crea una malla de triángulos y se texturiza a través de la proyección de las imágenes seleccionadas.

El sistema de medición, creado a partir de los elementos anteriores, consta de dos cámaras, una para el guiado y localización del usuario en tiempo real durante el escaneo, y la otra para la posterior reconstrucción 3D. El primer artículo (Sección I) se centra en una descripción detallada del concepto y de los elementos antes mencionados, así como de su interacción. La cámara videogramétrica ha sido evaluada y comparada con el láser escáner Faro Focus X330 en el artículo segundo (Sección II), obteniendo resultados prometedores en cuanto a tiempo de captura, precisión y textura de los resultados en entornos arqueológicos. En las secciones I y II, se realizan sendas evaluaciones; En la sección I se evalúa la precisión atendiendo a la distancia de captura, probando, para ello, tres distancias distintas y analizando la evolución, pero también, ya en la sección II, atendiendo a la configuración del elemento a escanear a través de trayectorias complejas. Los datos se han confrontado con los obtenidos en un software fotogramétrico comercial (Agisoft Metashape [2]) obteniendo menor resolución pero precisiones muy similares para ambos sistemas. La tecnología en sí, refiriéndonos al procedimiento de selección y reconstrucción 3D, tiene una proyección más amplia, pudiéndose utilizar en distintas áreas, como la medición en ingeniería y urbanismo a través de sistemas MMS o Unnamed Aerial Vehicles (UAV), o en otros muchos campos como la medicina, tal y como se expone en la sección III de esta Tesis Doctoral, en la cual se describe un trabajo de aplicación exitosa de reconstrucción 3D de partes de la articulación temporomandibular (ATM) a través de artroscopias. En este artículo de aplicación práctica de la tecnología desarrollada se consiguen, además, hitos interesantes, como la realización de las primeras reconstrucciones fotogramétricas de precisión a través de un artróscopo de la articulación ATM. La selección de imágenes y las técnicas de reconstrucción utilizadas fueron clave para la consecución de estos resultados tan favorables.

El trabajo de investigación concluye definiendo las aportaciones que realiza en el campo de los sistemas de medición, en el cual se habilita a la videocámara o sistemas de videocámaras, como un instrumento de medición profesional, cuyos resultados son equiparables a instrumentos actuales, en determinados ámbitos, como el arqueológico. Por otra parte, la tecnología de selección de imágenes y posterior reconstrucción 3D abre múltiples campos en los sistemas de *"mobile mapping"* o UAV, pero también en otros de un ámbito muy distinto, como es el caso, detallado en la sección III, de reconstrucción digital 3D de articulaciones a partir de endoscopias.

Índice

1.

INTRODUCCIÓN

1.1. Motivación

Entorno comercial y necesidades observadas en el mercado

La proliferación de nuevas tecnologías y productos en el ámbito de los escáneres 3D para ingeniería y arquitectura en las últimas décadas, ha sido el resultado de un interés creciente de los ámbitos académicos y profesionales en la sociedad. Incluso hoy, las proyecciones de crecimiento en el mercado de la tecnología LIDAR[1] certifican un interés en aumento, además de una mayor aceptación y uso por parte de la sociedad, de este tipo de instrumentación, que apenas existía hace tan solo 20 años atrás. En el año 2019 el mercado de la tecnología LIDAR movió en todo el mundo 844 millones de dólares, pero esa proyección alcista continúa en todos los continentes, hasta alcanzar los 2273 millones en el año 2024, según la publicación *Market and Market Journal*[1]. Dicha afirmación es confirmada por los datos de crecimiento observados en años anteriores en aplicaciones topográficas, arquitectónicas y de construcción (ver figura 1) según la publicación *Point of Beginning* [2].

	2018	***2017***	***2016***
Construcción	*57%*	*22%*	*20%*
Arquitectura/BIM	*44%*	*13%*	*46%*
Cartografía/Topografía	*44%*	*58%*	*44%*

Tabla 1. *Demanda de Laser escáner. Incremento de la demanda de laser escáner terrestre (TLS) en los años 2016, 2017 y 2018 en aplicaciones de la construcción, arquitectura y creación de mapas y planos topográficos. Fuente: 2019 Survey & Mapping Deep Dive Laser Scanning and GIS CLEAReport. Point of Beginning Journal.*

El aumento de ventas e interés del mercado por estas tecnologías, responde a la utilidad que los usuarios ven en ella, a los beneficios que le reportan en términos de completud de los modelos, aumento de precisión y reducción de tiempo empleado en los proyectos, entre otros factores. Pero también a que existe una mayor oferta de nuevas tecnologías y productos derivados de sistemas LIDAR, pero también de la fotogrametría, que permiten una mayor accesibilidad, más facilidad de uso y adaptabilidad del instrumento y del software de postproceso de datos, a las necesidades y requerimientos de los distintos profesionales. Asistimos, por tanto, a una transformación de los escáneres 3D en un producto más horizontal y accesible para un mayor número de profesionales, aumentando por tanto, el volumen de éstos que comienzan a utilizar instrumentos de medición y aumentando, también, las aplicaciones para las que estos pueden ser aplicados.

Como consecuencia, los laser escáneres terrestres (TLS) de medio y largo alcance, nacidos hace dos décadas, han evolucionado tecnológicamente siendo más rápidos, pequeños y precisos cada vez, pero además, uniéndolos a nuevos sensores y algoritmos, se pueden transportar y mover mientras escanean; de esta interesante variante podemos encontrar escáneres de mano de laser de tipo "*profile*", *sistemas "mobile mapping"* para automóviles (MMS) o mochilas, sistemas LIDAR para ser transportados en drones, denominados UAV (*Unnamed Aerial Vehicles*), etc. Los sistemas de adquisición de datos anteriormente mencionados, funcionan normalmente, con sensores activos tipo LIDAR, pero también son asistidos, cada vez más, por sensores pasivos como cámaras o multicámaras que ayudan en la localización y aportan texturas fotorrealistas a las nubes de puntos generadas.

La fotogrametría terrestre

El papel de la fotogrametría, como sistema de medición en la ingeniería y la arquitectura, es también fundamental; su uso se ha incrementado de forma proporcional, gracias sobre todo, a la automatización de

muchos de los procesos y, de forma muy especial, por la aparición y desarrollo de los UAV en los últimos años.

La fotogrametría que nos ocupa es la fotogrametría terrestre, cuyas tomas se realiza desde el suelo. El usuario debe conocer una serie de parámetros básicos de la cámara y también de las características de la toma, para garantizar el éxito de la reconstrucción 3D: por ejemplo, debe elegir cuando y donde realizar cada fotografía, esto es, la elección de la línea base, porcentaje de recubrimiento entre imágenes y de la geometría de la toma, pero también debe seguir una trayectoria adecuada [3] y adaptar los parámetros de la cámara a las condiciones de luz de la escena, que puede ser cambiante en cada fotografía, especialmente en capturas largas donde se intercalan distintas tipologías de escenarios e iluminaciones. También son elecciones del usuario el elegir la cámara adecuada, el sensor y la tipología de éste (por ejemplo "*global shutter" o "rolling shutter"*), el diafragma, el obturador, el ISO, etc. Es por tanto un procedimiento que requiere de un cierto conocimiento previo del usuario sobre conceptos básicos de fotografía y de fotogrametría.

El proceso para el modelado basado en imágenes podría dividirse en distintos puntos bien diferenciados [3], [4]: Diseño (calibración de la cámara, búsqueda de puntos homólogos, orientación relativa y cálculo de la geometría de la toma), mediciones 3D (generación de la nube de puntos), modelado 3D (segmentación, generación del mallado o "*mesh*", mapeado de texturas y visualización). De los avances en las investigaciones de los procedimientos fotogramétricos, que pueden consultarse en [5], y de la experiencia de diferentes estudios [3], [6] confirman que:

I. La precisión aumenta con tomas convergentes, mejor que con tomas paralelas, y aumentando la relación base-profundidad.
II. La precisión aumenta si un mismo punto aparece en múltiples imágenes, pero si aparece en más de 4 la precisión disminuye.
III. La precisión aumenta con el número de puntos medidos por imagen, siempre que la geometría de la toma sea robusta y su distribución esté repartida por toda la imagen.
IV. Una mayor resolución implica mayor precisión del modelo.

El video/videogrametría como sistema de medición.

Las reconstrucciones 3D a partir de videocámaras tienen, a su vez, dificultades básicas: el video está formado por una sucesión de "*frames*" y su frecuencia de toma no discierne si el usuario y la videocámara que porta, se ha parado durante la captura o si, en cambio, ha acelerado la velocidad; pero tampoco identifica si un objeto se ha cruzado de repente, o si el usuario ha realizado un movimiento o un giro demasiado rápido. También hay un inconveniente básico, y es que la resolución de las videocámaras comerciales suele ser notablemente inferiores que las de la toma fotográfica, con lo que ello afecta directamente a las calidades de los modelos 3D. Todos estos elementos pueden hacer que la toma no pueda generar una continuidad en la orientación o que la geometría no sea correcta, además de una mala calidad de los modelos 3D si la resolución de las imágenes es baja, entre otros problemas.

Debemos considerar que la selección de imágenes mediante videos puede realizarse, fundamentalmente, siguiendo tres metodologías [7] según la literatura científica:

a. Extrayendo un "*frame*" cada X "*frames*" existentes del video. Este método es el más básico y no responde ni a variaciones de la velocidad del usuario, ni cambios de angulación o distancia del objeto escaneado, entre otros; por lo que puede acarrear problemas importantes y limita su uso para grandes levantamientos y trayectorias complejas.

b. Método de 2D-"*feature-based*". [4] Esta metodología está basada en la evaluación del número de "*keypoints"* que tiene una imagen respecto a las anteriores, tras la aplicación de algún método de descriptores (FAST, ORB, SIFT, otros), y eliminando, además, los "*frames"* que no estén nítidos y aquellos cuyo porcentaje de "*keypoints"* esté por debajo de un valor de tolerancia dado.

c. Método de 3D-"*based selection"*. [1]. El algoritmo selecciona un nuevo "*keyframe"* si supera el mínimo establecido y si tiene menos de un 90% de puntos en común con el anterior *"keyframe"* seleccionado. Esta metodología considera la geometría del entorno y recupera la continuidad de la trayectoria al pasar por lugares donde se ha pasado anteriormente, pudiendo eliminar *"keyframes"* si el nuevo seleccionado tiene un 90% de puntos en común con los dos anteriores o con los *"keyframes"* de la zona de alrededor de éste. Este algoritmo es el utilizado en nuestro desarrollo.

La reconstrucción 3D de un escenario con las máximas garantías de éxito, a través de una sola videocámara en movimiento portada por un usuario, y en capturas de más de unos pocos minutos, requiere de un sistema de guiado, orientación y localización de los "*frames"* en tiempo real (Visual SLAM: Visual Simultaneous Localization and Mapping), que calcule la trayectoria constriñendo al usuario en sus movimientos e indicando si éste se ha perdido, para que vuelva a un lugar conocido por donde se ha pasado anteriormente, y generando así dicha trayectoria sin perder la continuidad. Al tratarse de capturas terrestres de tipo "*Large-scales"* y de un instrumento de mano o tipo "*handheld"*, asumimos que el objeto a escanear puede exigir una trayectoria compleja, y que el usuario puede realizar movimientos erráticos o que los condicionantes de la toma (escalones, pasillos, vegetación o zonas estrechas, entre otras) puedan crear una ruptura en la orientación de las imágenes, por lo que el usuario requiere realizar la captura de una determinada forma para garantizar el éxito y la continuidad de la misma. Las soluciones SFM (*Structure For Motion*)[8] requieren normalmente un mayor coste computacional, además de una geometría de la toma más específica, conservando la proporcionalidad entre las líneas base y el objeto a documentar para la obtención de un resultado óptimo. Por tanto, se precisa de un sistema Visual SLAM del tipo "*3D-based"* para la obtención de los *"frames"* óptimos extraídos del video en tiempo real, pero también de un procedimiento que complemente al anterior, ya que éste puede añadir imágenes no deseadas y, en ocasiones, el solape es insuficiente para realizar fotogrametría de precisión; por estas razones se ha diseñado un complejo algoritmo a través de distintos filtros que garantice la óptima selección de imágenes para que pueda realizarse una orientación relativa/SFM de las mismas y una reconstrucción 3D off-line (en postproceso) con la máxima precisión y garantías de éxito.

Motivación Personal

La motivación personal para investigar y desarrollar un sistema de reconstrucción 3D automático a través de videogrametría, nace de la experimentación con diferentes escáneres 3D, cámaras y softwares fotogramétricos en múltiples proyectos profesionales, pero también a través de proyectos de investigación y de relaciones profesionales con otros clientes. En una primera etapa profesional, realicé levantamientos arquitectónicos integrando distintos tipos de instrumentos como laser escáner, fotogrametría, GPS, estación total, etc. En una segunda etapa empresarial investigué y desarrollé un sistema fotogramétrico que trataba de facilitar el procedimiento ampliando su uso a usuarios no expertos, a partir de un sistema de procesamiento y captura móvil. En esta fase tuve contacto con múltiples usuarios y aprendí sobre los requerimientos y necesidades de éstos con gran nitidez. Todos estos años de experiencia profesional en mis distintas etapas, me sirvieron para aprender, de primera mano, el uso de hardware y software de distintas tipologías de instrumentos y conocer su problemática, pero también para investigar y desarrollar tecnologías que simplificaran su utilización, especialmente en el ámbito fotogramétrico.

De la observación del mercado y de mi propia experiencia nace la motivación en el desarrollo de un sistema para realizar reconstrucciones 3D, que sea sencillo e intuitivo. De ahí nació la investigación en los sistemas videogramétricos, en el guiado del usuario a través de Visual SLAM, en la selección automática

de imágenes de forma refinada y en las distintas fases de la reconstrucción 3D, objeto de estudio en esta Tesis Doctoral.

Durante el desarrollo del doctorado se observó que la tecnología desarrollada no sólo tenía una validez para la realización de un escáner videogramétrico de mano, sino que se podía aplicar a muchos campos donde se pretende realizar fotogrametría a partir de una o más cámaras. La aplicación se multiplica si, en vez de utilizar dos cámaras, una para VisualSLAM y otra para fotogrametría, que ambas entradas se implementen a través de una sola cámara. En este caso, con solo una cámara se podrían grabar las imágenes para fotogrametría y realizar, más tarde, la selección de imágenes a través de VisualSLAM, y posteriormente la reconstrucción. En este caso eliminaríamos el guiado del usuario, con lo que deberíamos de garantizar de otra forma que la captura sea correcta en términos de geometría de la toma.

Este esquema permite numerosas aplicaciones, como por ejemplo:

- Reconstrucciones 3D en endoscopias, como es el caso de la artroscopia (artículo sección III), laparoscopia, etc.
- Sistemas *"mobile mapping"* a través de automóvil, mochila o carro. En estos sistemas se suelen utilizar multicámaras cuyos *"frames"* se pueden seleccionar automáticamente y realizar fotogrametría integrándolo con los sistemas LIDAR y demás sensores.
- Sistemas UAV. La cámara del "*drone"* puede pasar a ser una cámara de video cuya selección de *"frames"* se realiza con la tecnología propuesta en este proyecto, evitando así un plan de vuelo, disminuyendo el tiempo empleado anterior al vuelo y garantizando que no falta ninguna imagen clave durante el vuelo. Esto sería muy útil para casos de emergencia, donde no existe mucho tiempo para hacer planificaciones de vuelo y en el cual, no puede faltar ninguna imagen que, posteriormente, limite una reconstrucción 3D completa de la escena.

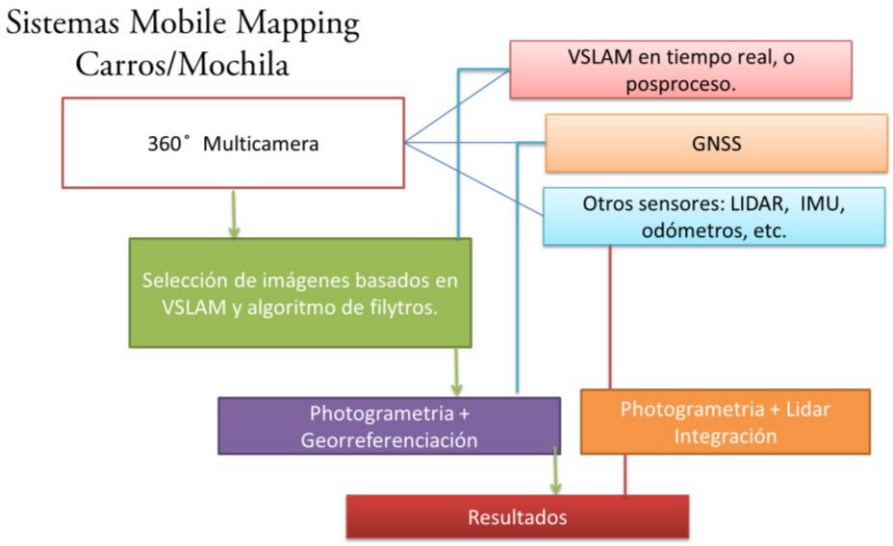

Figura 1. *Esquema de la aplicación tecnología del filtrado de imágenes y posterior reconstrucción 3D, en aplicaciones de sistemas "mobile mapping"(MMS). En éste esquema se detalla como un sistema multicámara, unido a otros sensores, como el LIDAR, y utilizando la selección de imágenes y posterior reconstrucción 3D, puede obtener resultados más completos que sin dicha integración.*

1.2. Objetivos

El objetivo general de este proyecto versa sobre la investigación de sistemas videogramétricos como alternativa o complemento de los instrumentos actuales de medición. Para ello se han explorado metodologías para la extracción de las imágenes óptimas de un video para la realización de fotogrametría, con la menor intervención humana posible. Para ello se ha construido un prototipo de cámara videogramétrica funcional. Finalmente se ha evaluado los resultados obtenidos y las aplicaciones posibles según los condicionantes que este sistema tiene.

Como **objetivos específicos** podemos destacar los siguientes puntos:

- Investigar y desarrollar un sistema videogramétrico que, a partir del diseño de un algoritmo para la selección automática y específica de *"frames"* provenientes de un video, se pueda realizar una reconstrucción 3D con garantías de continuidad y precisión utilizando únicamente los *"frames"* seleccionados.
  La cámara videogrametría desarrollada en este proyecto, es aquella que cumple los siguientes requisitos:
  i.La adquisición de imágenes se realiza de forma totalmente automática y sólo a través de imágenes, esto es, sin el apoyo de ningún otro sistema de medición.
  ii. Durante la adquisición de imágenes, el sistema utilizará el VisualSLAM para guiar al usuario y asegurar una continuidad de la trayectoria y del éxito del procesamiento off-line (posterior).
  iii. El procesamiento de datos (selección de *"frames"* y reconstrucción 3D) se realiza también de forma totalmente automática, una vez se termine la adquisición de datos.
- Consolidar la captura videogramétrica de forma específica en un escáner 3D de mano, con aplicaciones en la arquitectura, la arqueología y la ingeniería, entre otras. Se implementó un sistema de guiado del usuario en tiempo real a partir de una tablet, basado en la tecnología VisualSLAM que garantiza la continuidad de la toma y que el usuario realice movimientos compatibles con una posterior reconstrucción 3D. Por tanto, dicho sistema videogramétrico realiza reconstrucciones únicamente a través de imágenes y sin intervención del usuario, con la novedad de incluir una segunda cámara para la captura a alta resolución, y a través del procedimiento optimizado de selección y reconstrucción, que consiguen modelos 3D de alta resolución, precisión y calidades en las texturas de forma totalmente automática, pudiendo compararse con los sistemas más avanzados para estos fines(laser escáner), en la actualidad.
- Estudiar las posibilidades de aplicaciones posibles de la invención, para ello tanto en el sistema de guiado, que puede ser sustituído, como en el sistema de filtrado y selección de imágenes, y como en la reconstrucción 3D, se emplearon múltiples parámetros abiertos a ser ajustados a cada caso de aplicación. Es el caso de estudio expuesto en el tercer artículo (sección III), donde se muestra la aplicación del desarrollo en reconstrucciones 3D de la articulación temporomandibular a través de un artroscopio.

1.3. Estructura

La presente Tesis Doctoral sigue la reglamentación indicada por la Universidad de Extremadura y está basada en la modalidad de compendio de artículos científicos, los cuales deben ser publicados en revistas internacionales de índice de impacto. Esta Tesis Doctoral consta de tres secciones, y cada sección contiene un artículo original con índice de impacto; dos de los cuales están ya publicados y el tercero, presentado y en fase de revisión.

El primer artículo (Sección I) realiza un planteamiento del problema y detalla el sistema procedimental propuesto para el escaneo de estructuras arquitectónicas a través de un sistema videogramétrico desarrollado para dicho fin. En él se detalla el algoritmo de filtrado de imágenes y se realiza una primera aproximación al hardware a través de un primer prototipo. Se concluye dicha sección exponiendo una evaluación de los resultados a través de un estudio de precisión, realizando una comparativa con el software fotogramétrico Agisoft Metashape.

En la sección II, el segundo artículo plantea una evolución del dispositivo y se afina el procedimiento de filtrado. En esta sección se realiza una evaluación comparativa de mayor profundidad y se confrontan los resultados al láser escáner Faro Focus 3D. Para ello se escanean con los dos sistemas tres yacimientos arqueológicos. Se comparan diferentes elementos como los tiempos de procesamiento, resolución, precisión y texturas.

Finalmente en la sección III, el tercer artículo plantea una aplicación concreta de la tecnología de selección de imágenes y posterior reconstrucción 3D desarrollada; es el caso de aplicación de la generación de reconstrucciones 3D a través de artroscopias en la articulación temporomandibular. El artículo aplica la tecnología de selección de imágenes a partir de video y detalla el procedimiento de reconstrucción aplicado, obteniendo como resultado distintas nubes de puntos y mallas 3D con texturas de la articulación.

Se justifica, por tanto, la relación de los tres artículos como una evolución natural de la Tesis Doctoral, en el que se define la hipótesis, se desarrolla la tecnología y se aplica la misma en la cámara videogramétrica, como aplicación primaria. Se realiza una evaluación completa en las secciones I y II y, finalmente, se demuestra la viabilidad de la tecnología desarrollada en otros campos, como es el médico, donde a través de la sección III se obtienen interesantes resultados.

2. Sección I: El concepto tecnológico y su aplicación en arquitectura.

Esta sección contiene el artículo: "A Self-Assembly Portable Mobile Mapping System for Archeological Reconstruction Based on VSLAM-Photogrammetric Algorithm." Publicado el 12 de septiembre de 2019 en la revista Sensors, en el apartado especial de (special issue): Visual and Camera Sensors.

Resumen

El artículo plantea el contexto de los diferentes sistemas de medición basados en los tipos de sensores, los procesos de captura, los resultados que generan y las aplicaciones. Y en este ámbito se enuncia el sistema propuesto basado en un escáner de mano que, a través de dos cámaras de video, captura el escenario deseado para, posteriormente, procesar las imágenes, seleccionarlas y generar una nube de puntos, que es el resultado principal del dispositivo. El artículo plantea la aplicabilidad de dicho instrumento, entre otras posibilidades, para generar entornos BIM.

La carcasa es diseñada e impresa en 3D y, en ella se alojan dos cámaras industriales de la marca Imaging Source: Camera A (model DFK 42AUC03) and camera B (model DFK 33UX264). Se realizan sendas calibraciones de las cámaras y se extraen los parámetros para cada una de ellas; también se efectúa una calibración externa, calculando la posición de una cámara respecto a la otra, a través de una transformación 3D de 7 parámetros.

Se describe el modo de funcionamiento del sistema, desde un punto de vista de usuario y desde una perspectiva metodológica. El usuario se desplazará con el instrumento en paralelo a la zona a capturar y siguiendo las sugerencias del VisualSLAM que, en tiempo real, calcula la trayectoria y si ésta se ha perdido. Por otro lado se describe el esquema básico del algoritmo, donde la cámara A, a través del VisualSLAM, genera una información sobre el posicionamiento de la cámara de cada "*frame*" principal (o "*keyframe*") y, la cámara B, de mayor resolución, almacena todos los "*frames*". El algoritmo diseñado selecciona los "*frames*" de alta resolución obtenidos por la cámara B, basándose en los datos obtenidos de la cámara A y también a través de unos filtros: Filtro "*AntiStop*" y filtro de "*Divergent SelfRotation*", los cuales eliminan las imágenes si estas pertenecen a un momento donde el instrumento está parado o ha rotado sobre sí mismo.

Finalmente, se realiza una prueba experimental sobre el acueducto de los Milagros en la ciudad de Mérida, escaneándose a tres distancias distintas y comparando la precisión de los modelos a través de puntos individuales distribuidos por el monumento y medidos con estación total. Las precisiones obtenidas, en términos de error cuadrático medio (*root mean square error* -RMSE-) son de 8mm y de 33mm para distancias de observación de 5 m y 20 m respectivamente. Finalmente se confrontan los datos con el software fotogramétrico Agisoft Metashape obteniendo un modelo con más resolución que el obtenido con el sistema propuesto, pero con una precisión algo mejor. El instrumento se demuestra, por tanto, con un gran potencial de utilización y con precisiones equiparables a los sistemas fotogramétricos actuales.

Artículo I: A Self-Assembly Portable Mobile Mapping System for Archeological Reconstruction Based on VSLAM-Photogrammetric Algorithm.

SENSORS
Article

A Self-Assembly Portable Mobile Mapping System for Archeological Reconstruction Based on VSLAM-Photogrammetric Algorithm

Pedro Ortiz-Coder *,† and Alonso Sánchez-Ríos *,†

Department of Graphic Expression, University Centre of Mérida, University of Extremadura, 06800 Mérida, Spain

* Correspondence: peorco04@alumnos.unex.es (P.O.-C.); schezrio@unex.es (A.S.-R.)

† These authors contributed equally to this work.

Received: 19 July 2019 / Revised: 29 August 2019 / Accepted: 9 September 2019 / Published: 12 September 2019

Abstract: Three Dimensional (3D) models are widely used in clinical applications, geosciences, cultural heritage preservation, and engineering; this, together with new emerging needs such as building information modeling (BIM) develop new data capture techniques and devices with a low cost and reduced learning curve that allow for non-specialized users to employ it. This paper presents a simple, self-assembly device for 3D point clouds data capture with an estimated base price under €2500; furthermore, a workflow for the calculations is described that includes a Visual SLAM-photogrammetric threaded algorithm that has been implemented in C++. Another purpose of this work is to validate the proposed system in BIM working environments. To achieve it, in outdoor tests, several 3D point clouds were obtained and the coordinates of 40 points were obtained by means of this device, with data capture distances ranging between 5 to 20 m. Subsequently, those were compared to the coordinates of the same targets measured by a total station. The Euclidean average distance errors and root mean square errors (RMSEs) ranging between 12–46 mm and 8–33 mm respectively, depending on the data capture distance (5–20 m). Furthermore, the proposed system was compared with a commonly used photogrammetric methodology based on Agisoft Metashape software. The results obtained demonstrate that the proposed system satisfies (in each case) the tolerances of 'level 1' (51 mm) and 'level 2' (13 mm) for point cloud acquisition in urban design and historic documentation, according to the BIM Guide for 3D Imaging (U.S. General Services).

Keywords: self-assembly device; 3D point clouds; accuracy analysis; VSLAM-photogrammetric algorithm; portable mobile mapping system; low-cost device; BIM

1. Introduction

The tridimensional modeling of an object starts with its original design or with the process of acquiring the data necessary for its geometric reconstruction. In both cases, the result is a 3D virtual model that can be visualized and analyzed interactively on a computer [1,2]. In many cases, the process continues with the materialization of the model in the form of a prototype, which serves as a sample of what will be the final product, allowing us to check if its design is correct, thus changing the traditional manufacturing or construction industry [3–5].

The applications of 3D models (virtual or prototype) are numerous and widely used; they are usually used in the scope of clinical applications [6,7], geosciences [8–13], cultural heritage preservation [14,15] and engineering [16].

In this context, to address this wide variety of application areas, both data capture techniques and devices, as well as the specific software for data processing and management tend to be simplified. This is done in order to be accessible to the greatest number of users, even with limited knowledge in 3D measurement technologies.

In this sense, the classical methods of photogrammetry are combined with new techniques and procedures which are usually adopted for other areas [17], such as visual odometry (VO), the simultaneous localization and mapping (SLAM) and the visual slam (VSLAM) techniques. These are normally used to solve localization and mapping problems in the areas of robotics and autonomous systems [18–21], but also the combination of photogrammetry techniques with methodologies based on instruments like terrestrial or aerial laser scanners have obtained successful results [22,23].

These combined methods provide support and analytical robustness for the development of low/middle-cost capture systems, usually based on tablets or mobile devices that incorporate inertial sensors, absolute positioning and low cost cameras which can achieve medium 3D positional accuracy scanning, in compliance with technical requirements of a wide range of applications at a low cost and reduced learning curve [24–28]. As a result, handheld mobile mapping systems have appeared in recent years, using different technologies to perform 3D reconstructions that use fully automated processes [27,28]. Among which we can find systems based exclusively on images, requiring a fully automated process, taking into account the usual technical constraints in photogrammetry, and the free user movements in data capture [17]. In this field, different lines of research have been developed, depending on whether the final result is obtained in real time [29,30] or not. In the first case, the reduction in the time needed for data processing is the most important factor in the approach to research objectives (even at the expense of a metric accuracy reduction); in the second, however, metric accuracy is the most important factor, although the temporal cost is higher [17,31,32].

There are many commercial mobile mapping systems for urban, architectural or archaeological applications with high accuracy results [33]. Those systems are based on the integration on different sensors such as (Inertial Measurement Unit) IMU, line scanners [28], cameras, Global Navigation Satellite System (GNSS) [34], odometers and other sensors. The price and complexity of those systems are normally high [35].

The classical applications require a known level of data accuracy and quality, however, the emerging needs of Industry 4.0, building information modeling (BIM) or digital transformation, next to the appearance of new devices and information processing techniques pose new challenges and research opportunities in this field. Each capture method has its advantages and drawbacks, offering a particular level of quality in its results; in this sense, numerous investigations have linked these parameters, allowing people to choose the most cost-effective approach [35]. This can be achieved by way of evaluating the use of the laser scanner and the vision-based reconstruction among different solutions for progress monitoring inspection in construction and concluding (among other characteristics) that both of them are appropriate for spatial data capture. This could [36] include among 3D sensing technologies, photo/video-grammetry, laser scanning and the range of images that make a detailed assessment of the content (low, medium or high) into BIM working environments. It may also include [37] comparing photo/video-grammetry capture techniques with laser scanning, considering aspects such as accuracy, quality, time efficiency and cost needed for collecting data on site. The combination of data capture methods has also been traditionally analyzed; thus, [38] presently, there is a combined laser scanning/photogrammetry approach to optimize data collection, cutting around 75% of the time required to scan the construction site.

A common aspect, taken into account in most of the research, is the point cloud accuracy evaluation, that has been addressed in three different ways [39]: (a) By defining levels of quality parameters defined in national standards and guidelines that come from countries like the United States, Canada, the United Kingdom and Scandinavian countries that lead BIM implementation in the world [40], such as the U.S. General Services Administration (GSA) BIM Guide for 3D Imaging [41] that sets the quality requirements of point clouds in terms of their level of accuracy (LOA) and level of detail (LOD); (b) by evaluating quality parameters of a point cloud, in terms of accuracy and completeness [37] or (c) following three quality criteria: Reference system accuracy, positional accuracy and completeness [42].

Furthermore, in the specific environment of 3D indoor models, [43] we propose a method that provides suitable criteria for the quantitative evaluation of geometric quality in terms of completeness, correctness, and accuracy by defining parameters to optimize a scanning plan in order to minimize data collection time while ensuring that the desired level of quality is satisfied, in some cases, with the implementation of an analytical sensor model that uses a "divide and conquer" strategy based on segmentation of the scene [44], or one that captures the relationships between parameters like data collection parameters and data quality metrics [45]. In other cases, the influence of scan geometry is considered in order to optimize measurement setups [46], or are compared to different known methods for obtaining accurate 3D modeling applications, like in the work of [47], in the context of cultural heritage documentation.

This paper extends on past surveys of classical photogrammetry solutions, adopting an extended solution approach for outdoor environments based on the use of a simple and hand-held self-assembly device for data capture, based on images, that consist on two cameras: One, which data will be used to calculate in real time, the path followed by the device using a VSALM algorithm, while with other one; a high-resolution video recorded and used to achieve the scene reconstruction using photogrammetric techniques. Finally, after following simple data collection and fully automated processing, a 3D point cloud with associated color is obtained.

To determine the effectiveness of the proposed system, we evaluate it in one study site performed outdoors in the facades of the Roman Aqueduct of Miracles, in terms of the requirements laid down in the GSA BIM Guide for 3D Imaging. In this experiment, we obtain 3D point clouds from different data capture conditions, that vary according to the distance from the device and the monument; the measurements acquired by a total station serve to compare the coordinates of fixed points in both systems, and therefore, determining the LOA of each point cloud. The results obtained, with root mean square errors (RMSEs) between eight and 33 mm, stress the feasibility of the proposed system for urban design and historic documentation projects, in the context of allowable dimensional deviations in BIM and CAD deliverables.

This paper is divided into four sections. Following the Introduction, the portable mobile mapping system is described, including the proposed algorithm schema for the computations; therefore, a case study in which the system is applied is described in Section 2. The results are presented in Section 3 and finally, the conclusions are presented in Section 4.

2. Materials and Methods

This study was conducted with a simple and self-assembly prototype specifically built for data capture (Figure 1), that consists of two cameras from the Imaging Source Europe GmbH company (Bremen, Germany): Camera A (model DFK 42AUC03) and camera B (model DFK 33UX264) were fixed to a platform with the condition of its optical axes being parallel; each camera incorporated a lens; for camera A, the model was TIS-TBL 2.1 C, from the Imaging Source Europe GmbH company and for camera B, the model was the Fujinon HF6XA–5M, from FUJIFILM Corporation (Tokyo, Japan). The technical characteristics of cameras and lenses appear in Tables 1 and 2, respectively. Both cameras were connected to a laptop (with an Intel core i7 7700 HQ CPU processor and RAM of 16 Gb, running under Windows 10 Home), via

USB 2.0 (camera A) and 3.0 (camera B). This beta version of the prototype had an estimated base price under €2500.

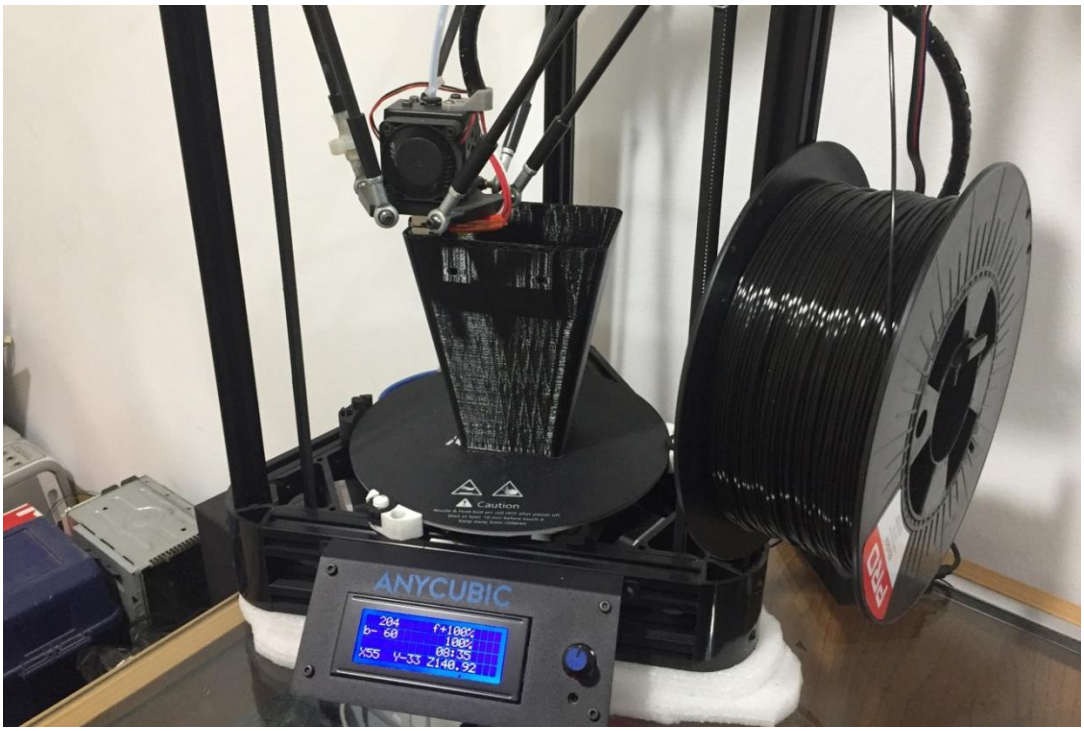

(**a**)

(**b**)

(**c**)

Figure 1. (**a**) 3D printing process of the prototype case; (**b**) cameras A and B with their placement inside the case; and (**c**) the final portable mobile mapping system prototype.

Table 1. Main technical characteristics of cameras used in the prototype (from the Imaging Source Europe GmbH company).

Model	Resolution (Pixels)	Megapixels	Pixel Size (µm)	Frame Rate (fps)	Sensor	Sensor Size	A/D (bit)
DFK 42AUC03	1280 × 960	1.2	3.75	25	Aptina MT9M021 C	1/3”CMOS	8
DFK 33UX264	2448 × 2048	5	3.45	”8	Sony IMX264	2/3” CMOS	8/12

Table 2. Main technical data of lenses used in the prototype (from the Imaging Source Europe GmbH company and FUJIFILM Corporation).

Model	Focal Length (mm)	Iris Range	Angle of view (H × V)
TIS-TBL 2.1 C	2.1	2	97° × 81.2°
Fujinon HF6XA–5M	6	1.9–16	74.7° × 58.1°

The calibration process of the cameras was carried out with a checkerboard target (60 cm × 60 cm) using a complete single camera calibration method [48], that provided the main internal calibration parameters: The focal length, radial and tangential distortions, optical center coordinates and camera axe skews. In addition, to know the parameters that related to the position of one camera compared to the other, we designed the following, practical test: To use as ground control points we placed 15 targets on two perpendicular walls and measured the coordinates of each target with a TOPCON Robotic total station, with an accuracy of 1" measuring angles (ISO 17123-3:2001) and 1.5 mm + 2 ppm measuring distances (ISO 17123-4:2001). After running the observations with the prototype, we used a seven-parameter transformation, using the 15 targets, to determine the relative position of one camera in relation to the other [17].

Camera A and camera B had different configuration parameters which defined image properties such as brightness, gain or exposure between others. In order to automate the capture procedure, automatic parameters options had been chosen. In such a way, the data collection was automatic and the user didn't need to follow specials rules since the system accepted convergent or divergent turns of the camera, stops or changes in speed. The algorithm processed all this data properly using the proposed methodology.

During the capture (Figure 2), the user needed to see the VSLAM tracking in the screen of the computer in real time. In this way, the user was sure he didn´t make a fast movement or if an item appeared that interrupted camera visualization and, therefore, the tracking could not continue. In this case, the user must return again to a known place and continue the tracking from this point.

Figure 2. In-field data capture. The white arrow indicates the user direction movement, parallel to the monument façade, followed during this test.

Workflow of the Proposed Algorithm for the Computation

The application of the VSLAM technique on a low weight device, normally with limited calculation capabilities, needed the implementation of a low computational cost VSLAM algorithm to achieve effective results. The technical literature provided a framework that consisted of the following basic modules: The initialization module; to define a global coordinate system, and the tracking and mapping modules; to continuously estimate camera poses. In addition, two additional modules were used for a more reliable and accurate result: The re-localization module, that has to be used when, due to a fast device motion or some disruptions in data capture, the camera pose must be computed again and the global map optimization, which is performed to estimate and remove accumulative errors in the map, produced during camera movements.

The characteristics of the VSLAM-photogrammetric algorithm, including identified strong and weak points, depend on the methodology used for each module which sets its advantages and limitations. In our case, we proposed the following sequential workflow (Figure 3) divided into four threaded processes, which have been implemented in C++.

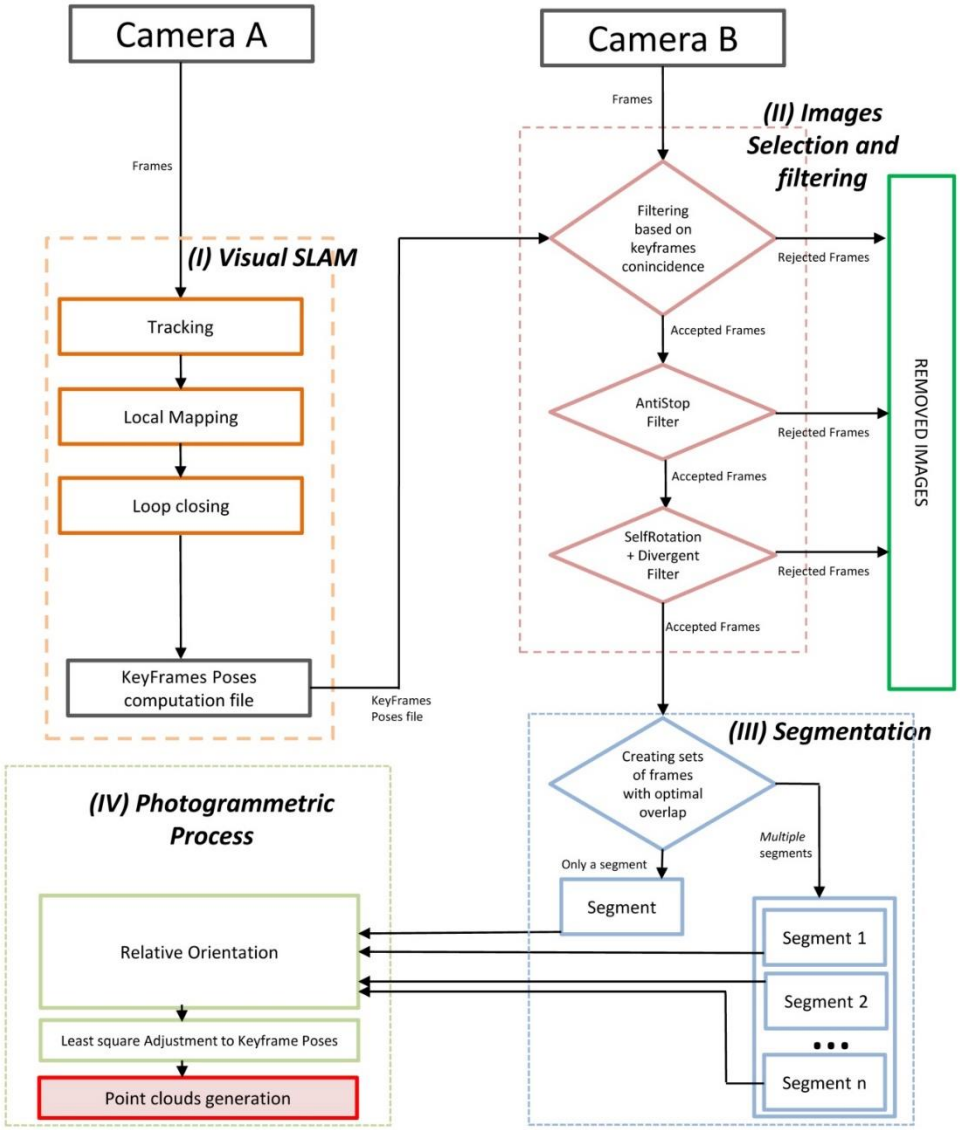

Figure 3. General workflow of the algorithm implemented in C++ for the computations.

Basically, the four processes consisted in the following: (I) A VSLAM algorithm to estimate both motion and structure, that is applied in frames obtained from camera A, (II) an image selection and filtering process of frames obtained with camera B, (III) the application of an image segmentation algorithm and finally, (IV) a classical photogrammetric process applied to obtain the 3D point cloud. Each process is explained in more detail below.

The first process (I) started with the simultaneous acquisition of videos with cameras A and B, with speeds of 25 FPS and 4 FPS, respectively. With the frames from camera A, used as an ORB descriptor [49] for object recognition, detection and matching was used. This descriptor built on the FAST key-point detector and the BRIEF descriptor, with good performance and low cost, and therefore, was appropriate for our case. An ORB-SLAM algorithm was then applied to estimate camera positioning and trajectory calculation [50]; this was an accurate monocular SLAM system that worked in real time and can be applied in indoor/outdoor scenarios, and has modules to loop closure detection, re-localization (to recover from situations where the system becomes lost) and to a totally automatic initialization, taking into account the calibration parameters of the camera. From these remarks, our process was carried out in three steps as follows [50]. The first step was the tracking, which calculated the positioning of the camera for

each frame and selected keyframes and decided which frames were added to the list; the second one was local mapping, which performed keyframes optimization, incorporating those that were being taken and removing the redundant keyframes. With these data, through a local bundle adjustment, in addition to increasing the quality of the final map, it was possible to reduce the computational complexity of the processes that were just running, and equally for the subsequent steps. The third one was loop closing, which looked for redundant areas where the camera had already passed before, which could be found in each new keyframe; the transformation of similarity on the accumulated drift in the loop was calculated, the two ends of the loop were aligned [50], the duplicate points were merged and the trajectory was recalculated and optimized to achieve overall consistency. The result of this process was a text file with UNIX time parameters and camera poses of the selected keyframes.

The above information together with the frames recorded by camera B, was used to start the second process (II), in which a selection and filtering of the images obtained by camera B was carried out, which consisted in the direct deletion of images whose baseline was very small, and therefore, which made it difficult to compute an optimum relative orientation [17,51,52]. The filtering process was performed in three consecutive steps: The first, a filtering based on keyframes coincidence, which consisted of incorporating a β number of frames (in our case β = 2) from camera B between each two consecutive frames from camera A and, at the same time, the remaining frames were removed. To run this filter, it was necessary that the cameras were synchronized by UNIX time. The second process, applied the so-called AntiStop filter, which removed those frames obtained in the event that the camera had been in a static position, or with a very small movement, recorded images of the same zone, which we described as redundant and which should, therefore, be eliminated. To determine the redundant frames, it was assumed that cameras A and B were synchronized and that we knew the coordinates of the projection center of each frame, computed in (I). We continued with the calculation of the distances between the projection centers of every two consecutive keyframes i and j (D_{ij}) as well as the mean value of all the distances between consecutive frames (D_m) and the definition of the minimum distance (D_{min}) from which the device was either stopped or was in motion, by the expression:

$$D_{min} = D_m * p,$$

where p is a parameter that depends on the data capture conditions (in our case, after performing several tests, we defined a value of p = 0.7). Finally, the keyframes took by camera B in which the distance between the projection centers of each two consecutive keyframes was less than the minimum distance ($D_{ij} < D_{\min}$) were removed.

The third, called the divergent self-rotation filter, was able to remove those keyframes captured by camera B when they met two conditions: The rotation angles of the camera ω_i (X axis) and κ_i (Z axis) (Figure 4) increase or decrease their value permanently during data capture for of at least three consecutive frames at a value of ±9° (in our case), and besides, their projection centers were very close to each other; for the calculation of the same procedure is the same one used as the one used for the AntiStop filter, but with a different value of p (in our case, we considered a value of p = 0.9).

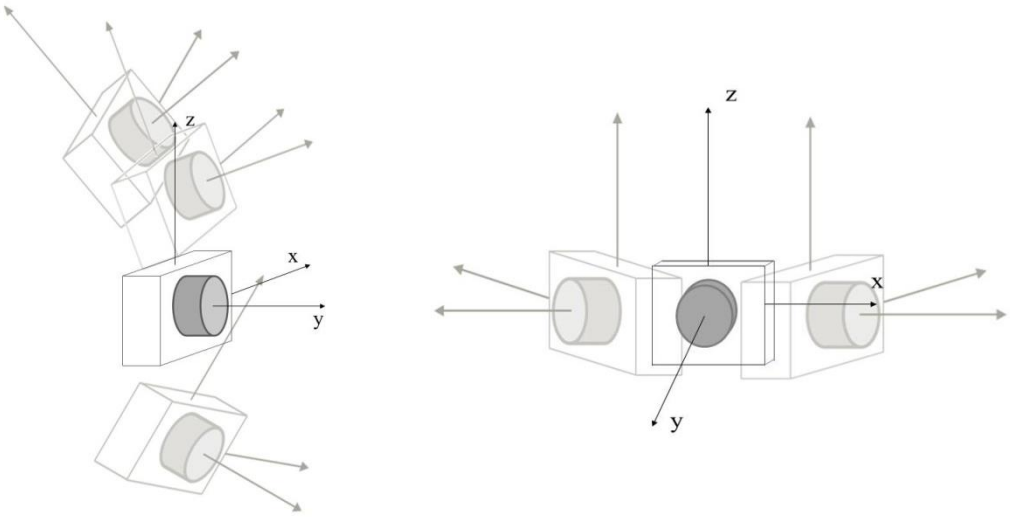

(**a**) (**b**)

Figure 4. Divergent self-rotation in the (**a**) *X*-axis; and (**b**) *Z*-axis.

The next process (III) was segmentation, which aimed to obtain more significant and easy to analyze images in the subsequent photogrammetric process. It started searching for the homologous points belonging to the keyframes resulting from the filtering process carried out in (II) [53–55], which was performed between an image, the earlier one and the later one. The resulting images were stored in a set, called a "segment". The result of this process generated one or more independent segments among themselves, which had a number of homologous points and an appropriate distribution to be properly oriented (in our case, 200 points and 10% of these points were in each quadrant of the image; in addition, if the segment did not have at least three images, it was discarded and its images were removed).

The last process (IV) was called the photogrammetric process, which was structured in three steps: The first was to compute a relative image orientation [53] setting the first image as the origin of the relative reference system and used the homologous points of each segment and algorithms leading to direct solutions [17,51,53]; then, a bundle adjustment) was used on the oriented images to avoid divergences [56], obtaining the coordinates of the camera poses and computed tie points. The second step consisted of an adjustment of the camera poses in each segment to adapt them to the overall trajectory, computed in (I). This procedure was performed using minimum square techniques [57] in each segment, and a three-dimensional transformation [10] to correct the positions of camera B with respect to camera A.

In the third step, the scene was reconstructed using MICMAC software [54], in order to obtain dense cloud points with color. MICMAC is a free open-source photogrammetry software developed by the French National Mapping Agency (IGN) and the National School of Geographic Sciences (ENSG) [58]. This software generates a depth map from the main image and a series of secondary images to obtain parallax values. The calculation was carried out having taken into account that the scene could be described by a single function $Z = f(X; Y)$ (with X; Y; Z using Euclidean coordinates) with several parameters of MICMAC to calculate the density correlation and obtain the cloud of dense points with color [54,55,59] which was the final result of the process.

3. Accuracy Assessment and Results

This work determined the accuracy of a set of point clouds obtained with the prototype in order to validate the device for BIM work environments. Additionally, the results were compared with a usual photogrammetric procedure, using a reflex camera and photogrammetric software (Agisoft Metashape [60]), in order to compare the advantages and disadvantages of the proposed prototype in respect to this known methodology. For this, an experimental test was carried out in the Roman aqueduct of "The Miracles" in the city of Mérida (Spain). This monument, built in the first-century A.C, has a total dimension of 12 km in length between underground and aerial sections with arches. The test was carried out on an archery stretch which was 23 m high and 60 m wide, performing a set of three data capture scenarios at different observation distances (5, 12, and 20 m) from the prototype to the base of the monument (Figure 5).

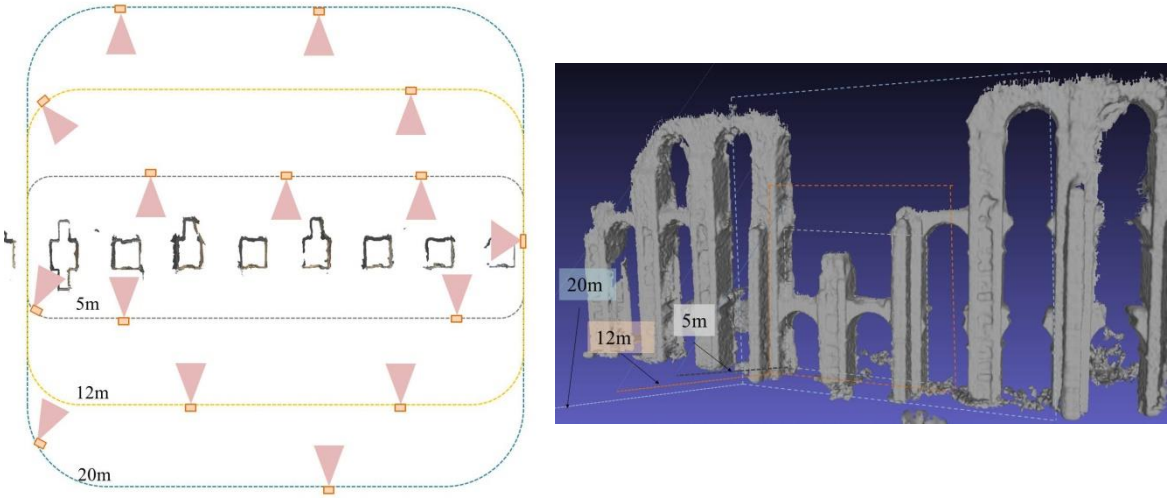

(**a**) (**b**)

Figure 5. (**a**) Scheme with the data capture trajectories and (**b**) the areas covered by a frame, for 5, 12 and 20 m of distance prototype-monument. The figure that appears in (**b**), is a 3D model (mesh) generated by the software Meshlab [61] from the 20m points cloud made only for visualization purposes.

In this test, the data collection was carried out in such a way that the movement of the user followed a perpendicular direction to the camera optical axe (Figure 2), avoiding divergent turns since this kind of movement was not necessary in this case. In this way, this prevented the algorithm from using the divergent self-rotation filter in an unnecessary situation.

In order to evaluate the metric quality of the measures obtained with the prototype and the Agisoft Metashape photogrammetric procedure, a control network was performed to be used in the dimensional control study, following the procedures carried out by [62] and [63]. The network was used as reference points and consisted on a set of targets and natural targets whose three-dimensional coordinates in a local coordinate system were obtained by a second measuring instrument (more precise than the device we want to evaluate). In this case, a total station Pentax V-227N (Pentax Ricoh Imaging Company, Ltd, Tokyo, Japan) was used, with an accuracy of 7′ for angular measurements (ISO 17123-3:2001) and 3 mm ± 2 ppm for distance measurements (ISO 17123-3:2001) with which a total of 40 uniformly distributed targets have been measured (Figure 6).

Then, the method proposed by [62] was used, in which the accuracy of the 3D point cloud was quantified according to the Euclidean average distance error (δ_{avg}) as:

$$\delta_{avg} = \frac{1}{n}\sum_{i=1}^{n} | Ra_i - T - b_i | \quad (1)$$

where a_i is the ith checkpoint measured by the prototype, b_i is the corresponding reference point acquired by the total station, R and T are the rotation and translation parameters for 3D Helmert transformation.

And the quality of the 3D point cloud was also evaluated by the root mean square error (RMSE) as:

$$RMSE = \sqrt{\frac{1}{n}\sum_{i=1}^{n}(a_i^t - b_i)^2} \quad (2)$$

where a_i^t indicates the a_i point after the 3D conformal transformation to bring the model coordinates in the same system of the reference points.

(**a**) (**b**)

(**c**) (**d**)

Figure 6. (**a**,**c**) Reference points spread on the two fronts of the monument. (**b**) Target model used in the test and (**d**) total station Pentax V-227N used to measure the network coordinates.

As mentioned previously in Section 1 of this paper, the point cloud accuracy evaluation can be done according to different criteria. In our case, we have used the GSA BIM Guide for 3D Imaging criteria, that defines four levels of detail (LOD) with dimensions of the smallest recognizable feature ranging between 13 mm × 13 mm to 152 mm × 152 mm; and also defines the level of accuracy (LOA) associated to each LOD, ranging between three and 51 mm of tolerance, considering it as the allowable dimensional deviation in the deliverable from truth (that has been obtained by some more precise other means). In the case of a point cloud, the guide specifies that the distance between two points from the model must be compared to the true distance between the same two points, and be less than or equal to the specified tolerance; the guide also defines the area of interest as a hierarchical system of scale in which each scan is registered, depending on the LOD. In Table 3, we summarize the data quality parameters defined by the GSA for registering point clouds.

Table 3. Data quality parameters defined by U.S. General Services Administration (GSA) for registering point clouds. (Unit: Millimeters).

Level of Detail (LOD)	Level of Accuracy (LOA, Tolerance)	Resolution	Areas of Interest (Coordinate Frame, c. f.)
Level 1	±51	152 × 152	Total Project area (Local or State c. f.)
Level 2	±13	25 × 25	e.g., building (local or project c. f.)
Level 3	±6	13 × 13	e.g., floor level (project or instrument c. f.)
Level 4	±3	13 × 13	e.g., room or artifact (instrument c. f.)

In order to complete the study, other photogrammetric system was analyzed under conditions similar to the prototype (Figure 7). The camera used was a Canon EOS 1300D and the lens was an EFS 18–55mm, but we only used the focal length of 18mm for this experiment. Multiple images were taken in this experiment for each distance (35 images for 5 m, 41 images for 12 m and 43 images for 20 m) and the camera was configured with a resolution of 2592 pixels × 1728 pixels with the aim of comparing the results in an equitable way with the proposed approach which have a similar image resolution. The reflex camera´s parameters (shutter, diaphragm, ISO, etc.) were chosen in automatic mode during the test to match the conditions to the prototype test. The pictures were taken standing on the same trajectories previously followed by the prototype, at the same distances from the aqueduct: 5, 12 and 20 m. These circumstances increase the time consumed in the field during the data capture, as can be seen in the Table 4, because the user must focus each image and ensure that the picture has been taken with enough overlap and quality. On the other hand, the prototype cameras also have a configuration with automatic parameters which allowed the user, along with the methodology used, to make a continuous capture, without stopping to take the images. The images of the Canon camera were processed using the software Agisoft Metashape 1.5.4 [60] which is commercialized by the company Agisoft LLC, sited in St. Petersburg, Russia (Figure 8).

Point cloud density for each system was measured. Two points clouds, one for each system, were processed using the same 10 images of the aqueduct at a distance of 5 m. The density [37] of the point cloud was 328 points/dm^2 for the proposed prototype system and 332 points/dm^2 for the Agisoft Metashape photogrammetric software.

Table 4. Comparison between the proposed approach and the camera with Agisoft Metashape software in regards to the time spent in the field for data capture and processing time using the same laptop (Intel core i7 7700 HQ CPU processor, 16Gb RAM, Operative System Windows 10 Home). Distance values are measured from the camera to the monument.

System	Data Capture Distance (m)	Data Capture Time (min)	Processing Time (min)
Prototype and Visual Slam (VSLAM)-Photogrammetric Algorithm	5	4.25	80
	12	4.53	85
	20	4.65	99
Canon Camera and Agisoft Metashape Software	5	7.83	72
	12	9.08	80
	20	9.50	89

With the prototype and VSLAM-Photogrammetric algorithm we have computed the average error and the RMSE in each direction (x, y, and z) of each data capture distance, that are listed in Table 5, with overall accuracies of 12, 26 and 46 mm for 5, 12 and 20 m respectively and the RMSEs on each axis ranging between 5 to 8 mm (5 m), 10 to 21 mm (12 m) and 30 to 38 mm (20 m) (Figure 7) which satisfied the error tolerance of 'level 1' (51 mm) for data capture distances from 12–20 m and 'level 2' (13 mm) for data capture distances about 5 m.

Table 5. This table compares the accuracy assessment results with the root mean square errors (RMSEs) and average errors for data capture distances from 5 to 20 m from the camera to the monument, between the prototype and VSLAM-photogrammetric algorithm and the Canon camera with Agisoft Metashape software. The RMSE error values have been computed in the three vector components: *X*, *Y* and *Z*.

	Methodology							
	Prototype and VSLAM-Photogrammetric Algorithm				**Canon Camera and Agisoft Metashape Software**			
Distance 5 m								
	Error Vector *X* (mm)	**Error Vector *Y* (mm)**	**Error Vector *Z* (mm)**	**Error (mm)**	**Error Vector *X* (mm)**	**Error Vector *Y* (mm)**	**Error Vector *Z* (mm)**	**Error (mm)**
Average Error				12				11
RMSE	5	8	8	8	4	9	8	12
Distance 12 m								
AVERAGE Error				26				23
RMSE	21	16	10	16	12	18	17	28
Distance 20 m								
Average Error				46				35
RMSE	32	30	38	33	18	24	24	39

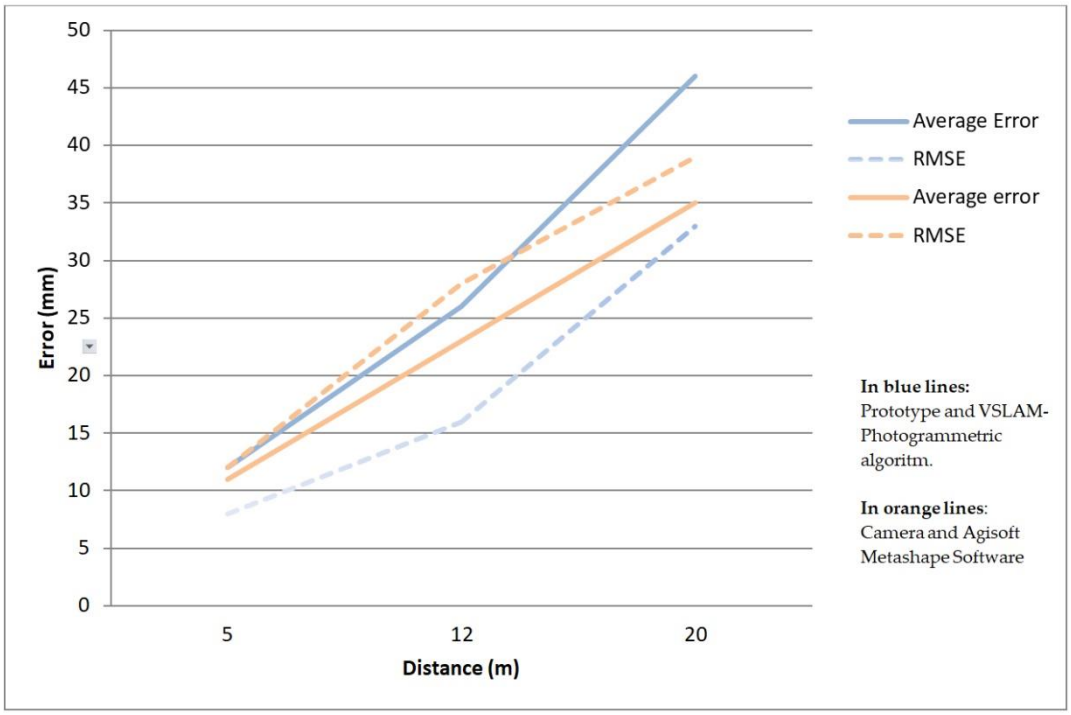

Figure 7. Graphic on the evolution of the average errors and RMSEs for the distances of 5, 12 and 20m from the camera to the monument. The results are shown for both systems: Prototype and VSLAM-photogrammetric algorithm and Canon camera with Agisoft Metashape software.

Figure 8. Comparison between points clouds resulting from both systems (with a data capture distance of 12 m): (**a**) Prototype and VSLAM-photogrammetric algorithm; and (**b**) Canon camera EOS 1300D with Agisoft Metashape software.

The point clouds obtained at the different distances of observation shown in Figure 9. Small holes or missing parts can be seen in those points clouds. This occurs due to the camera's trajectory, since it needs to focus directly on all the desired areas and capture a minimum number of images to perform optimal triangulation. No filter has been applied in the results shown in Figure 9.

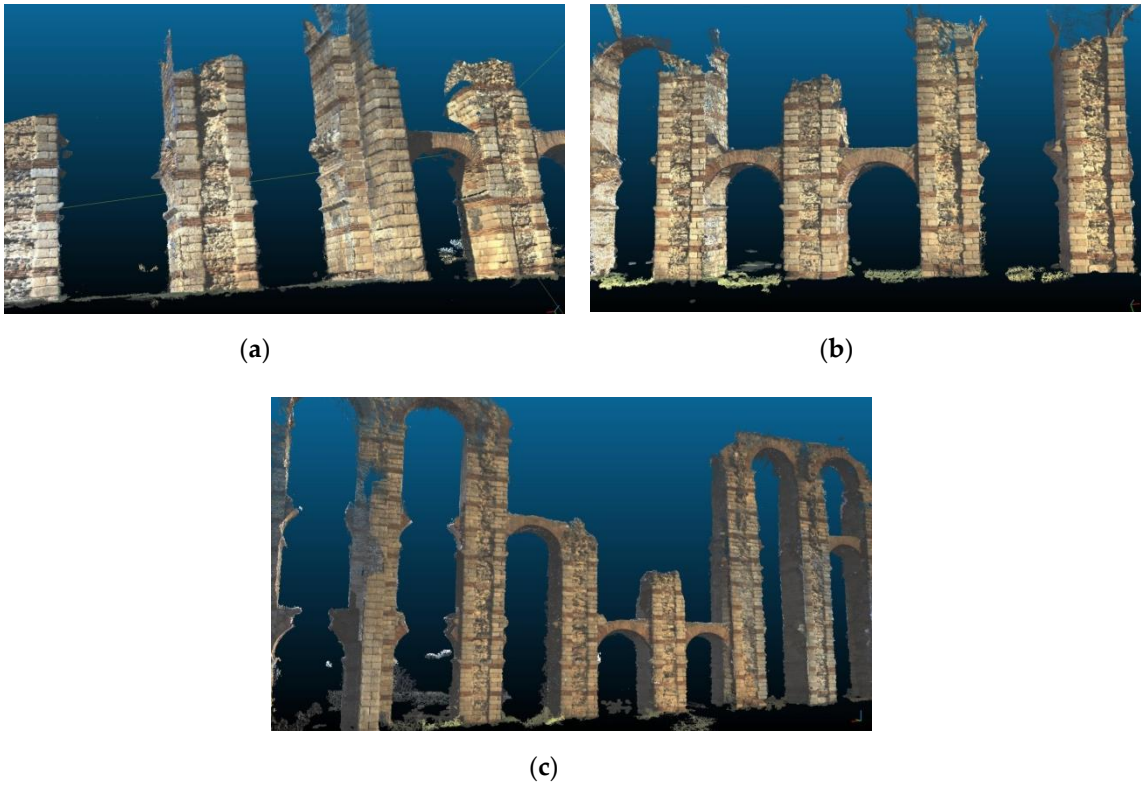

(**a**) (**b**)

(**c**)

Figure 9. Points clouds resulted at the distances established in the experimental test: (**a**) 5 m; (**b**) 12 m; and (**c**) 20 m. The images show the central part of the color points clouds that resulted from the test. The points clouds have not been filtered or edited.

4. Conclusions

The major innovations of this study are as follows: First, the proposed approach for the 3D data capture and the implementation of the VSLAM-photogrammetric algorithm has been materialized in a functional and low-cost prototype, which has been checked in an experimental test, the results of which have been presented in the context of the BIM work environment.

Second, the results obtained in the experimental test comply with the precision requirements of the GSA BIM Guide for 3D Imaging for point cloud capture work with a resolution (minimum artifact size) of 152 mm × 152 mm, for observation distances of approximately 20 m. For distances between 5 and 12 m, we saw that better accuracies and resolution results were achieved.

Third, the possibility of using the instrument at different distances facilitates the data capture in shaded areas or areas with difficult access. This, together with the fact that the device has been designed for outdoor data collection, makes it suitable for urban design and historic documentation, which are usually carried out in outdoor environments, registering information for plans, sections, elevations and details and 3D point cloud in PLY format (positioning: x, y, z and color: R, G, B), following the GSA PBS(Public Building Service) CAD standards (2012) and the GSA BIM Guide for 3D Imaging Standards.

In order to increase the knowledge of the proposed approach, it has been compared with a well-known photogrammetric methodology consisting of a Reflex Canon 1300D camera and the

software Agisoft Metashape. The results of the comparison test have provided interesting conclusions:

1. The accuracy results of both methods are similar as can be seen in Table 5. Although the average error is slightly higher in the proposed approach, the RMSE is a bit lower than with the Agisoft Metashape methodology. This indicates a small, but greater dispersion of the points of the proposed approach in respect to the Agisoft software. But as can be seen in the results, this factor does not imply an increase of RMSE, but this error is slightly less in the proposed approach in relation to Agisoft software.
2. The processing time was a bit higher in the proposed approach for the distances of 5 and 12 m but not for 20 m, for which the time was slightly less. The differences are not significant, in our opinion, and indicate that the proposed method optimizes the number of images extracted and the photogrammetric process, thus equating well-known procedures such as the use of a Reflex camera and the Agisoft Metashape software.
3. In our opinion, the greatest improvement occurred in the data capture field. The user does not worry about how to use the camera or where to take the picture, because in the proposed approach, the capture is continuous and the system chooses the images automatically, as is explained in Section 2. In this way, the learning curve changes significantly, provided the user doesn´t need to have previous knowledge about photography or photogrammetry. For this reason, the proposed approach here described, reduces significantly the time spent in the field, as can be seen in Table 4.

A new handheld mobile mapping system based on images have been presented in this paper. This proposed methodology does not adversely affect the known photogrammetric process (accuracy, processing time, point cloud density) but it proposes a new, easier and faster way to capture the data in the field, based on continuous data capture and fully automatic processing, without human intervention in any phase.

Author Contributions: Conceptualization, P.O.-C.; data curation, P.O.-C. and A.S.-R.; formal analysis, A.S.-R.; investigation, P.O.-C.; methodology, P.O.-C.; resources, P.O.-C.; software, P.O.-C.; supervision, A.S.-R.; validation, A.S.-R.; writing—original draft, P.O.-C.; writing—review, A.S.-R.

Funding: This research received no external funding.

Acknowledgments: We are grateful to the "Consorcio de la Ciudad Monumental de Mérida" for allowing the work in this monument.

Conflicts of Interest: The authors declare no conflicts of interest.

References

1. Remondino, F.; El-Hakim, S. Image-Based 3D Modelling: A Review. *Photogramm. Rec.* **2006**, *21*, 269–291, doi:10.1111/j.1477-9730.2006.00383.x.
2. Raza, K.; Khan, T.A.; Abbas, N. Kinematic Analysis and Geometrical Improvement of an Industrial Robotic Arm. *J. King Saud Univ. Eng. Sci.* **2018**, *30*, 218–223, doi:10.1016/j.jksues.2018.03.005.
3. Rayna, T.; Striukova, L. From Rapid Prototyping to Home Fabrication: How 3D Printing Is Changing Business Model Innovation. *Technol. Soc. Chang.* **2016**, *102*, 214–224, doi:10.1016/j.techfore.2015.07.023.
4. Wu, P.; Wang, J.; Wang, X. A Critical Review of the Use of 3-D Printing in the Construction Industry. *Autom. Constr.* **2016**, *68*, 21–31, doi:10.1016/j.autcon.2016.04.005.
5. Tay, Y.W.D.; Panda, B.; Paul, S.C.; Mohamed, N.A.N.; Tan, M.J.; Leong, K.F. 3D Printing Trends in Building and Construction Industry: A Review. *Virtual Phys. Prototyp.* **2017**, *12*, 261–276, doi:10.1080/17452759.2017.1326724.
6. Yan, Q.; Dong, H.; Su, J.; Han, J.; Song, B.; Wei, Q.; Shi, Y. A Review of 3D Printing Technology for Medical Applications. *Engineering* **2018**, *4*, 729–742, doi:10.1016/j.eng.2018.07.021.
7. Moruno, L.; Rodríguez Salgado, D.; Sánchez-Ríos, A.; González, A.G. An Ergonomic Customized-Tool Handle Design for Precision Tools Using Additive Manufacturing: A Case Study. *Appl. Sci.* **2018**, *8*, doi:10.3390/app8071200.

8. Liang, X.; Wang, Y.; Jaakkola, A.; Kukko, A.; Kaartinen, H.; Hyyppä, J.; Honkavaara, E.; Liu, J. Forest Data Collection Using Terrestrial Image-Based Point Clouds from a Handheld Camera Compared to Terrestrial and Personal Laser Scanning. *IEEE Trans. Geosci. Remote Sens.* **2015**, *53*, doi:10.1109/TGRS.2015.2417316.
9. Behmann, J.; Mahlein, A.-K.; Paulus, S.; Kuhlmann, H.; Oerke, E.-C.; Plümer, L. Calibration of Hyperspectral Close-Range Pushbroom Cameras for Plant Phenotyping. *ISPRS J. Photogramm. Remote Sens.* **2015**, *106*, 172–182, doi:10.1016/j.isprsjprs.2015.05.010.
10. Abellán, A.; Oppikofer, T.; Jaboyedoff, M.; Rosser, N.J.; Lim, M.; Lato, M.J. Terrestrial Laser Scanning of Rock Slope Instabilities. *Earth Surf. Process. Landf.* **2014**, *39*, 80–97, doi:10.1002/esp.3493.
11. Ghuffar, S.; Székely, B.; Roncat, A.; Pfeifer, N. Landslide Displacement Monitoring Using 3D Range Flow on Airborne and Terrestrial LiDAR Data. *Remote Sens.* **2013**, *5*, 2720–2745, doi:10.3390/rs5062720.
12. Lotsari, E.; Wang, Y.; Kaartinen, H.; Jaakkola, A.; Kukko, A.; Vaaja, M.; Hyyppä, H.; Hyyppä, J.; Alho, P. Gravel Transport by Ice in a Subarctic River from Accurate Laser Scanning. *Geomorphology* **2015**, *246*, 113–122, doi:10.1016/j.geomorph.2015.06.009.
13. Harpold, A.; Marshall, J.; Lyon, S.; Barnhart, T.; Fisher, A.B.; Donovan, M.; Brubaker, K.; Crosby, C.; Glenn, F.N.; Glennie, C.; et al. Laser Vision: Lidar as a Transformative Tool to Advance Critical Zone Science. *Hydrol. Earth Syst. Sci.* **2015**, *19*, 2881–2897 doi:10.5194/hess-19-2881-2015.
14. Cacciari, I.; Nieri, P.; Siano, S. 3D Digital Microscopy for Characterizing Punchworks on Medieval Panel Paintings. *J. Comput. Cult. Herit.* **2014**, *7*, 19, doi:10.1145/2594443.
15. Jaklič, A.; Erič, M.; Mihajlović, I.; Stopinšek, Ž.; Solina, F. Volumetric Models from 3D Point Clouds: The Case Study of Sarcophagi Cargo from a 2nd/3rd Century AD Roman Shipwreck near Sutivan on Island Brač, Croatia. *J. Archaeol. Sci.* **2015**, *62*, 143–152, doi:10.1016/j.jas.2015.08.007.
16. Camburn, B.; Viswanathan, V.; Linsey, J.; Anderson, D.; Jensen, D.; Crawford, R.; Otto, K.; Wood, K. Design Prototyping Methods: State of the Art in Strategies, Techniques, and Guidelines. *Des. Sci.* **2017**, *3*, 1–33, doi:10.1017/dsj.2017.10.
17. Luhmann, T.; Robson, S.; Kyle, S.; Harley, I. Close Range Photogrammetry: Principles, Techniques and Applications; Whittles Publishing: Dunbeath, UK, 2006.
18. Ciarfuglia, T.A.; Costante, G.; Valigi, P.; Ricci, E. Evaluation of Non-Geometric Methods for Visual Odometry. *Robot. Auton. Syst.* **2014**, *62*, 1717–1730, doi:10.1016/j.robot.2014.08.001.
19. Yousif, K.; Bab-Hadiashar, A.; Hoseinnezhad, R. An Overview to Visual Odometry and Visual SLAM: Applications to Mobile Robotics. *Intell. Ind. Syst.* **2015**, *1*, 289–311, doi:10.1007/s40903-015-0032-7.
20. Strobl, K.H.; Mair, E.; Bodenmüller, T.; Kielhöfer, S.; Wüsthoff, T.; Suppa, M. Portable 3-D Modeling Using Visual Pose Tracking. *Comput. Ind.* **2018**, *99*, 53–68, doi:10.1016/j.compind.2018.03.009.
21. Kim, P.; Chen, J.; Cho, Y. SLAM-Driven Robotic Mapping and Registration of 3D Point Clouds. *Autom. Constr.* **2018**, *89*, 38–48, doi:10.1016/j.autcon.2018.01.009.
22. Balsa-Barreiro, J.; Fritsch, D. Generation of Visually Aesthetic and Detailed 3D Models of Historical Cities by Using Laser Scanning and Digital Photogrammetry. *Digit. Appl. Archaeol. Cult. Herit.* **2018**, *8*, 57–64, doi:10.1016/j.daach.2017.12.001.
23. Balsa-Barreiro, J.; Fritsch, D. Generation of 3D/4D Photorealistic Building Models. The Testbed Area for 4D Cultural Heritage World Project: The Historical Center of Calw (Germany). In Proceedings of the International Symposium on Visual Computing, Las Vegas, NV, USA, 14–16 December 2015; pp. 361–372, doi:10.1007/978-3-319-27857-5_33.
24. Dupuis, J.; Paulus, S.; Behmann, J.; Plümer, L.; Kuhlmann, H. A Multi-Resolution Approach for an Automated Fusion of Different Low-Cost 3D Sensors. *Sensors* **2014**, *14*, 7563–7579, doi:10.3390/s140407563
25. Sirmacek, B.; Lindenbergh, R. Accuracy Assessment of Building Point Clouds Automatically Generated from Iphone Images. *ISPRS Int. Arch. Photogramm. Remote Sens. Spat. Inf. Sci.* **2014**, *45*, 547–552, doi:10.5194/isprsarchives-XL-5-547-2014.
26. Lachat, E.; Macher, H.; Landes, T.; Grussenmeyer, P. Assessment and Calibration of a RGB-D Camera (Kinect v2 Sensor) Towards a Potential Use for Close-Range 3D Modeling. *Remote Sens.* **2015**, *7*, 13070–13097, doi:10.3390/rs71013070.

27. Sánchez, A.; Gómez, J.M.; Jiménez, A.; González, A.G. Analysis of Uncertainty in a Middle-Cost Device for 3D Measurements in BIM Perspective. *Sensors* **2016**, *16*, 1557–1574, doi:10.3390/s16101557.
28. Zlot, R.; Bosse, M.; Greenop, K.; Jarzab, Z.; Juckes, E.; Roberts, J. Efficiently Capturing Large, Complex Cultural Heritage Sites with a Handheld Mobile 3D Laser Mapping System. *J. Cult. Herit.* **2014**, *15*, 670–678, doi:10.1016/j.culher.2013.11.009.
29. Pollefeys, M.; Nistér, D.; Frahm, J.-M.; Akbarzadeh, A.; Mordohai, P.; Clipp, B.; Engels, C.; Gallup, D.; Kim, S.-J.; Merrell, P.; et al. Detailed Real-Time Urban 3D Reconstruction from Video. *Int. J. Comput. Vis.* **2008**, *78*, 143–167, doi:10.1007/s11263-007-0086-4.
30. Zingoni, A.; Diani, M.; Corsini, G.; Masini, A. Real-Time 3D Reconstruction from Images Taken from an UAV. *ISPRS Int. Arch. Photogramm. Remote Sens. Spat. Inf. Sci.* **2015**, *40*, 313–319, doi:10.5194/isprsarchives-XL-3-W3-313-2015.
31. Sapirstein, P. Accurate Measurement with Photogrammetry at Large Sites. *J. Archaeol. Sci.* **2016**, *66*, 137–145, doi:10.1016/j.jas.2016.01.002.
32. O'Driscoll, J. Landscape Applications of Photogrammetry Using Unmanned Aerial Vehicles. *J. Archaeol. Sci. Rep.* **2018**, *22*, 32–44, doi:10.1016/j.jasrep.2018.09.010.
33. Campi, M.; di Luggo, A.; Monaco, S.; Siconolfi, M.; Palomba, D. Indoor and Outdoor Mobile Mapping Systems for Architectural Surveys. *ISPRS Int. Arch. Photogramm. Remote Sens. Spat. Inf. Sci.* **2018**, *42*, 201–208, doi:10.5194/isprs-archives-XLII-2-201-2018.
34. Petrie, G. Mobile Mapping Systems: An Introduction to the Technology. *Geoinformatics* **2010**, *13*, 32–43.
35. Kopsida, M.; Brilakis, I.; Antonio Vela, P. A Review of Automated Construction Progress Monitoring and Inspection Methods; In Proceedings of the 32nd CIB W78 Conference, Eindhoven, The Netherlands, 27–29 October 2015.
36. Omar, T.; Nehdi, M.L. Data Acquisition Technologies for Construction Progress Tracking. *Autom. Constr.* **2016**, *70*, 143–155, doi:10.1016/j.autcon.2016.06.016.
37. Dai, F.; Rashidi, A.; Brilakis, I.; Vela, P. Comparison of Image-Based and Time-of-Flight-Based Technologies for Three-Dimensional Reconstruction of Infrastructure. *J. Constr. Eng. Manag.* **2013**, *139*, 69–79, doi:10.1061/(ASCE)CO.1943-7862.0000565.
38. El-Omari, S.; Moselhi, O. Integrating 3D Laser Scanning and Photogrammetry for Progress Measurement of Construction Work. *Autom. Constr.* **2008**, *18*, 1–9, doi:10.1016/j.autcon.2008.05.006.
39. Rebolj, D.; Pučko, Z.; Babič, N.Č.; Bizjak, M.; Mongus, D. Point Cloud Quality Requirements for Scan-vs-BIM Based Automated Construction Progress Monitoring. *Autom. Constr.* **2017**, *84*, 323–334, doi:10.1016/j.autcon.2017.09.021.
40. Wu, P. *Integrated Building Information Modelling*; Li, H.; Wang, X. Eds; Bentham Science Publishers: Sharjah, UAE, 2017; doi:10.2174/9781681084572117010l.
41. U.S. General Services Administration, Public Buildings Service. *GSA Building Information Modeling Guide Series: 03—GSA BIM Guide for 3DImaging*; General Services Administration: Washington, DC, USA, 2019.
42. Akca, D.; Freeman, M.; Sargent, I.; Gruen, A. Quality Assessment of 3D Building Data: Quality Assessment of 3D Building Data. *Photogramm. Rec.* **2010**, *25*, 339–355, doi:10.1111/j.1477-9730.2010.00598.x.
43. Tran, H.; Khoshelham, K.; Kealy, A. Geometric Comparison and Quality Evaluation of 3D Models of Indoor Environments. *ISPRS J. Photogramm. Remote Sens.* **2019**, *149*, 29–39, doi:10.1016/j.isprsjprs.2019.01.012.
44. Zhang, C.; Kalasapudi, V.S.; Tang, P. Rapid Data Quality Oriented Laser Scan Planning for Dynamic Construction Environments. *Adv. Eng. Inf.* **2016**, *30*, 218–232, doi:10.1016/j.aei.2016.03.004.
45. Tang, P.; Alaswad, F.S. Sensor Modeling of Laser Scanners for Automated Scan Planning on Construction Jobsites. In *Construction Research Congress 2012*; American Society of Civil Engineers: West Lafayette, IN, USA, 2012; pp. 1021–1031, doi:10.1061/9780784412329.103.
46. Soudarissanane, S.; Lindenbergh, R.; Menenti, M.; Teunissen, P. Scanning Geometry: Influencing Factor on the Quality of Terrestrial Laser Scanning Points. *ISPRS J. Photogramm. Remote Sens.* **2011**, *66*, 389–399, doi:10.1016/j.isprsjprs.2011.01.005.

47. Shanoer, M.M.; Abed, F.M. Evaluate 3D Laser Point Clouds Registration for Cultural Heritage Documentation. *Egypt. J. Remote Sens. Space Sci.* **2018**, *21*, 295–304, doi:10.1016/j.ejrs.2017.11.007.
48. Zhang, Z. A Flexible New Technique for Camera Calibration. *IEEE Trans. Pattern Anal. Mach. Intell.* **2000**, *22*, 1330–1334, doi:10.1109/34.888718.
49. Rublee, E.; Rabaud, V.; Konolige, K.; Bradski, G. ORB: An Efficient Alternative to SIFT or SURF. In Proceedings of the 2011 International Conference on Computer Vision, Barcelona, Spain, 6–13 November 2011; pp. 2564–2571, doi:10.1109/ICCV.2011.6126544.
50. Mur-Artal, R.; Montiel, M.M.J.; Tardós, J.D. ORB-SLAM: A Versatile and Accurate Monocular SLAM System. *IEEE Trans. Robot.* **2017**, *31*, 1255–1262.
51. Hartley, R.; Zisserman, A. *Multiple View Geometry in Computer Vision*, 2nd ed.; Cambridge University Press: Cambridge, UK, 2004; doi:10.1017/CBO9780511811685.
52. Stewénius, H.; Engels, C.; Nistér, D. Recent Developments on Direct Relative Orientation. *ISPRS J. Photogramm. Remote Sens.* **2006**, *60*, 284–294, doi:10.1016/j.isprsjprs.2006.03.005.
53. Pierrot Deseilligny, M.; Clery, I. Apero, an Open Source Bundle Adjusment Software for Automatic Calibration and Orientation of Set of Images. *ISPRS Int. Arch. Photogramm. Remote Sens. Spat. Inf. Sci.* **2012**, *269277*, doi:10.5194/isprsarchives-XXXVIII-5-W16-269-2011.
54. Georgantas, A.; Brédif, M.; Pierrot-Desseilligny, M. An Accuracy Assessment of Automated Photogrammetric Techniques for 3D Modeling of Complex Interiors. *ISPRS Int. Arch. Photogramm. Remote Sens. Spat. Inf. Sci.* **2012**, *39*, 23–28, doi:10.5194/isprsarchives-XXXIX-B3-23-2012.
55. Cerrillo-Cuenca, E.; Ortiz-Coder, P.; Martínez-del-Pozo, J.-Á. Computer Vision Methods and Rock Art: Towards a Digital Detection of Pigments. *Archaeol. Anthropol. Sci.* **2014**, *6*, 227–239, doi:10.1007/s12520-013-0147-2.
56. Triggs, B.; Mclauchlan, P.; Hartley, R.; Fitzgibbon, A. Bundle Adjustment—A Modern Synthesis. In Proceedings of the International Workshop on Vision Algorithms, Singapore, 5–8 December 2000; pp. 198–372.
57. Fischler, M.A.; Bolles, R.C. Random Sample Consensus: A Paradigm for Model Fitting with Applications to Image Analysis and Automated Cartography. *Commun. ACM* **1981**, *24*, 381–395, doi:10.1145/358669.358692.
58. Rupnik, E.; Daakir, M.; Pierrot Deseilligny, M. MicMac—A Free, Open-Source Solution for Photogrammetry. *Open Geospat. Data Softw. Stand.* **2017**, *2*, 14, doi:10.1186/s40965-017-0027-2.
59. Deseilligny, M.; Paparodit, N. A Multiresolution and Optimization-Based Image Matching Approach: An Application to Surface Reconstruction from SPOT5-HRS Stereo Imagery. *Int. Arch. Photogramm. Remote Sens. Spat. Inf. Sci.* **2012**, *36*, 1–5.
60. Agisoft Metashape. Available online: https://www.agisoft.com/ (accessed on 28 August 2019).
61. Meshlab. Available online: http://www.meshlab.net/ (accessed on 27 May 2015).
62. Hong, S.; Jung, J.; Kim, S.; Cho, H.; Lee, J.; Heo, J. Semi-Automated Approach to Indoor Mapping for 3D as-Built Building Information Modeling. *Comput. Environ. Urban Syst.* **2015**, *51*, 34–46, doi:10.1016/j.compenvurbsys.2015.01.005.
63. Koutsoudis A, Vidmar B, Ioannakis G, Arnaoutoglou F, Pavlidis G, Chamzas C. Multi-image 3D reconstruction data evaluation. Journal of Cultural Heritage. 2014;15(1):73-79. doi:10.1016/j.culher.2012.12.003

3.

Sección II: Evaluación en aplicaciones arqueológicas.

Esta sección contiene el artículo "An Integrated Solution for 3D Heritage Modeling Based on Videogrammetry and V-SLAM Technology" Publicado el 11 de Mayo de 2020 en la revista Remote Sensing, en el apartado especial de (special issue): Photogrammetry and Image Analysis in Remote Sensing.

Resumen

El presente artículo enumera las tipologías de sensores de adquisición de datos y reconstrucción 3D en arquitectura, urbanismo y arqueología que existen en el mercado actual, y analiza sus características más esenciales, como el sensor, la velocidad de adquisición de datos en campo, la precisión a través del error medio, el alcance y su precio al público, entre otros detalles. El texto analiza los láser escáners terrestres (TLS), los escáneres de mano ("*handheld scanners*"), la fotogrametría, los sistemas MMS basados en LIDAR y los sistemas "*mobile mapping*" basados en imágenes ("*Imaging Mobile Mapping*"), mencionando también aquellos transportados en mochilas y los transportados en carros. Finaliza este análisis enumerando las aplicaciones fotogramétricas hasta concretar las diseñadas para uso en smartphones.

El análisis de los productos actuales, junto al de la literatura científica más relevante en el ámbito de la videogrametría y de la selección de imágenes basados en los tres distintos métodos (selección automática, basado en características 2D, basado en características 3D), desemboca en la definición detallada de la propuesta de desarrollo principal de éste artículo: se trata de un escáner 3D de mano basado únicamente en imágenes y que, a partir de un procedimiento de selección de la imágenes proveniente de videocámaras y de una metodología para la reconstrucción 3D, genera nubes de puntos con color de forma automática. El artículo describe detalladamente los materiales utilizados para la creación del prototipo, planteando cómo se ha realizado un cambio de cámaras con la pretensión de mejorar su funcionamiento y el desempeño en el campo, especialmente cuando hay grandes variaciones de luz o si la luz está de frente al sistema de cámaras.

La cámara A se emplea para calcular la localización simultanea (VisualSLAM) y la cámara B, de más resolución, para capturar los "*frames*" que se utilicen en el proceso fotogramétrico. El texto describe con detalle los filtros que se han diseñado para la selección de imágenes provenientes de la cámara B, dichos filtros son: Filtro "*AntiStop*", filtro "*Divergent SelfRotation*" y el nuevo filtro de ruptura ("*Break Filter*") el cual analiza la continuidad de los frames seleccionados a partir del número de puntos homólogos, insertando imágenes si es necesario y creando nuevas secciones si la ruptura es insalvable. Estos filtros maximizan la posibilidad de que no haya ruptura de la orientación relativa en ningún punto y que la geometría de la toma sea óptima. Posteriormente se detalla el procedimiento fotogramétrico seguido a través de diferentes fases hasta la generación de la nube de puntos, filtrado de la nube de puntos, generación del mallado ("*mesh*") y del mapa de texturas ("*texture mapping*") tras el cual el modelo 3D contiene una textura asociada producto de una fusión balanceada de las imágenes más relevantes utilizadas en el modelado.

Para evaluar convenientemente los resultados se realiza un test experimental sobre tres zonas en el yacimiento arqueológico del conocido como Casa de Mitreo, en la ciudad de Mérida (España). Cada una de las zonas tiene unas características determinadas que ayudarán a un examen más exahustivo a la cámara videogramétrica propuesta. Para completar la evaluación, y compararlo con un instrumento actual y habitual de éste tipo de yacimientos arqueológicos, se decidió confrontarlo con el láser escáner Faro Focus X330. Se realizaron capturas de las tres zonas con ambos instrumentos y se procesaron los datos hasta la extracción de las tres nubes de puntos, una para cada zona de trabajo. Primeramente se comparó los tiempos de adquisición de datos, siendo el sistema propuesto 17 veces más rápido que el láser escáner; posteriormente se analizó la resolución y distribución de ambas nubes de puntos, donde se puede observar una mayor resolución (10X) del láser escáner respecto del sistema propuesto. Por otro lado se

calculó la precisión de todos los modelos a partir de 150 dianas distribuidas por las tres áreas de trabajo; los resultados arrojaban una precisión muy similar para ambos sistemas, de unos RMSE de 6mm de media. También se analizó la precisión de forma pormenorizada para dos zonas concretas a través de estadística circular, donde se observaron las tendencias de dirección y módulo de los errores, concluyendo que no existía una deformación con una tendencia clara y cuyos módulos entraban dentro de los errores previstos, por lo que se descartó algún posible error sistemático del instrumento y se confirmó la similitud de las precisiones. Se realizaron secciones a los modelos de ambas tecnologías y también se analizaron las texturas y, en ambos casos, no existían diferencias apreciables, ahondando en la similitud de resultados.

Se concluye por tanto que éste escáner videogramétrico, el cual ha sido mejorado en hardware y en software, ofrece unos resultados equiparables al láser escáner en múltiples aspectos y en entornos arqueológicos, mejorando los tiempos de captura y empeorando en los tiempos de procesamiento, eso sí, siendo dicho procesamiento totalmente automático.

Articulo II: An Integrated Solution for 3D Heritage Modeling Based on Videogrammetry and V-SLAM Technology

remote sensing

MDPI

Article

An Integrated Solution for 3D Heritage Modeling Based on Videogrammetry and V-SLAM Technology

Pedro Ortiz-Coder [1,*] and Alonso Sánchez-Ríos[1]

[1] University Centre of Mérida, University of Extremadura, 06800 Mérida, Spain;
* Correspondence: peorco04@alumnos.unex.es (P.O-C.); schezrio@unex.es (A.S-R.)

Received: 12 April 2020 / Revised: 5 May 2020 / Accepted: 8 May 2020 / Published: 11 May 2020

Abstract: This paper presents an approach for 3D reconstruction of heritage scenes using a videogrammetric-based device. The system, based on two video cameras with different characteristics, uses a combination of visual simultaneous localization and mapping (SLAM) and photogrammetry technologies. VSLAM, together with a series of filtering algorithms, is used for the optimal selection of images and to guarantee that the user does not lose tracking during data acquisition in real time. The different photogrammetrically adapted tools in this device and for this type of handheld capture are explained. An evaluation of the device is carried out, including comparisons with the Faro Focus X 330 laser scanner, through three case studies in which multiple aspects are analyzed. We demonstrate that the proposed videogrammetric system is 17 times faster in capturing data than the laser scanner and that the post-processing of the system is fully automatic, but takes more time than the laser scanner in post-processing. It can also be seen that the accuracies of both systems and the generated textures are very similar. Our evaluation demonstrates the possibilities of considering the proposed system as a new professional-quality measurement instrument.

Keywords: videogrammetry; photogrammetry; 3d reconstruction; handheld scanner; visual SLAM; survey instrument.

1. Introduction

The wide-spread use of 3D models in fields such as architecture, urban planning, and archaeology [1–3] means that some professionals cannot generate 3D models without advanced technical knowledge in surveying. In this context, many investigations carried out in recent years have been aimed at the development of new products[1] and working methods that simplify the necessary requirements both for data acquisition and processing, without harming the accuracies of the resulting products [4–6]. In parallel, multiple 3D data acquisition systems based on active or passive sensors have appeared in recent decades, obtaining 3D models either as point clouds or textured surfaces. These new systems have revolutionized the possibilities of users, obtaining results that assist in understanding digitized elements and facilitating studies that could hardly be carried out in any other way [7–9].

Among the various systems that are commonly used for data acquisition in architecture, urban planning, and archaeology, mid-range terrestrial laser scanners (TLS) [10] are commonly used, which are survey instruments that use laser pulses to measure distances and a rotating mirror to measure angles, generating a point cloud of the environment with a range of 0.5–300

m and root mean square error (RMS) between 1 and 4 mm. Mobile mapping systems (MMS) [9,11] are based on multiple synchronized components, such as LIDAR, IMU, GNSS, cameras, odometers, and so on, with which 3D models can be constructed with up to 2 cm RMS errors. Handheld scanners, normally based on active sensors such as lidar or structured light sensors, are considered MMS. With handheld scanners, data are captured while the user moves through a work area. Lidar-based handheld scanners, which are applicable to the fields of interest in this article, achieve RMSE errors of 1–3 cm, with ranges usually no greater than 150 meters [1]. Finally, we consider photogrammetric techniques [12] as a perfectly viable and growing means for generating 3D models in the fields of architecture, urban planning, and heritage. Such 3D models have been generated using 10–12 Mpx commercial cameras and commercial photogrammetric software, with a variable distance between 1 and 15 m in these applications, following certain proven capture procedures and conditions [13,14]., the RMSE of these models ranges from 2 mm for the closest distances to 1 cm for longer distances. In the aerial photogrammetric case [15,16], if we consider a flight height of 30 m, the accuracy can reach 2–9cm.

In the cases of TLS and MMS, in competition between companies to satisfy the market requirements, research has normally been directed towards simplifying the procedures and facilitating the interaction of the instrument with users, creating ever simpler and more user-friendly interfaces. Thus, these technologies can now be used by non-expert users [9,17,18]. Among commercial TLS, we mention the Faro Focus 150, manufactured by FARO Technologies Inc. (Lake Mary, Florida, U.S.A.); the Leica RTC360, manufactured by Leica geosystems (Heerbrugg, Switzerland); the RIEGL VZ-400i, manufactured by RIEGL Laser Measurement Systems (Horn, Austria); and the Z+F imager, manufactured by Zoller & Frölich GmbH (Wangen im Allgäu, Germany) [19–22]. Manufacturers have opted to facilitate their use by simplifying user interfaces, connectivity, and scan pre-registration procedures (automatic or semi-automatic). Still, the reading and loading data processes in the software and the inconvenience of having to process millions of points at once, especially at very high resolutions, is a major challenge for users; especially for non-experts. The most widely used MMS for large-scale scanning and mapping projects in urban, architectural, and archaeological environments are vehicle-based mobile mapping platforms or those that must be transported by backpack or trolley. In the former, we mention the UltraCam Mustang, manufactured by Vexcel Imaging GmbH (Gra, Austria); the Leica Pegasus:Two Ultimate, manufactured by Leica geosystems (Heerbrug, Switzerland); and the Trimble MX9, manufactured by Trimble (Sunnyvale, CA, U.SA.) [23–25], which use inertial systems and GNSS for positioning, and are equipped with LIDAR profilers with high scanning speeds (up to 500 scans/sec) and 360 º cameras to achieve street-level scenery with geo-positioned panoramic imagery. The latter type (i.e., systems transported by a backpack or by a trolley) are usually used for indoor/outdoor middle-scale scanning and mapping projects with difficult access (buildings, urban centers, construction areas, caves, and so on). These products include systems based on different technologies, including active capture sensors (e.g., Lidar) and passive sensors (e.g., cameras), as well as GNSS and IMU systems, which assist the system in positioning and orienting itself. In this type of product, we mention the Leica Pegasus: Backpack, manufactured by Leica Geosystems (Heerbrugg, Switzerland); the bMS3D LD5+, manufactured by Viametris (Louverné, France); and the trimble Indoor Mobile Mapping solution (TIMMS), manufactured by Applanix (Richmond Hill, Canada)[26–28].

Data acquisition in MMS is automatic and normally easy and fast. However, there is still the inconvenience of having to manage clouds of millions of points, increasing the time required in data processing [29]; in addition to the fact that the price of the equipment is usually high, ranging between €350,000 and €650,000 for vehicle-based mobile mapping platform systems and €60,000 and €350,000 for systems carried by a backpack or trolley.

However, in the case of systems based on photogrammetric techniques, many investigations have been aimed at both simplifying data processing and obtaining the final results as automatically as possible. In the dynamics of simplification such that photogrammetry can be used by non-experts, the use of modern smart phones and tablets to capture high-resolution images [30–32], following which the obtained data are processed in the cloud. This process has been used in applications such as the Photogrammetry App created by Linearis HmbH & Co (Braunschweig, Germany) and ContextCapture mobile created by Bentley systems Incorporated (Exton, U.S.A.)[33,34], among others. In general terms, the technical knowledge required of the user has been practically reduced to adapting the parameters of the camera to manage the scene lighting conditions and ensuring good camera poses geometry [35]; therefore, a semi-automated process is followed using the captured information, in which the user practically does not intervene [32]. In this line, companies have focused their objectives on achieving data capture without prior technical knowledge and almost fully automatic data processing. In short, their main goal is achieving fast and accurate data capture with which high-quality end products can be obtained, while being accessible to a non-specialized user. Thus, some manufacturers have chosen to use photogrammetric techniques in their MMS capture systems (instead of using laser scanning systems), such as the Trimble MX7 manufactured by Trimble (Sunnyvale, CA, U.S.A.)[36], which consists of a vehicle-mounted photogrammetric system equipped with a set of six 5 megapixel cameras using GNSS and inertial referencing system for precise positioning; as well as the imajing 3D Pro system from imaging SAS (Labège, France) [37], in which photogrammetric tools are used to process the 2D images obtained by a sensor which, for precise and continuous positioning, is equipped with an inertial system, a GNSS receiver, and a barometric sensor, thus constituting a complete portable mobile mapping system for high-speed data collection.

From the above, it follows that the most commonly used positioning and measurement systems are based on inertial systems, GNSS, cameras, and LIDAR. However, some recent research [1,38,39] has been directed at combining laser measurement systems with positioning systems based on visual odometry (VO) or simultaneous localization and mapping (SLAM) techniques. With this type of design, the company Geoslam (Nottingham, UK) has launched ZEB systems with three configurations—Revo, Horizon, and Discovery—which are handheld or carried in a backpack, and have capture ranges between 5–100 m and relative accuracies ranging between 1–3 cm. Videogrammetric 3D reconstruction through smartphones using a 3D-based images selection have been also explored [40]. In this paper, VisualSLAM [41] and photogrammetry techniques using high-resolution images from an industrial video-camera have been combined for 3D reconstruction; 3D-based and ad hoc algorithms has been used for an optimal images selection and for the calculations, to obtain longer data sets and more complex 3D and precise 3D scenarios. To explore this possibility, a new system has been designed: A simple handheld imaging scanner based on two commercial cameras, one of which is used to compute the camera position in real time using the VisualSLAM algorithm; the other camera is a high-resolution frame recorder, which continuously saves images of the scene which, using photogrammetry, is used to generate a 3D color point cloud. To evaluate the effectiveness of the proposed system, a set of three studies were performed in the House of Mitreo (Mérida, Spain), a dwelling from Roman times with ongoing archaeological excavations. In these experiments, different aspects such as the data acquisition and processing time, the average density of the point clouds, and the level of accuracy (LOA) of each point cloud, are evaluated, taking as reference a set of 150 targets distributed throughout the entire area, whose coordinates were observed with a total station. Likewise, the same areas were scanned with a Focus3D X 330 laser scanner manufactured by FARO Technologies Inc. (Lake Mary, Florida, U.S.A.) [19], in order to compare the results obtained with the proposed system and ensure the absence of systematic errors between both systems. The results obtained with acquisition times and human intervention in the data processing using the proposed system were 31 and 0

minutes, respectively (compared to 520 and 97 minutes with the laser scanner), the mean point cloud density value is 1.6 points/mm (compared to 0.3 pts/mm with the laser scanner), and accuracy values between 5–6 mm (RMSEs) to evaluate LOA (compared to the 6–7 mm obtained with the laser scanner). In addition, circular statistics were computed to confirm of the absence of systematic errors between both systems, stressing the feasibility of the proposed system in archaeological environments.

This paper is divided into four sections: In Section 2, the proposed system is described, from the first idea to its current state. In Section 3, the experimental tests carried out with the system are described, and the results are also presented. Finally, Section 4 presents our final conclusions.

2. Materials and Methods

The process of point cloud generation by the proposed system, which combines VisualSLAM and photogrammetry, is shown in Figure 1. This scheme is based on simultaneous video capture by two cameras, A and B: With the images obtained with camera A, the camera pose is computed in real time (applying the VSLAM algorithm) and, therefore, the camera trajectory data are obtained. High-resolution images are extracted from the video obtained by camera B, with which point clouds and associated textures are generated using photogrammetric techniques (after image selection and filtering).

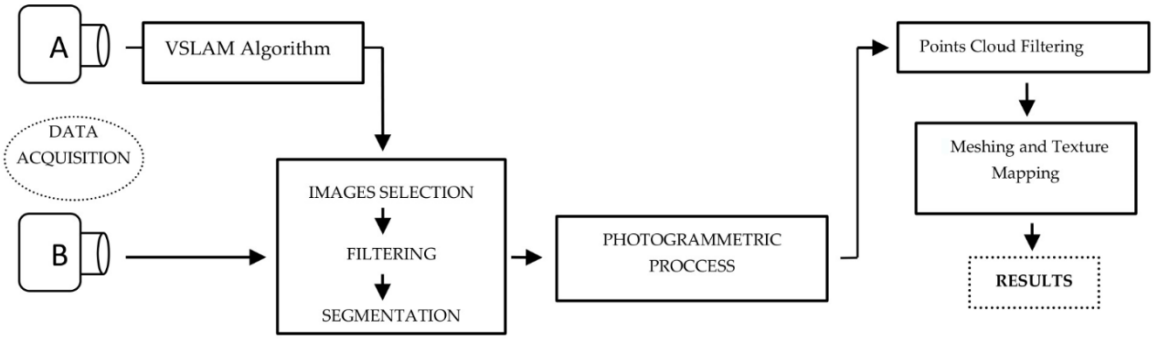

Figure 1. General procedure overview.

For data collection, the construction of a prototype was considered, using plastic material (acrylonitrile butadiene styrene, ABS), based on two cameras connected to a laptop in an ad-hoc designed housing for easy handling during field work. The first version of this prototype (P-1) incorporated two camera models from The Imaging Source Europe GmbH company (Bremen, Germany), each with a specific lens model: camera A (model DFK 42AUC03), with a model TIS-TBL 2.1 C lens (The Imaging Source Europe GmbH company, Bremen, Germany) (see Table 1), fulfilled the main mission of obtaining images for calculation of the real-time positioning of the capture system by the VSLAM algorithm; Camera B (model DFK 33UX264), with a Fujinon HF6XA–5M model lens (FUJIFILM Corp., Tokyo, Japan), was used to acquire the images, which were later used in the photogrammetric process. Although the first metric studies were satisfactory, it was observed that camera A had a higher resolution and performance than was required for the intended purpose, and that Camera B had a low dynamic range, such that it lacked optimal automatic adaptation to different lighting conditions; producing, in some cases, effects of excessive darkening of images. To solve these problems, a second prototype (P-2) was designed, with a lighter and smaller housing. Inside, two new cameras were installed next to each other, with parallel optical axes: The ELP-USB500W05G, manufactured by Ailipu Technology Co., Ltd. (Shenzhen, Guangdong, China), as camera A, and the GO-5000C-USB

camera, manufactured by JAI Ltd. (Copenhagen, Denmark), as camera B. The main technical characteristics of the cameras used in both prototypes are given in Table 1.

Table 1. Main technical characteristics of cameras and associated lenses used in the two prototype versions P-1 and P-2 (from The Imaging Source Europe GmbH company, FUJIFILM Corporation, Ailipu Technology Co., Ltd., and JAI Ltd.). *Focal length have been computed using Scaramuzza model [42].

Prototype Version	Camera/Model	Resolution (pixels)	Focal (mm)	Angle of View (H°xV°)	Sensor Size (inch or mm)	Frame Rate (fps)
P-1	A/ DFK 42AUC03	1280×960	2.1	97º x 81.2º	1/3"	25
	B/ DFK 33UX264	2448 x 2048	6	74.7º x 58.1º	2/3"	38
P-2	A/ ELP-USB500W05G	640 x 480	*	170˚x 126˚	3.9 x 2.9 mm	30
	B/ GO-5000C-USB	2560 x2048	6.5	89˚x 76.2˚	12.8 x 10.2 mm	6

Regarding functionality, in the P-2 prototype, three simple improvements were planned: An anchor point to an extendable pole to facilitate working in high areas; a patella system, which allows the user to direct the device towards the capture area and to connect to a lightweight and portable laptop (around 1.5 kg), to facilitate data collection. In our case, the chosen laptop model was the HP Pavillion Intel Core i5-8250U 14", with a 256 GB SSD and 16 GB RAM, manufactured by HP Inc. (Palo Alto, California, U.S.A.). The two configurations of the P-1 and P-2 prototypes are shown in Figure 2.

Figure 2. Initial prototype configuration P-1 (top) and the actual prototype P-2 (bottom), 14 cm long and lighter, with an extendable pole anchor point (red arrow) and a ball joint system (yellow arrow) to facilitate data capture.

a) 2.1. Cameras Calibration

Once the P-2 prototype was built, it was necessary to determine the internal and external calibration parameters of the cameras. For internal calibration, two widely known calibration

algorithms, which have been used in the computer vision field, were considered: For camera A, the calibration algorithm proposed by Scaramuzza et al. (2006) [42] for fisheye camera models and, for camera B, the algorithm proposed by Zhang (2000) [43]. In both cases, a checkerboard target (60 x 60 cm) and a set of multiple images, taken from different positions in order to cover the entire surface, were used. For the computations, Matlab 2019 software, from the company MathWorks (Natick, Massachusetts), was used to obtain the values of focal length, principal point, and distortions (radial and tangential), in order to calibrate cameras A and B.

To calculate the external calibration parameters, a total of 15 targets were first spread over two vertical and perpendicular walls, whose cartesian coordinates were measured with a calibrated robotic total station with accuracies of 1" and 1.5 mm + 2 ppm for angles and distances, respectively. Subsequently, multiple observations were made of these walls with both cameras of the prototype, obtaining the set of coordinates of the 15 targets with which, after applying the seven-parameter transformation [44], the external calibration parameters that relate the relative positions of cameras A and B were obtained.

b) 2.2. Data Acquisition and Preliminary Images Selection

For data capture in the field, the user must carry the device (hand-held type) connected to the reversible laptop. The VSLAM algorithm (implemented in C ++) was based on ORB-SLAM [45], with which, through the geometry of the objects themselves, a preliminary selection of the main frames (denominated keyframes) is made (in addition to the calculation of the trajectory). Thus, through the user interface, the operator can observe, in real time, which zone is being captured by camera A, the trajectory followed, and whether there has been any interruption in its follow-up; in this case, the trajectory returns to a working zone already captured and the trajectory is recovered. This procedure is carried out in three phases [46]: In the first, called tracking, the positions of the cameras are calculated to generate the keyframes, which will be part of the calculation process; in the second, called local mapping, keyframes are optimized and redundant keyframes are eliminated; in the last, the loop closing phase, the areas where the camera had previously passed, are detected and the trajectory is recalculated and optimized. The process generates a file with the camera pose and time UNIX for each keyframe. While capturing images with camera A and during trajectory and keyframe calculations, camera B records high-resolution images onto the laptop's hard drive at a speed of 6 fps, different from the speed of camera A (30 fps). Subsequently, the algorithm makes a selection of images from camera B based on the keyframes calculated with camera A, and applies different filters.

c) 2.3. Image Selection by Filtering Process.

In this phase, we start from a set of images from cameras A and B with different characteristics (see Table 1). In order to ensure the consistency of the data that will be used in the photogrammetric process (camera images B), the following filters were designed [7]: A) The AntiStop filter, with which it is possible to delete images where the user stopped at a specific point in the trajectory and the system continuously captured data, resulting in nearby positions. This filter is based on the calculation of distances between the camera centers of the keyframes, which are related to the shot times. In this way, the system detects whether the user has stopped and eliminates redundant keyframes; B) the divergent self-rotation filter, which eliminates those keyframes that meet two conditions for at least three consecutive keyframes, and the angle of rotation of the camera with respect to the X and Z axes must increase its value by a maximum of $\pm 9^0$ and its projection centers must be very close; and C) the break area filter, which was specifically designed to detect whether there is less than a minimum value of homologous points in an image. The algorithm used to extract the main characteristics of the images is the so-called scale-invariant feature transform (SIFT), developed by Lowe (2004) [47]; in our case, the calculation is performed at low resolution (around 1 megapixel) at a speed of 2 images every 3.5 seconds, thus reducing the computational cost of the procedure. Figure 3

describes, in detail, the workflow followed in the application of the break area filter, the end result of which is that the images selected for incorporation into the photogrammetric process are grouped into a set of interrelated segments, where each forms a group of images connected to each other by a determined number of homologous points, guaranteeing the consistency and success of the photogrammetric process.

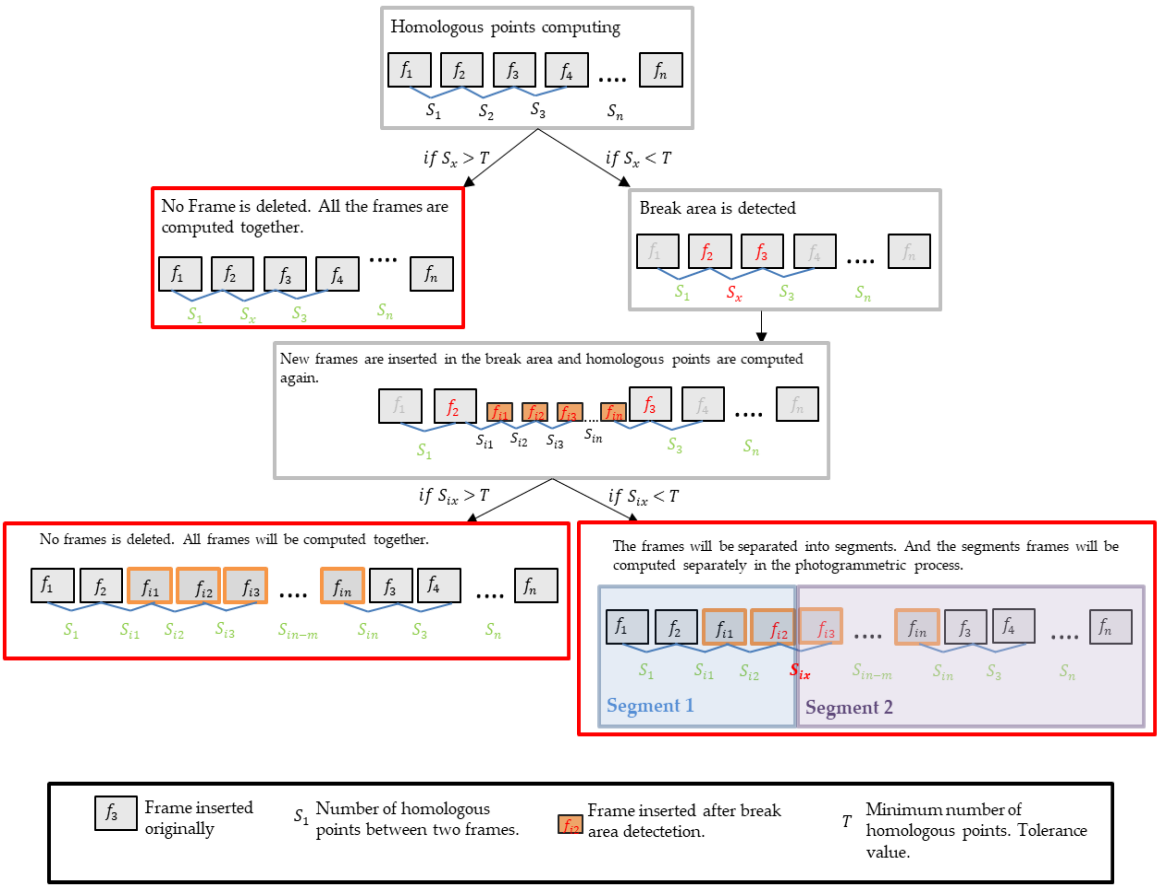

Figure 3. Break area filter workflow.

d) 2.4. Photogrammetric Process.

The photogrammetric procedure is applied independently to each of the segments obtained in the previous phases, and is structured in three steps: First, after a search for homologous points between the images of each segment (using the SIFT algorithm [47]), a filtering process is performed using a random sample consensus algorithm (RANSAC) [48]. The search for homologous points is carried out in the following three grouping criteria: 1) In the set of images that form the starting image with four previous images and four subsequent images, 2) in the set of images characterized by their proximity according to data from the trajectory calculated with the VSLAM algorithm, and 3) in all the images of the segment. Each criterion has a different computational cost, less in criterion 1 and more in criteria 2 and 3. The choice of criterion depends on the intake conditions; thus, if the user makes a trajectory in a single direction, it is appropriate to use criterion 1. In the case of trajectories in several directions, in which the user passes through the same place several times, we can use criterion 2; although, we obtain a more robust solution with criterion 3, albeit with a higher computational cost.

In the second step, the relative orientation of the images is calculated, in order to calculate all the camera positions in a relative reference system at the time of the shot. For this, we start

from the homologous points of each segment, to which algorithms leading to direct solutions [49,50] and bundle adjustment [50] are applied to minimize divergence, obtaining a sparse point cloud and camera poses as a result, which are then adjusted to the general trajectory through minimum square techniques and a 3D transformation.

The last step is the generation of depth maps of the scene. For this, we start with a main image and eight adjacent secondary images, according to the direction of data capture. Depth values are calculated for each X and Y position of the image [49]; subsequently, all the generated point clouds are merged together, aligning them in a general co-ordinate system (Figure 4a).

2.4.1. Point Cloud Filtering

When collecting data from the prototype, it is typical that the obtained point clouds have noise and artifacts that must be removed. In reality, these are outliers, which can be numerically separated from the rest and which must be eliminated (Figure 4b). In our case, we applied two filters [51,52]: 1) First, a statistical outlier removal (SOR) filter, which analyzes a set of n points by calculating the average distance between them; any point that is more than σ standard deviation from the mean distance is detected as an outlier and removed (in our case, the values used for n and σ were 200 and 0.8, respectively); 2) subsequently, a radius outlier removal (ROR) filter is applied, with which a set of k points is fitted to a local plane, following which the normal of the plane through the points is computed and the radius (R) of a virtual sphere is defined, which is used to count the excess neighbors. As a result, the points outside of this sphere are detected as outliers and removed—only those points closest to the adjusted plane and that best define the object are kept.

2.4.2. Mesh and Texture Mapping Generation.

Once the point clouds and depth maps have been generated (as in Section 2.4), an algorithm to eliminate distortions [53] is applied to the selected images, using the camera calibration parameters obtained in Section 2.1. Subsequently, to carry out the texture mapping, the Poisson algorithm [54] is used, in which a mesh formed by a series of triangles adapted to the point cloud is generated (see Figure 4c). Taking into account the position of the camera's projection center, the size and position of the triangle, and the orientation of its normal vector, each triangle will be associated with one or more main images corrected for distortions (with their original color) [55]. To transfer the generated textures to the point cloud, a two-step procedure [55,56] is carried out: First, an algorithm that transfers the color of the texture projecting it onto the vertices of the mesh is used; then, the colors of the vertices are transferred to the point cloud, following the criterion of associating the color of the vertex with the closest points (Figure 4c); the result will be optimal if the average length of the sides of the triangles of the mesh coincides with the distance between points of the point cloud; otherwise, a loss of resolution may be observed in the projected texture.

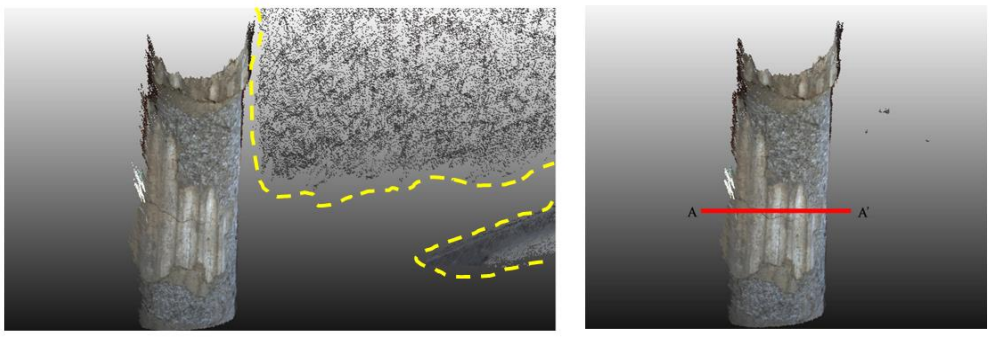

(a) **(b)**

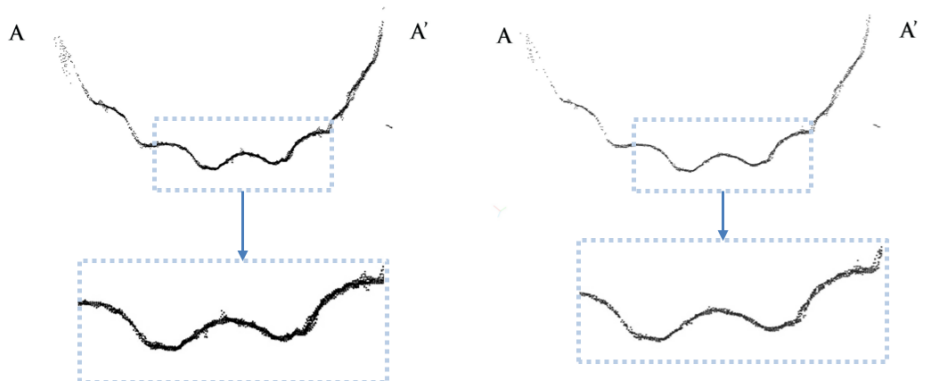

(c) (d)

Figure 4. Effect of statistical outlier removal (SOR) and radius outlier removal (ROR) filters on a point cloud on the surface of a Roman column: (a) Point cloud with outliers in areas marked with dashed lines in yellow; (b) point cloud after applying the SOR filter, section AA is marked with a red line; (c) point cloud of section AA after applying the SOR filter; and (d) point cloud of section AA after the application of the SOR and ROR filters, with a better definition of the contour of the column section.

3. Experimental Test

To evaluate the effectiveness of the system proposed in this paper, a set of various studies were performed in the House of Mitreo (Mérida, Spain), a dwelling from Roman times built between the first century BC and the seocnd century AD. Within this archaeological set, three working areas were chosen, due to their own characteristics, in which different aspects of the proposed system were tested:

Working area 1: Pond and peristilium. In this area, it was intended to observe the behavior of the device in areas with different height levels and horizontal and vertical construction elements, as the area consists of a water tank (currently empty) located below the ground, and columns that rise up to 2.5 m above the ground (Figure 5a). One aspect to be evaluated was the behavior of the device in capturing the columns due to their geometry, which can pose a challenge for the calculation of homologous points and subsequent relative orientations. Another aspect to evaluate was that, as the data collection required two different trajectories—one inside the pond courtyard and the other outside (through the peristilium)—we checked if the system adjusted both trajectories properly and whether the drift error was acceptable.

Working area 2: Underground rooms. This part of the house was used in the summer season. Being excavated below ground level, there was a lower temperature inside than in the upper area. These are accessed through a staircase with a narrow corridor, surrounded by high walls and with remains of paintings and notable differences in lighting between the lower and upper parts (Figure 5b). It was, therefore, an interesting area to study the behavior of the proposed system in narrow areas, as well as the adaptability of the system to different lighting levels and complex trajectories.

Working area 3: Rooms with mosaic floors (Figure 5c). Mosaics are typically repetitive geometric figures materialized by a multitude of small tiles. Thus, their 3D reconstruction could pose a challenge for the proposed system, leading to errors in matching homologous points causing gross errors or even the impossibility of orienting the images. Regarding data capture, work in this area requires long and complex trajectories, in order to cover all areas without accumulating drift errors. In addition, the small size of the tiles that make up the mosaic floors and their different colors demand a high capacity in the resolution and definition of the captured textures.

(a) (b) (c)

Figure 5. Work areas in the "Casa del Mitreo": (**a**). Working area 1: Pond and Peristilium (left); (**b**). Working area 2: Underground rooms (center); and (**c**). Working area 3: Rooms with mosaic floors (right).

To carry out validation of the proposed system, the same work areas were scanned, in addition to the proposed system, by a Faro Focus3D X 330 laser scanner, with a range of 0.6–330 m, a scanning speed of 976,000 points/seg, and a maximum precision, according to the manufacturer, of 1 mm @ 5 m. In addition, to perform a metric control of both systems, a total of 150 targets were placed throughout the three areas. Their co-ordinates were measured by the total station Pentax V-227N (Pentax Ricoh Imaging Company, Ltd., Tokyo, Japan) with an angular precision of 7" and 3 mm+2 ppm of error in distance measurement (ISO 17123-3: 2001) (Figure 6).

(a) (b)

(c) **(d)**

(e) **(f)**

Figure 6. Total station (a) and target model (b) used to co-ordinate control points; Faro Focus3DX330 laser scanner recording data in working areas 1 (c) and 3 (d); and data capture with the proposed system in working area 2 (e and f).

With these data, we carried out a set of tests in which both systems (i.e., the proposed system and the laser scanner) were evaluated and compared:

The first test compared the time spent in data acquisition and data processing.

In the second test, a series of calculations and experiments were performed to determine the resolution and distribution of the point cloud of both systems in a comparative way.

The third test evaluated the precision of both systems through three different sub-tests. In the first sub-test, 150 targets were measured as control points and a comparative study was carried out on the accuracy assessment of both systems; in the second sub-test, precision and zonal deformations were evaluated, in which the presence of systematic errors between the proposed system and the laser scanner were ruled out by means of circular statistical analysis. In the third sub-test, a visual comparison was made between cross-sections of the point clouds resulting from both systems.

The last test evaluated the resulting textures of both systems through the analysis of different variables.

The tests mentioned above are described in detail below.

e) 3.1. Comparison Times for Data Acquisition and Processing

Data acquisition with the proposed system consists of focusing the device towards the area to be measured and moving along a trajectory which the VSLAM algorithm continuously calculates, the graph of which appears in real time on the laptop screen; in this way, the user can ensure that there is continuity in the capture and that the system is not interrupted (Figure 7). The distances between the measured elements and the device varied from 0.4 to 2 m in working areas 1, 2, and 3; likewise, the parameters that defined the resolution were not chosen until the post-processing phase and did not determine the times used for data acquisition.

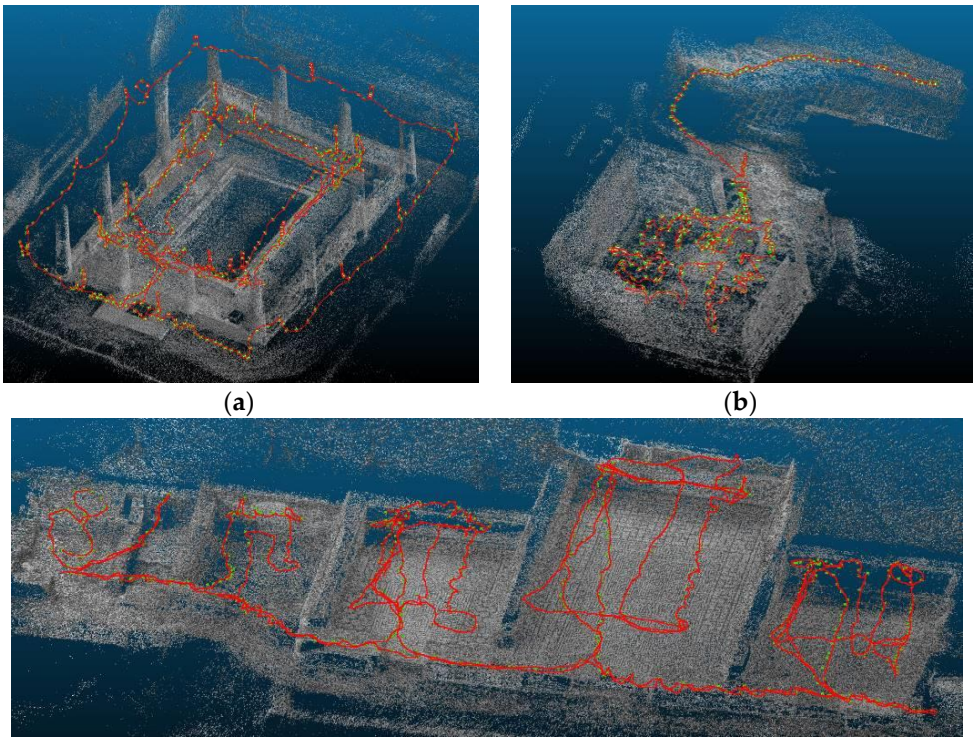

(**a**) (**b**)

(**c**)

Figure 7. Trajectory followed (red lines) during data acquisition in the three work zones: orking area 1 **(a)**; working area 2 **(b)**; and working area 3 **(c).**

For data collection with the Faro Focus X 330 laser scanner, a resolution of ½ of the total was chosen among the configuration parameters, along with a quality of 4x, which, according to the manufacturer's data [19], achieves a resolution of 3.06 mm @ 10 m distance. Furthermore, the scanner took 360 º images at each scanning station. In the methodology used, different positioning of the instrument was necessary to avoid occluded areas.

Regarding the subsequent phase of data processing, the proposed system acts autonomously; that is, practically without user intervention, where the user only has to choose some initial parameters when starting the process. However, the laser scanner's post-processing work required more operator intervention or, in some cases, the performance of operations that require a high time cost, such as the scan loading process, which may takes several minutes, registration of the reference spheres, which must be supervised manually, the assignment of colors to the scans, and so on. The results can be seen in Table 2, where the times used by each system in different areas are shown, both for data collection and data processing. Regarding the results obtained, the time required for data acquisition with the proposed system was 31 min (0.52 h) in total for the three working areas, compared to 520 min (8.67 h) with the Faro Focus3D X330 laser scanner; that is, the proposed system was about 17 times faster in capturing data than the laser scanner. The preliminary work of the laser scanner, the placement of reference spheres, and the necessary station changes were also considered in this time measurement. However, in data processing (CPU time), the laser scanner system was about 10 times faster than the proposed system: 176 min (2.93 h) for the former, compared to 1716 min (28.60 h) for the latter. However, it should be noted that the user spent a total of 97 min (1.62 h) in the data processing operations with the laser scanner system but, with the proposed system, the user's time-cost was nil, as the processing is done fully automatically.

Table 2. Summary of total and partial times (working areas 1, 2, and 3) used in the acquisition and processing of data with the Faro Focus3D X 330 system and the proposed system.

	Working Area 1		**Working Area 2**		**Working Area 3**		**Total**	
Data Acquisition Time (min)								
FARO FOCUS X 330	200 10 scans		100 5 scans		220 11 scans		520	
Proposed System	11		8		12		31	
Processing Time (min)								
	User time	CPU Time	User time	CPU Time	User time	CPU Time	User time	CPU Time
FARO FOCUS X 330	35	61	22	40	40	75	97	176
Proposed System	0	605	0	421	0’	690	0	1716

f) 3.2. Points Cloud Resolution and Distribution

The point clouds generated by both systems had a non-uniform point-to-point separation, where the magnitude depended mainly on the capture distance between the device and the scanned area. In order to estimate an optimal value of this parameter, the average resolution values in the three study areas were calculated. For this, the minimum distances between all points of the cloud was obtained and their average value was calculated. However, in some cases, the mean density values may have been distorted; for example, if the point clouds were obtained by merging multiple point clouds. Therefore, in order to have an independent value that confirmed the previous results, a test was carried out with the proposed system on a flat 1 m^2 surface, following movement in a direction perpendicular to the optical axis of the main image (at 1 m distance). The outlier data were removed and the resulting points were projected onto the plane; with these points, we calculated the average resolution value, as was done in the first case. The results with the resolution values of each technique are shown in Table 3, in which the resolution obtained with the laser scanner in all cases was about 3.5 times higher than that obtained with the proposed system.

Table 3. Resolution of both systems in the work areas and resolution of an individual scan on a flat 1 m2 surface at 1 m distance. * according to manufacturer data.

Resolution in the Study Areas (mm)				
	Working Area 1	**Working Area 2**	**Working Area 3**	**Mean Resolution**
Faro Focus3DX330	0.4	0.4	0.5	0.4
Proposed System	1.6	1.2	1.4	1.4
Individual Scan Resolution(mm)				
	Number of Points		**Resolution**	
Faro Focus3DX330	11.108.889		0.3*	
Proposed System	576.255		1.3	

g) 3.3. Accuracy Assessments

Evaluation of the precision of both systems was carried out through the precise measurement of 150 control targets in both systems. At the same time, detailed calculation of a control area was carried out through circular statistics and, finally, the results were obtained of a series of comparative cloud cross-sections resulting from both systems. Figure 8 shows the results of the point clouds of both systems for the three work areas.

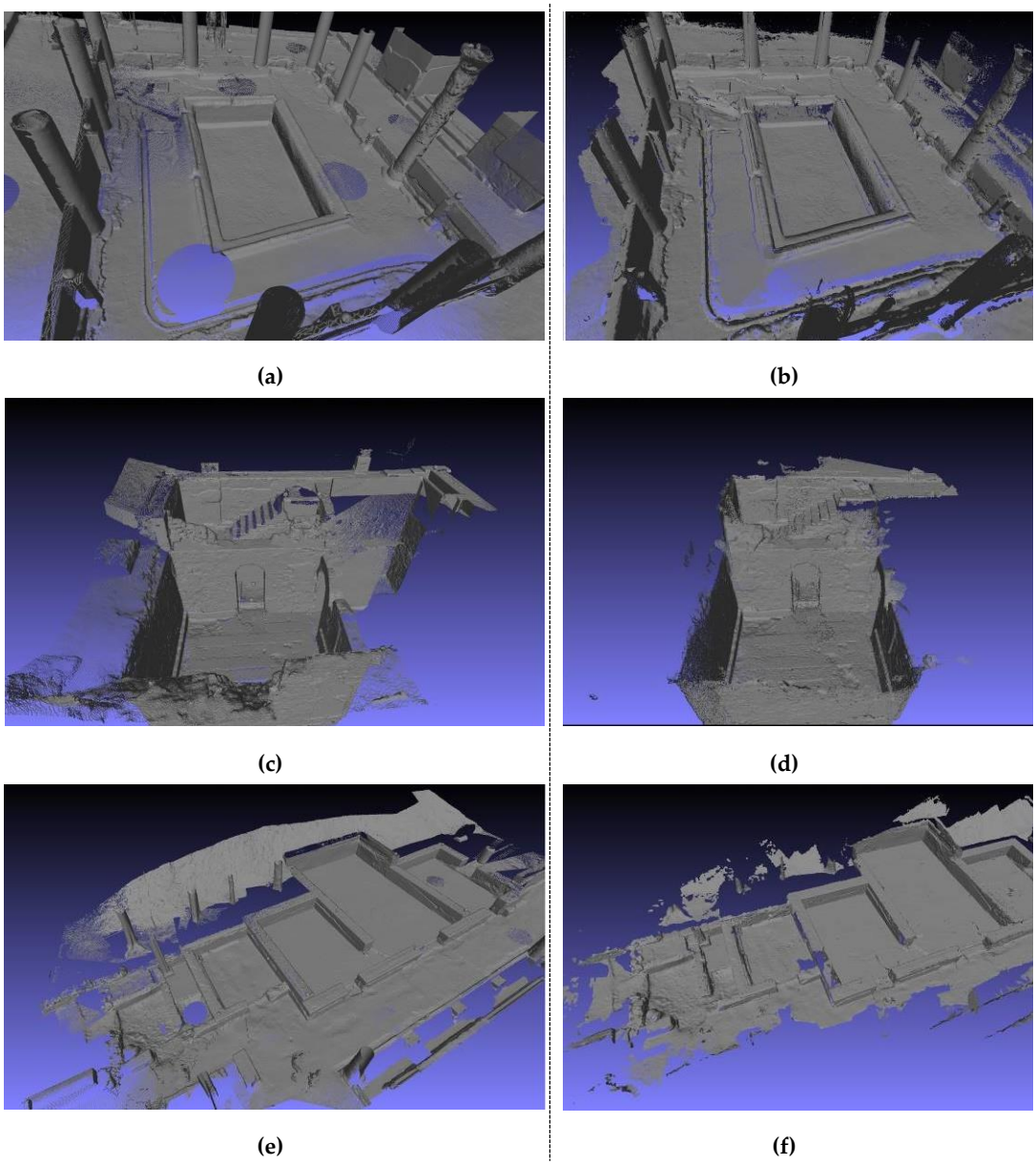

Figure 8. Comparison of the point cloud resulting from the LS Faro Focus3D X 330 (**a**,**c**,**e**) and the proposed system (**b**,**d**,**f**) of working area 1 (**a**,**b**), working area 2 (**c**,**d**), and working area 3 (**e**,**f**). Visualization was carried out in Meshlab [52] with a homogeneous normal calculation for both systems, with the aim of eliminating textures and favoring a balanced geometric comparison.

3.3.1. Control Points Accuracy Test

To assess the metric quality of the measurements, we analyzed the point clouds of each work area generated by both the proposed system and the Faro Focus3D X 330 system. For this, the coordinates of the 150 targets were used as control points, which were evenly distributed on pavement, walls, columns, baseboards, and so on. These coordinates were measured with the total station; in this way, each check point (target) had three coordinates: The coordinate obtained with the proposed system, that obtained with the laser scanner, and that with the total station. The results were compared following the method proposed by Hong, et al. [57]:

First, the precision of both the measurements made by the proposed system and by the laser scanner system were evaluated using the Euclidean average distance error (δ_{avg}).

$$\delta_{avg} = \frac{1}{n}\sum_{i=1}^{n} |Ra_i - T - b_i|, \quad (1)$$

where a_i is the i^{th} check point measured by the proposed system (or the scanner laser), b_i is the corresponding check point acquired by the total station, and R and T are the rotation and translation parameters for the 3D Helmert transformation, respectively.

Then, the error vectors in the x, y, and z directions and the average error were computed. Finally, the root mean square error (RMSE) was calculated as

$$RMSE = \sqrt{\frac{1}{n}\sum_{i=1}^{n} (a_i^t - b_i)^2}, \quad (2)$$

where a_i^t indicates the point transformed to the coordinate system of the total station.

The results obtained are shown in Table 4, where it can be seen that the accuracy values are very similar between both systems, taking into account that the observation distances used with the proposed system were in the range of 0.4–2 m.

Table 4. Accuracy assessment result for the Faro Focus3D X 330 and proposed system in working areas 1, 2, and 3 (unit: Millimeter).

	Faro Focus3D X 330				**Proposed System**			
Working Area 1								
	Error Vector X	Error Vector Y	Error Vector Z	Error	Error Vector X	Error Vector Y	Error Vector Z	Error
δ_{avg}				10				7
RMSE	9	6	4	7	6	4	4	5
Working Area 2								
	Error Vector X	Error Vector Y	Error Vector Z	Error	Error Vector X	Error Vector Y	Error Vector Z	Error
δ_{avg}				8				8
RMSE	5	9	4	6	4	6	6	6
Working Area 3								
	Error Vector X	Error Vector Y	Error Vector Z	Error	Error Vector X	Error Vector Y	Error Vector Z	Error
δ_{avg}				11				8
RMSE	5	8	7	6	6	4	5	5

3.3.2. Analysis of Systematic Errors Using Circular Statistics.

In the previous section, the metric quality of the point clouds was analyzed from the point of view in which only linear magnitudes were taken into account. However, we are obviating the possible existence of anisotropic behaviors, in which the magnitudes of error would follow a particular direction, which, in the case of the measurement instruments used (i.e., the laser scanner and proposed system), would confirm the existence of some systematic error between both systems, which should be corrected. To analyze this possibility, we resorted to circular statistics [58,59], designed exclusively for the analysis of directions or azimuths, whose basic descriptive statistics are as follows:

- Average azimuth ($\bar{\theta}$) obtained by the vector sum of all the vectors in the sample, as calculated by the following equations:

$$\bar{\theta} = arctan\frac{S}{C}\text{; with } s = \sum_{i=1}^{n}\sin\theta_i \text{ and } c = \sum_{i=1}^{n}\cos\theta_i \quad (3)$$

- Modulus of the resulting vector (R), obtained by the following expression:

$$R = \sqrt{c^2 + s^2}. \quad (4)$$

- Average modulus ($\bar{R}$), obtained by the following expression, where n is the number of observations:

$$\bar{R} = \frac{R}{n}. \quad (5)$$

- Circular variance of the sample (V), which is calculated by

$$V = 1 - \bar{R}. \quad (6)$$

- Sample standard circular deviation (υ), being

$$\upsilon = \sqrt{-2\,log(1 - V)}. \quad (7)$$

Concentration parameter (κ), which measures the deviation of our distribution from a uniform circular distribution. Its values are between $\kappa = 0$ (uniform distribution) and $\kappa = \infty$ (maximum concentration). For values of κ > 2, this parameter indicates concentration. The value of κ is calculated using the following expressions:

$$\kappa = \begin{cases} 2\bar{R} + \bar{R}^3 + \dfrac{5\bar{R}^5}{6} & \bar{R} < 0.53 \\ -0.4 + 1.39\bar{R} + \dfrac{0.43}{(1 - \bar{R})} & 0.53 \le \bar{R} \le 0.85 \\ 1/(\bar{R}^3 - 4\bar{R}^2 + 3\bar{R} & \bar{R} > 0.85 \end{cases} \quad (8)$$

Likewise, to check the uniformity of the data, uniformity tests such as Rayleigh, Rao, Watson, or Kuiper [59–61] were applied.

In our case, we carried out two data samples from both systems: One on a horizontal mosaic and another on a vertical wall with the remains of decorative paintings. In both cases, in the resulting point clouds, we identified a set of uniformly distributed common points; each set formed a data sample: Sample M1, in which points belonging to the vertices of the mosaic tiles were identified (42 points), and sample M2, consisting of points identified in the details and color changes of the paintings on the vertical wall (28 points). In both cases, we obtained their co-ordinates in each system using the CloudCompare (GPL Lisence) software.

With these data, we obtained the descriptive statistics of Table 5 and, further, we used the Oriana v4 software (Kovach Computing Services, Anglesey, Wales) to obtaining the data in Table 6, in which it can be observed that the values obtained for the mean modulus ($\bar{R}$) were relatively low (0.13 and 0.56 for samples M1 and M2, respectively), compared to the minimum and maximum values of 0 and 1 between which it can oscillate. Therefore, we can rule out the existence of a preferred data address. Likewise, the concentration parameter (κ) presented values of 0.27 and 1.35, far from the value 2, which would indicate the concentration of data. Another indicator of vector dispersion were the high values reached by the circular standard deviations (υ) of the samples (115.3° and 61.9°, respectively). Therefore, we are assured that, in both statistical samples, the error vectors were not grouped, they did not follow a preferential direction, and there was no unidirectionality in the data. Likewise, there was a high probability that the data were evenly distributed in M2, with a lower probability in M1. In Figure 9, the modules and azimuths referring to a common origin are represented to evaluate both their orientation and their importance. From the above, it follows that we can reject the existence of systematic errors between both systems.

Table 5. Main descriptive statistics of samples M1 and M2 (units: m).

Estatistical	Sample M1	Sample M2
Average	0.012	0.010
Standard error	0.001	0.001
Median	0.012	0.008
Mode	0.011	0.008
Standard Deviation	0.006	0.007
Variance	0.000	0.000
Mínimun	0.001	0.003
Máximum	0.025	0.032

Table 6. Results of the basic statistics and the tests of fit to the uniform distribution (Rayleigh test) in samples M1 and M2.

Statistical sample	Number of Observations	$\overline{\theta}$	$\overline{R}$	υ	κ	Data Grouped?	Rayleigh Test
M1	42	297.3°	0.13	115.3°	0.27	no	0.48
M2	28	133.5°	0.56	61.9°	1.35	no	$8.7*10^{-5}$

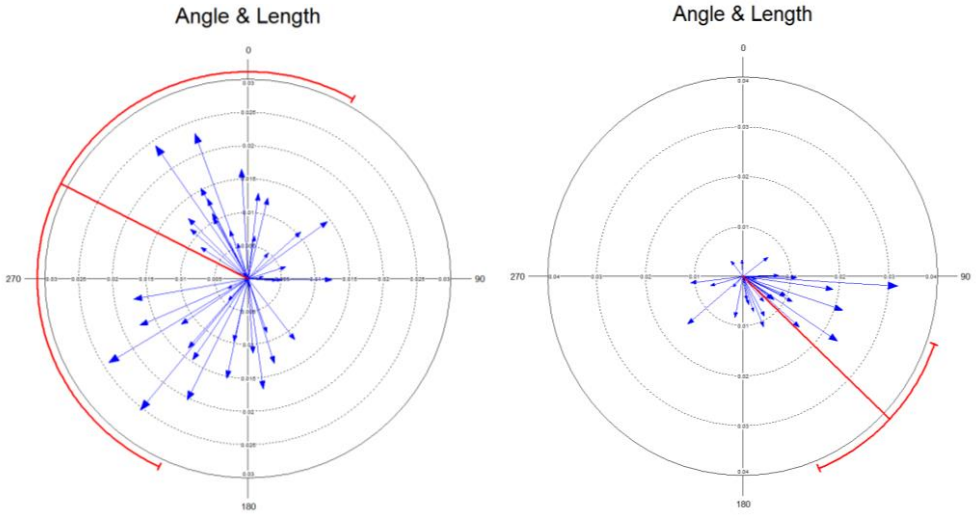

Figure 9. Graphs of distribution of angular and linear magnitudes in samples M1 and M2.

3.3.3. Cross-Sections

To complete the precision analysis of the proposed system, and for comparison with the laser scanner, horizontal sections were taken from the point clouds obtained with both systems in work zones 1 and 3. The section was formed by using a horizontal plane parallel to the horizontal reference plane at a height of 0.50 m from the ground and with a thickness of 2 cm. If we superimpose both sections, we obtain the results of Figure 10, in which the points in red correspond to the section of the cloud taken with the laser scanner and those in green to that of the proposed system, observing that they are practically coincident.

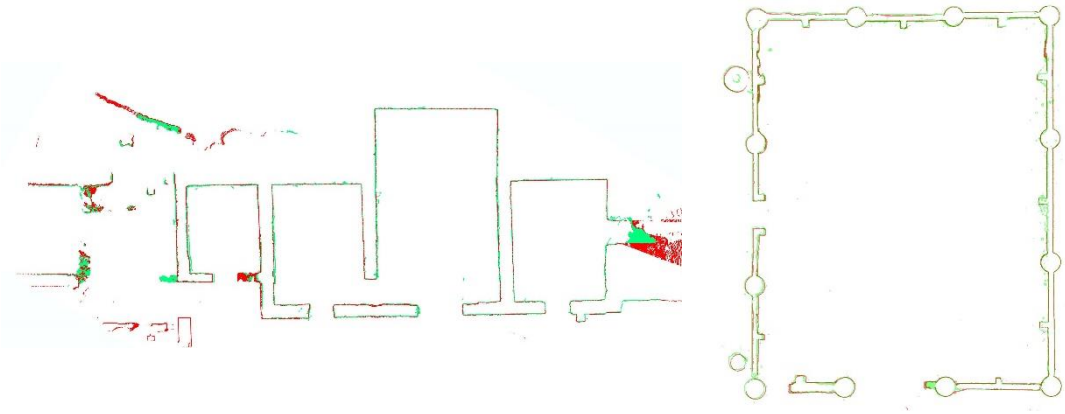

Figure 10. Overlapping cross sections generated in both point clouds, obtained using a horizontal plane at a height of 0.50 m above the ground. The result of the section of the cloud captured by the laser scanner appears in red, and that with the proposed system in green: Work zone 1 (**a**) at scale 1/235; and work zone 3 (**b**) at scale 1/180.

h) 3.4. Points Color Evaluation

We compared the quality and resolution of the color in both capture systems visually, with similar lighting conditions. To analyze the color of the point clouds of both systems, the resolution of the clouds must be considered, as a noticeable decrease in the resolution of one cloud with respect to another would indicate a loss of detail in textures. In parallel, the different characteristics of the images of each system must be also considered (Table 7); as well as the resolution of the cameras of both systems, as the capture distances were different in each system (maximum of 5 m and 2 m, respectively). Furthermore, in order to carry out an evaluation in comparative terms, the ground sample data (GSD) [44] of both systems was calculated at the same distance of 1.5 m: The GSD of the LS camera was 0.46 mm and the GSD of the videogrammetric system was 0.57 mm (see table 7). Given that the difference in GSD was sub-millimeter and that the resolution of both systems was high enough, despite their differences, it can be seen in Figure 11 that there were no significant differences in the results obtained in work areas 2 and 3.

Table 7. Main characteristics of the images registered by both systems.

Image Data Adquisition		
	Laser scanner Faro Focus x330	**Proposed system**
Format	.jpg	.jpg
Resolution (pixels)	20,198×8534	2560×2048
Images files size (Mb)	7.68	20
Acquisition time (seg)	180”	0.25“
GSD at 1.5 m distance.	0.46 mm	0.57 mm

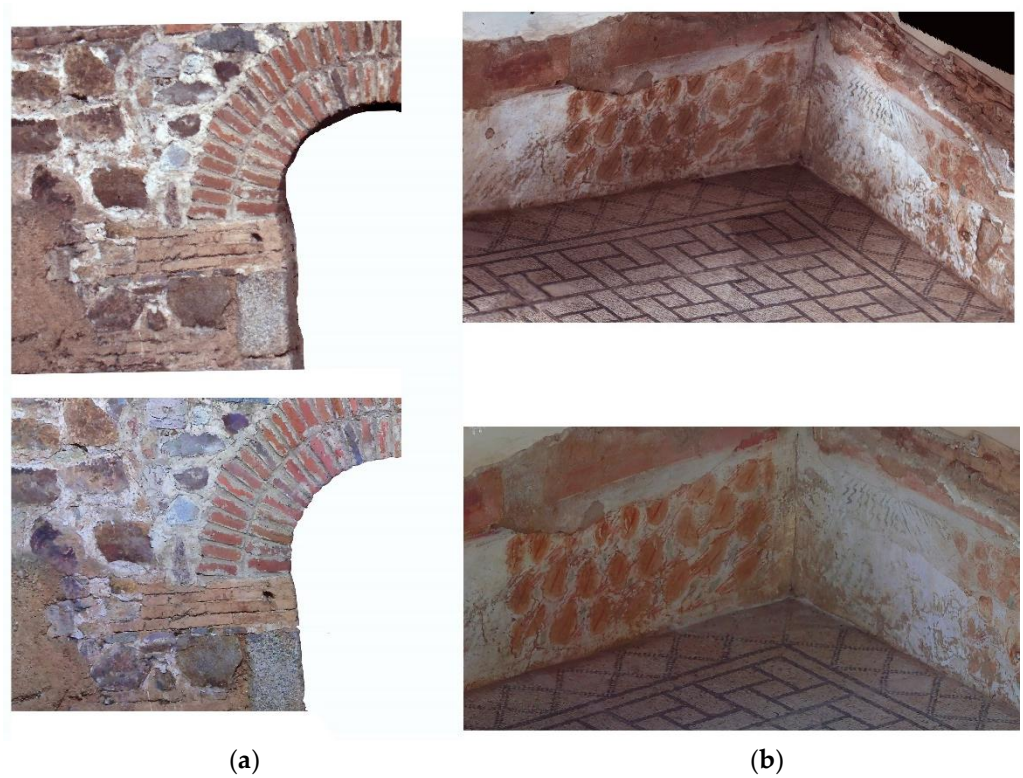

(**a**) (**b**)

Figure 11. Detail of the point clouds of work zones 2 (**a**) and 3 (**b**) obtained with both systems. The two images in the upper part belong to those obtained with the proposed system and those obtained with the Focus3DX330 are shown in the lower part.

4. Conclusions

In this article, we present a new data acquisition and 3D reconstruction device, which was evaluated and compared with the laser scanner Faro Focus3D X 330 in three case studies within the archaeological site Casa del Mitreo in Mérida, Spain.

The videogrammetric prototype that we evaluated in this paper represents an innovation, given that it is one of the first videogrammetric systems whose results are comparable to other professional capture systems. The image selection system, based on a 3D-based methodology according to Mur-Artal et al. (2017), allows for the choice of keyframes, which are more adjusted to photogrammetric needs Remondino et al. (2017). Furthermore, the filters that are applied and the generation of segments increase ostensibly the guarantee of success and precision of the procedure. Thanks to this smart and adaptable algorithm, longer and more complex captures can be scanned without orientation errors or areas without enough overlap, which hinder the relative orientation process of the images. This is an important innovation in this area, in our opinion.

In this article, we demonstrate the effectiveness of the prototype, comparing it with a laser scanner in three complex case studies. The capture times, in the case of videogrammetry, were 11, 8, and 12 min for case studies I, II, and II, respectively, which highlights the complexity and length of the trajectories (see Figure 7). We observe that the capture times of the videogrammetric system demonstrated a significant improvement over the scanner laser in a substantial way, being about 17 times faster on average. It also improves on the amount time a user needs to spend in post-processing the data, as the videogrammetric post-processing system is fully automatic. However, the processing time without human intervention is notably higher in the videogrammetric system than in the laser scanner, with processing performed by the LS being 10 times faster.

One of the most notable results of the experimental test is that the precision of both systems are very similar, yielding good precision on the measured targets and on the intermediate data reflected in the circular statistics, whose vectors did not show any significant deformation. The same applies to cross-sections and textures, the results of which were visually similar.

The videogrammetric prototype presented here is, therefore, proposed as a professional capture system with exceptional rapidity of capture and high precision for short capture ranges. Likewise, it can be used in connection with other orientation and 3D reconstruction algorithms, thus expanding its potential.

For future work, we will focus our efforts on reducing the processing time, as well as increasing the completeness of the data, trying to guide and assist users in the field to ensure that they have scanned the entire desired area, avoiding forgotten areas. Also, a new error analysis can be implemented to obtain a better understanding of the photogrammetric survey uncertainties, according to James M.R. et al. (2017)[62].

The videogrammetric method with high-resolution cameras here presented opens new opportunities for automatic 3D reconstruction (e.g., using drones), especially considering the need for quick capture and without prior flight planning; for example, in emergencies. Furthermore, it may be considered as complementary to MMS systems, where it can be used as a unique 3D reconstruction system or to complement Lidar systems.

Author Contributions: Both authors have contributed equally to this manuscript.

Funding: This research received no external funding.

Acknowledgments: They are grateful to the "Consorcio de la Ciudad Monumental de Mérida" for allow the works in this monument.

Conflicts of Interest: The authors declare no conflict of interest.

References

1. Zlot, R.; Bosse, M.; Greenop, K.; Jarzab, Z.; Juckes, E.; Roberts, J. Efficiently Capturing Large, Complex Cultural Heritage Sites with a Handheld Mobile 3D Laser Mapping System. *J. Cult. Herit.* **2014**, *15*, 670–678, doi:10.1016/j.culher.2013.11.009.
2. Wang; Chen; Zhu; Liu; Li; Zheng. A Survey of Mobile Laser Scanning Applications and Key Techniques over Urban Areas. *Remote Sens.* **2019**, *11*, 1540, doi:10.3390/rs11131540.
3. Mill, T.; Alt, A.; Liias, R. Combined 3D building surveying techniques laser scanning (TLS) and total station surveying for bim data management purposes. *J. Civ. Eng. Manag.* **2013**, *19* (Suppl. 1), S23–S32.
4. Omar, T.; Nehdi, M.L. Data Acquisition Technologies for Construction Progress Tracking. *Autom. Constr.* **2016**, *70*, 143–155, doi:10.1016/j.autcon.2016.06.016.
5. Moruno, L.; Rodríguez Salgado, D.; Sánchez-Ríos, A.; González, A.G. An Ergonomic Customized-Tool Handle Design for Precision Tools Using Additive Manufacturing: A Case Study. *Appl. Sci.* **2018**, *8*, doi:10.3390/app8071200.
6. Navarro, S.; Lerma, J.L. Accuracy Analysis of a Mobile Mapping System for Close Range Photogrammetric Projects. *Measurement* **2016**, *93*, 148–156, doi:10.1016/j.measurement.2016.07.030.
7. Ortiz-Coder, P.; Sánchez-Rios, A. A Self-Assembly Portable Mobile Mapping System for Archeological Reconstruction Based on VSLAM-Photogrammetric Algorithm. *Sensors* **2019**, *19*, 3952, doi:10.3390/s19183952.
8. Vanneschi, C.; Eyre, M.; Francioni, M.; Coggan, J. The Use of Remote Sensing Techniques for Monitoring and Characterization of Slope Instability. *Procedia Eng.* **2017**, *191*, 150–157, doi:10.1016/j.proeng.2017.05.166.
9. Puente, I.; González-Jorge, H.; Martínez-Sánchez, J.; Arias, P. Review of Mobile Mapping and Surveying Technologies. *Measurement* **2013**, *46*, 2127–2145, doi:10.1016/j.measurement.2013.03.006.
10. Boehler, W.; Marbs, A. 3D Scanning Instruments. Proceedings of the CIPA WG, 2002, vol. 6, no 9

11. Campi, M.; di Luggo, A.; Monaco, S.; Siconolfi, M.; Palomba, D. INDOOR AND OUTDOOR MOBILE MAPPING SYSTEMS FOR ARCHITECTURAL SURVEYS. *ISPRS - Int. Arch. Photogramm. Remote Sens. Spat. Inf. Sci.* **2018**, *XLII–2*, 201–208, doi:10.5194/isprs-archives-XLII-2-201-2018.
12. Luhmann, T. *Recent Developments in Close-Range Photogrammetry a Measurement Technology in Transition*; GIM International: Lemmer, The Netherlands, 14 February 2019.
13. Cerrillo-Cuenca, E.; Ortiz-Coder, P.; Martínez-del-Pozo, J.-Á. Computer Vision Methods and Rock Art: Towards a Digital Detection of Pigments. *Archaeol. Anthropol. Sci.* **2014**, *6*, 227–239, doi:10.1007/s12520-013-0147-2.
14. Martínez, S.; Ortiz, J.; Gil, M.L.; Rego, M.T. Recording Complex Structures Using Close Range Photogrammetry: The Cathedral of Santiago De Compostela. *Photogramm. Rec.* **2013**, *28*, 375–395, doi:10.1111/phor.12040.
15. Beretta, F.; Shibata, H.; Cordova, R.; Peroni, R.D.L.; Azambuja, J.; Costa, J.F.C.L. Topographic Modelling Using UAVs Compared with Traditional Survey Methods in Mining. *REM - Int. Eng. J.* **2018**, *71*, 463–470.
16. Kršák, B.; Blišťan, P.; Pauliková, A.; Puškárová, P.; Kovanič, Ľ.; Palková, J.; Zelizňaková, V. Use of Low-Cost UAV Photogrammetry to Analyze the Accuracy of a Digital Elevation Model in a Case Study. *Measurement* **2016**, *91*, 276–287, doi:10.1016/j.measurement.2016.05.028.
17. González-Aguilera, D.; Rodríguez-Gonzálvez, P.; Gómez-Lahoz, J. An Automatic Procedure for Co-Registration of Terrestrial Laser Scanners and Digital Cameras. *ISPRS J. Photogramm. Remote Sens.* **2009**, *64*, 308–316, doi:10.1016/j.isprsjprs.2008.10.002.
18. Liu, W.I. Novel Method for Sphere Target Detection and Center Estimation from Mobile Terrestrial Laser Scanner Data. *Measurement* **2019**, *137*, 617–623, doi:10.1016/j.measurement.2019.02.025.
19. Faro Focus. Available online: https://www.faro.com/products/construction-bim/faro-focus/features/ (accessed on 27 November 2019).
20. Leica RTC360. Available online: https://leica-geosystems.com/en-gb/products/laser-scanners/scanners/leica-rtc360 (accessed on 27 November 2019).
21. Riegl VZ-400i. Available online: http://www.riegl.com/nc/products/terrestrial-scanning/produktdetail/product/scanner/48/ (accessed on 27 November 2019).
22. Z+F Imager. Available online: https://www.zf-laser.com/z-f-imager-r-5016.184.0.html (accessed on 27 November 2019).
23. Vexcel Imaging Ultracam Mustang: Available online: https://www.vexcel-imaging.com/ultracam-mustang/ (accessed on 27 November 2019).
24. Leica Pegasus: Two. Available online: https://leica-geosystems.com/products/mobile-sensor-platforms/capture-platforms/leica-pegasus_two (accessed on 29 November 2019).
25. Trimble MX9. Available online: https://geospatial.trimble.com/products-and-solutions/trimble-mx9#product-downloads (accessed on 29 November 2019).
26. Leica Pegasus BackPack. Available online: https://leica-geosystems.com/products/mobile-sensor-platforms/capture-platforms/leica-pegasus-backpack (accessed on 29 November 2019).
27. Viametris BMS3D LD5+. Available online: https://www.viametris.com/backpackmobilescannerbms3d (accessed on 29 November 2019).
28. Trimble TIMMS Aplanix Indoor MMS. Available online: https://www.applanix.com/products/timms-indoor-mapping.htm (accessed on 29 November 2019).
29. Cura, R.; Perret, J.; Paparoditis, N. A Scalable and Multi-Purpose Point Cloud Server (PCS) for Easier and Faster Point Cloud Data Management and Processing. *ISPRS J. Photogramm. Remote Sens.* **2017**, *127*, 39–56, doi:10.1016/j.isprsjprs.2016.06.012.
30. Gruen, A.; Akca, D. Evaluation of the Metric Performance of Mobile Phone Cameras. In Proceedings of the International Calibration and Orientation Workshop EuroCOW 2008, Castelldefels, Spain, 30 January–1 February 2008.
31. Roberts, J.; Koeser, A.; Abd-Elrahman, A.; Wilkinson, B.; Hansen, G.; Landry, S.; Perez, A. Mobile Terrestrial Photogrammetry for Street Tree Mapping and Measurements. *Forests* **2019**, *10*, 701, doi:10.3390/f10080701.

32. Sirmacek, B.; Lindenbergh, R. Accuracy Assessment of Building Point Clouds Automatically Generated from Iphone Images. *ISPRS - Int. Arch. Photogramm. Remote Sens. Spat. Inf. Sci.* **2014**, *XL–5*, 547–552, doi:10.5194/isprsarchives-XL-5-547-2014.
33. Photogrammetry App. Company<: Linearis GmbH & Co. KG. Available online: http://www.linearis3d.com/ (accessed on 9 may 2020).
34. Contextcapture Mobile. Company: Bentley. Available online: www.bentley.com (accessed on).
35. Remondino, F.; Nocerino, E.; Toschi, I.; Menna, F. A CRITICAL REVIEW OF AUTOMATED PHOTOGRAMMETRICPROCESSING OF LARGE DATASETS. *Int. Arch. Photogramm. Remote Sens. Spat. Inf. Sci.* **2017**, *XLII-2/W5*, 591–599, doi:10.5194/isprs-archives-XLII-2-W5-591-2017.
36. Trimble MX7. Available online: https://geospatial.trimble.com/products-and-solutions/trimble-mx7#product-support (accessed on 27 November 2019).
37. Imaging Imajbox. Available online: https://imajing.eu/mobile-mapping-technologies/sensors/ (accessed on 27 November 2019).
38. Chiabrando, F.; Della Coletta, C.; Sammartano, G.; Spanò, A.; Spreafico, A. "TORINO 1911" PROJECT: A CONTRIBUTION OF A SLAM-BASED SURVEY TO EXTENSIVE 3D HERITAGE MODELING. *Int. Arch. Photogramm. Remote Sens. Spat. Inf. Sci.* **2018**, *XLII–2*, 225–234, doi:10.5194/isprs-archives-XLII-2-225-2018.
39. Chiabrando, F.; Sammartano, G.; Spanò, A.; Spreafico, A. Hybrid 3D Models: When Geomatics Innovations Meet Extensive Built Heritage Complexes. *IJGI* **2019**, *8*, 124, doi:10.3390/ijgi8030124.
40. Torresani, A.; Remondino, F. VIDEOGRAMMETRY vs. PHOTOGRAMMETRY FOR HERITAGE 3D RECONSTRUCTION. *Int. Arch. Photogramm. Remote Sens. Spat. Inf. Sci.* **2019**, *XLII-2/W15*, 1157–1162, doi:10.5194/isprs-archives-XLII-2-W15-1157-2019.
41. Gálvez-López, D.; Salas, M.; Tardós, J.D. Real-Time Monocular Object SLAM. *Robot. Auton. Syst.* **2016**, *75*, 435–449.
42. Scaramuzza, D.; Martinelli, A.; Siegwart, R. A Toolbox for Easily Calibrating Omnidirectional Cameras. In *2006 IEEE/RSJ International Conference on Intelligent Robots and Systems*; IEEE: Beijing, China, 2006; pp 5695–5701, doi:10.1109/IROS.2006.282372.
43. Zhang, Z. A Flexible New Technique for Camera Calibration. *IEEE Trans. Pattern Anal. Mach. Intell.* **2000**, *22*, 1330–1334, doi:10.1109/34.888718.
44. Luhmann, T.; Robson, S.; Kyle, S.; Harley, I. *Close Range Photogrammetry: Principles, Techniques and Applications*; Whittles Publishing: Caithness, UK, 2006.
45. Rublee, E.; Rabaud, V.; Konolige, K.; Bradski, G. ORB: An Efficient Alternative to SIFT or SURF. In *2011 International Conference on Computer Vision*; IEEE: Barcelona, Spain, 2011; pp 2564–2571, doi:10.1109/ICCV.2011.6126544.
46. Mur-Artal, R.; Montiel, J.M.M.; Tardós, J.D. ORB-SLAM: A Versatile and Accurate Monocular SLAM System. *IEEE Trans. Robot.* **2017**, *31*, 1255–1262.
47. Lowe, D.G. Distinctive Image Features from Scale-Invariant Keypoints. *Int. J. Comput. Vis.* **2004**, *60*, 91–110, doi:10.1023/B:VISI.0000029664.99615.94.
48. Dung, L.-R.; Huang, C.-M.; Wu, Y.-Y. Implementation of RANSAC Algorithm for Feature-Based Image Registration. *JCC* **2013**, *01*, 46–50, doi:10.4236/jcc.2013.16009.
49. Pierrot-Deseilligny, M.; Clery, I. Apero, an Open Source Bundle Adjustment Software for Automatic Calibration and Orientation of Set of Images. *Int. Arch. Photogramm. Remote Sens. Spat. Inf. Sci.* **2011**, *38*, 269–276.
50. Triggs, B.; Mclauchlan, P.; Hartley, R.; Fitzgibbon, A. Bundle Adjustment - A Modern Synthesis. In Proceedings of the ICCV '99 Proceedings of the International Workshop on Vision Algorithms: Theory and Practice, Corfu, Greece, 21–22 September 1999; Springer: Berlin/Heidelberg, Germany, 2000; pp. 198–372.
51. Rusu, R.B.; Cousins, S. 3D Is Here: Point Cloud Library (PCL). In *2011 IEEE International Conference on Robotics and Automation*; IEEE: Shanghai, China, 2011; pp 1–4, doi:10.1109/ICRA.2011.5980567.
52. PCL Point Cloud Library. Available online: http://pointclouds.org/ (accessed on).
53. Bradski, G.; Kaehler, A. *Learning OpenCV: Computer Vision in C++ with the OpenCV Library*, 2nd ed.; O'Reilly Media, Inc.: Newton, MA, USA, 2013.

54. Hoppe, H. Poisson Surface Reconstruction and Its Applications. In *Proceedings of the 2008 ACM Symposium on Solid and Physical Modeling - SPM '08*; ACM Press: Stony Brook, NY, USA, 2008; p 10, doi:10.1145/1364901.1364904.
55. Cignoni, P.; Callieri, M.; Corsini, M.; Dellepiane, M.; Ganovelli, F.; Ranzuglia, G. MeshLab: An Open-Source Mesh Processing Tool. *Eurographics Ital. Chapter Conf.* **2008**, *8*, doi:10.2312/LOCALCHAPTEREVENTS/ITALCHAP/ITALIANCHAPCONF2008/129-136.
56. Ranzuglia, G.; Callieri, M.; Dellepiane, M.; Cignoni, P.; Scopigno, R. MeshLab as a Complete Tool for the Integration of Photos and Color with High Resolution 3D Geometry Data. In *Archaeology in the Digital Era Volume II, e-Papers from the 40th Conference on Computer Applications and Quantitative Methods in Archaeology, Southampton, 26–30 March 2012*; Amsterdam University Press: Amsterdam, The Netherlands, 2013; pp. 406–416.
57. Hong, S.; Jung, J.; Kim, S.; Cho, H.; Lee, J.; Heo, J. Semi-Automated Approach to Indoor Mapping for 3D as-Built Building Information Modeling. *Comput. Environ. Urban Syst.* **2015**, *51*, 34–46, doi:10.1016/j.compenvurbsys.2015.01.005.
58. Fisher, N.I.; Lewis, T.; Embleton, B.J.J. *Statistical Analysis of Spherical Data*, 1st ed.; Cambridge University Press: Cambridge, UK, 1987, doi:10.1017/CBO9780511623059.
59. Polo, M.-E.; Felicísimo, Á.M. Full Positional Accuracy Analysis of Spatial Data by Means of Circular Statistics: Analyzing the Positional Error in Spatial Data. *Trans. GIS* **2010**, *14*, 421–434, doi:10.1111/j.1467-9671.2010.01223.x.
60. Fisher, N.I. *Statistical Analysis of Circular Data*, 1st ed.; Cambridge University Press: Cambridge, UK, 1993, doi:10.1017/CBO9780511564345.
61. Oden, N. Circular Statistics in Biology. Edward Batschelet. *Q. Rev. Biol.* **1983**, *58*, 312–312, doi:10.1086/413381.
62. James, M.R.; Robson, S.; Smith, M.W. 3-D Uncertainty-Based Topographic Change Detection with Structure-from-Motion Photogrammetry: Precision Maps for Ground Control and Directly Georeferenced Surveys: 3-D Uncertainty-Based Change Detection for SfM Surveys. *Earth Surf. Process. Landf.* **2017**, *42*, 1769–1788, doi:10.1002/esp.4125.

4.

Sección III: Aplicación tecnológica en medicina.

Esta sección contiene el artículo: "Automatic 3d dense reconstruction using VSLAM and photogrammetric algorithms: approach in the temporomandibular arthroscopy case." Presentado el 23 de junio de 2020 en la revista Measurements..

Resumen

El artículo analiza las principales técnicas fotogramétricas utilizadas para reconstrucción 3D a partir de las distintas tipologías de endoscopias. Entre las técnicas principales se encuentran "*Shape-from-shading"* en la que se realiza el modelo 3D a través del movimiento del foco de luz respecto del objeto, y la técnica "*Shape from motion"*, en la que el elemento móvil es la cámara respecto del objeto a reconstruir. Dentro de la evaluación contextual, se hace referencia al caso que nos ocupa: a la reconstrucción 3D a partir de artroscopias sobre la articulación temporomandibular (ATM), cuyo caso concreto apenas existe literatura previa. La artroscopia es una cirugía de mínima invasión que, en el caso de la ATM, tiene un entorno o espacio de actuación minúsculo, de apenas unos 3 cm^2 y en una zona donde es fácil encontrar movimientos del paciente durante la cirugía y, para que la ésta pueda realizarse, necesita ingresarse suero. Todos estos elementos son puestos de manifiesto como dificultades para una reconstrucción 3D de calidad.

Primeramente se analiza el artróscopo, que es la cámara que se utiliza en esta intervención, la cual es calibrada. Las primeras pruebas se realizan sobre simuladores, que son réplicas de la mitad de la cabeza de una persona con una reproducción de la articulación ATM idéntica en forma y texturas, para que se puedan realizar intervenciones y prácticas sobre dicho simulador con el máximo realismo.

En el texto se define la metodología a seguir, basada en la tecnología desarrollada en esta Tesis Doctoral, que integra VisualSLAM y un procedimiento para la reconstrucción 3D, además de la aplicación de una serie de filtros para afinar la selección de imágenes extraídas del video. En este caso, solo existe una cámara y por tanto las imágenes para realizar la localización simultánea, como para la posterior reconstrucción 3D, parten de la misma cámara y del mismo video. Esto es una pequeña novedad en cuanto al procedimiento metodológico que abre un nuevo campo y amplia el número y tipología de aplicaciones. La metodología de selección de imágenes diseñada detecta si hay movimientos en las articulaciones y elimina dichas imágenes por contener un número de puntos homólogos por debajo de la tolerancia, después del filtrado RANSAC. Esto significa que dicha tecnología actúa como garante de que los grupos de imágenes seleccionados puedan ser reconstruidos con ciertas garantías de precisión y óptima geometría de la toma. Para que este procedimiento pueda hacerse con éxito, en algunos casos se le aplica un filtro para la extracción de características, que permite obtener grupos de imágenes más amplios en sets de imágenes donde, previamente, no se podía extraer un grupo válido.

El procedimiento se aplica a distintos casos de estudio: El caso 1 se realiza sobre un simulador, y se genera una reconstrucción 3D de una porción de la fosa y del disco articular de la ATM. La reconstrucción consta de una nube de puntos y una malla con textura, y, para poder realizar un estudio métrico, se calcula un mapa de alturas (hipsometría) y una sección longitudinal. De forma análoga se procede con el caso 2, pero en este ejemplo se realiza sobre una artroscopia real en un paciente vivo y en un entorno hospitalario. Se reconstruyen dos partes de una adherencia y se generan las nubes de puntos, el mallado, un modelo de tipo "*wireframe"* y un mapas de alturas. En uno de los casos se realiza el mapa de alturas sobre la imagen preprocesada con el filtro de Wallis.

Se concluye que el procedimiento es novedoso y se obtienen resultados óptimos y esperanzadores, aún con grupo de imágenes muy pequeños por las difíciles condiciones de toma de este tipo de intervenciones.

Artículo III: Automatic 3d dense reconstruction using VSLAM and photogrammetric algorithms: approach in the temporomandibular arthroscopy case.

Article

Automatic 3d dense reconstruction using VSLAM and photogrammetric algorithms: approach in the temporomandibular arthroscopy case.

Pedro Ortiz-Coder [1], Florencio Monje Gil[2] and Alonso Sánchez-Ríos[1,*]

1 University Centre of Mérida, University of Extremadura, 06800 Mérida, Spain;
2 Department of Oral and Maxillofacial Surgery, University Hospital of Badajoz, Badajoz 06001, Spain.
* Correspondence: peorco04@alumnos.unex.es (P.O.-C); schezrio@unex.es (A.S.-R.); fmonje@oralmaxilofacial.com (F.M.G).

Abstract:

3D reconstructions through the different types of endoscopies is a complex issue that is becoming increasingly relevant in the field of computational vision. The different types of endoscopies and the places where they can be applied, force the use of different strategies to obtain good results. This article shows a methodology for 3d reconstructions of the temporomandibular joint (TMJ) through arthroscopies. For this, VisualSLAM and a series of filters are used for images selection, and a precise 3d photorealistic reconstruction methodology is also explained in this manuscript. Despite the fact that, in this case, the joint is really small (3cm^2) and the conditions, especially in living patients, are complex, given small movements, wet areas and reflections, different photorealistic 3d models are generated, in addition to different geometric analysis. The results represent an important advance, since they are the first time that a photogrammetric 3d reconstruction of this joint has been performed on living patients, under these conditions.

Keywords: 3D reconstruction; endoscopy; arthoscopy, videogrammetry, VSlam.

1. Introduction

Minimally invasive surgery has been significantly improved in recent years, among other reasons because very small cameras are being used. Endoscopy consists of a camera which is inserted in the body through a small incision or also through a natural body hole, to obtain images and videos of different parts of the internal organs and obtain a diagnosis or guide and help the surgeon in operations [1].

The visual environment of A endoscopy is usually about narrow areas, tissues that may move easily, bones, blood, and other fluids. In those cases a light focus is located in the same place as the camera or, otherwise, it is located in another cannula or artefact but, in this case, it is also mobile. In order to generate a 3d reconstruction of internal parts of the body, multiples approaches has been developed to date [2], [3]–[5]. But there is a wide state of the art depending on whether the operation is performed on corpses [6] or on living people[6], or if the operation is carried out in wider environments of the human body [4] or in smaller areas [6], but also depend on the 3d reconstruction methodology, that can be applied depending on the concrete case of endoscopy, for example, shape from shading [7]–[10] and shape from motion types [5], [10]–[12]. Shape from shading type obtain the 3d reconstruction analyzing the shadows of the elements while the light focus is moving; and the shape from motion methodology can

reconstruct an element moving the camera respect to the element, in this case, the theory indicates that the light focus should be fixed. The endoscopy environment, especially if it is done manually, is not suitable for any of the techniques previously mentioned, since the tissues and all the internal elements move, to a greater or lesser extent, during the intervention, and this includes the camera and light bulb. In addition there are reflections of humidity in the surfaces, blood and other remains in suspension. For that reason, there are big efforts of the computer vision community to improve the results in 3d reconstruction in this scenario[13], [14].

One of the concrete kinds of surgery which use endoscopy is the arthroscopy[1], [15]; this is a minimally invasive surgical procedure which uses a camera with a long, small, and thin lens, called endoscope, which is inserted in the human body through a small incision. This technique is used for diagnosis and to repair a different kind of joint tissues. This technique is relatively new being invented in the 1960s by Masaki Watanabe. In this paper, the arthroscopy is applied in the temporomandibular joint (TMJ) (see figure 1). Arthroscopy [8] of the temporomandibular joint (TMJ) is a technique that, on one hand, brings us close to the knowledge of the psychopathy of this joint and, on the other, has revolutionized the treatment of this joint for essentially what is known as the TMJ pain-dysfunction syndrome (TMDS). This article describes the 3D reconstruction of different parts of the TMJ through the use of arthroscopic surgery. The main objectiv to perform 3D reconstruction is to improve the visualization of all parts of the TMJ measuring different parameters inside of this joint. On the other hand these parameters could be prognosis factors in the result of arthroscopic surgery.

A 3D reconstruction based on arthroscopies can be found in [6] where the surgery is done in a cadaver knee and the incision is done via robotic procedures, the 3d reconstruction is based on multiview stereo (MVS) techniques, generating the surface through the motion of the camera. Structure from Motion (SfM) 3d reconstruction can be found also in the literature [4] through the different kind of endoscopies like laparoscopies [12], gastric endoscopies [4] or other cases[3], [5]. The literature of 3d reconstruction in the temporomandibular joint through arthroscopy with manual procedures in living patients is very limited. This operation requires extensive training and skills of the surgeon, given, among other reasons, the little space available to operate. In the same manner, the video captured through the arthroscope show small and narrows spaces, with hidden areas, provide to the joint topography characteristics, in addition to the general endoscopies complexities. Endoscope camera has a pretty narrow and long lens which the light focus is coaxial to the camera axe and, therefore, the lens and the light coexist in this same small cannula. The camera can focus automatically the different surfaces, adapting rapidly to the distance; this effect generates usually unfocused frames that need to be deleted.

Visual simultaneous localization and mapping (VSLAM) is a known technique in computer vision which has been improved in the latest years [16], [17]. In some cases the VSLAM has been used, together with a designed algorithm[18], [19], to select the most optimal images for 3d dense reconstruction using structure from motion techniques. Automatic images selection for a posterior relative orientation and 3d model generation can be done through three methodologies: 1. Extracting 1 frame each *n;* This is the most basic method but may have problems if there are changes in the speed or in the geometry. 2. 2D-feature-based [Guan et al, Nocerino et al]; this methodology analyzes the number of key points between the images based on the different descriptors and choosing the best-related images. 3. 3D based selection [Resch et al.]; the algorithm designates some frames as keyframes based on common tie points in the 3d sparse reconstruction. Thus, the geometry is taken into consideration. A good image

selection based on 3d geometry is necessary to guarantee the posterior 3d reconstruction provide to in photogrammetry an optimal images pose geometry [20] is required to guarantee an accurate relative accuracy and an optimal posterior 3d reconstruction.

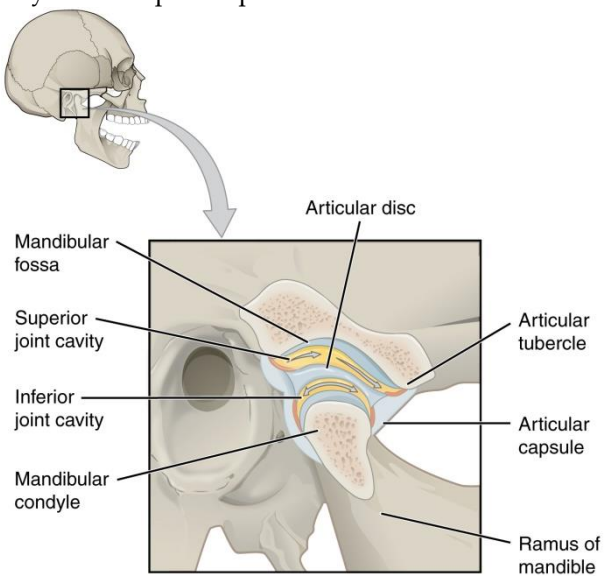

Figure 1. *Temporomandibular Joint. Parts.*[21]

This paper describes a methodology for an automatic 3D reconstruction in temporomandibular articulation using arthroscopy. This surgery area [1] in this joint is very small, no higher than 2 cm^3. The operations in the temporomandibular joint through arthroscopy can be done manually or using a robot [6]. In this case, only manual procedures are being carried out. The arthroscope camera is calibrated and the images captured through video are selected based on VSLAM and an algorithm filters-based are applied. The manuscript details the procedure of how the point cloud, the mesh and the texture mapping have been generated. Different results are exposed to reconstructions made on simulators and also on a living patient case. The innovation lies in the 3d reconstruction of such a small and complex articulation and the application of an image selection methodology based on VSLAM and image filters that guarantee optimal images for relative orientation using small segments of images and preprocessing the frames selected to extract more features and improve the results.

2. Materials

The arthroscopy instruments used in the surgery in this paper is from the Striker brand (Kalamazoo, Miami,USA). The arthroscopy instruments consist of multiples materials[22], small instruments and tools and mechanics systems for fluid management between others. In the arthroscopy surgery two thin cannulas which are inserted in the TMJ, and which inside the cannulas different crossblades with tools are also introduced. In one of the cannulas the arthroscope camera is inserted; the camera consists on a camera head, C-Mount coupler, a cable, a soaking cap and a connector; but the part of the camera inserted into the cannula is part of the lens: it's a rod of 5cm long. The rod contains the image rays the camera sensor, and it has 2mm of diameter. This lens consists of [1][22] a series of glass cylinders, convex and wide with small spaces of air between the lenses. This system improves the light-transmission of the endoscope and expands the field of vision. The magnification of the object can vary from 1 to 30 times the original size, depending on the type of arthroscope used and the distance of the object to the tip of the arthroscope. The optical parts should be handled with extreme care to avoid breakage

during surgery as well as during subsequent manipulation of washing and sterilization. The system of lenses is surrounded by glass fibres that transmit light from a source to illuminate the joint. This fibre-optics cable, which can be sterilized, needs to be inserted into the arthroscope. The light source should be capable of providing a colour temperature of 5000 K. (see figure 2). The camera has a 1/3" CCD sensor (4.8 x 3.6 mm) into the camera head and the resolution is 1100x600 [22]. The arthroscope camera varies in diameter and angle, but an arthroscope measuring 1.7 to 2.3 mm diameter and with a visual angle of 30º is desirable.

The video framerate is 25 frames per second, and its recording is saved in *mov format. The frames of the video have a final useful resolution of 570 x 720 and a field of view of 48˚x 60˚.

To practice the arthroscopy technique, a simulator is highly recommended provide the difficulties of the technique and the skills required. This simulator [23](see figure 2) consist of a highly realistic reproduction of the midface of the patient, with real dimensions, manufactured with different plastics and silicon-based materials, that reproduce the internal temporomandibular aspect, cavities and elements to allow the surgeon have as most realistic experience as possible. In this investigation, two simulators have been used for 3d reconstruction to obtain a concrete knowledge of the spaces and camera movements, available in the temporomandibular joint.

In this paper are exposed to different 3d models results from real arthroscopies carried out on living patients at the hospital environment. In both cases, in a simulator and in real cases, the 3d reconstruction has been done using the same arthroscope camera. During the arthroscopy operation, the camera has been focused carefully to the interested area and advance slowly from one extreme to the other and going back to the previous places. In this period time, no serum have been introduced and the patient has not been moved.

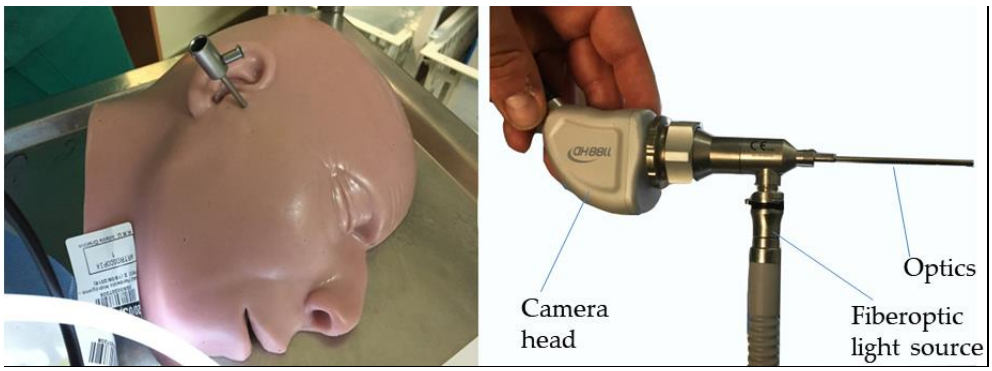

Figure 2. *Simulator for TMJ arthroscopy practice (left). Arthroscope Camera (right).*

The computer used for the 3D reconstruction in this project was in the notebook ASUS Strix Intel Core i7-7700HQ @2.80GHz, RAM 16GB and the hard disk have SSD technology; SSOO Windows 10 Home.

3. Methodology

In this section, we describe the different phases (Figure 3), from the data acquisition using the arthroscope camera to obtain the final result.

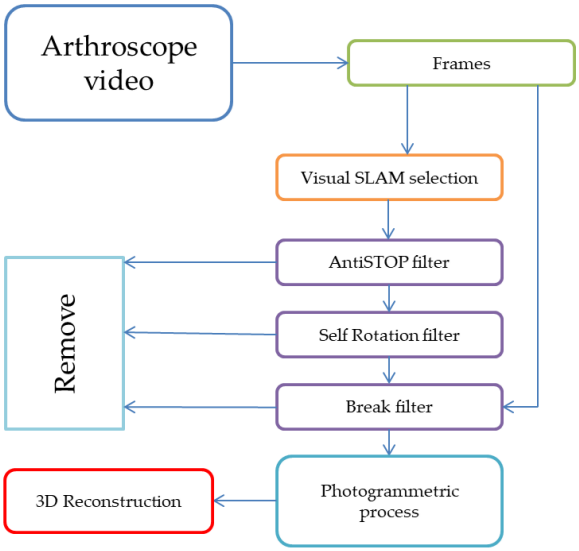

Figure 3. *Phases of the algorithm for 3d reconstruction from the arthoscope video.*

2.1. Data acquisition

Camera calibration. The arthroscope camera is the only monocular sensor used for data acquisition in this procedure. Due to there is no way to obtain a real dimension inside the body, no scale assignation is possible too, for this reason, a small rule with millimetres division has been developed to being introduced for the other cannula and, in this way, the arthroscope camera can capture the rule and obtain a real dimension of de scenario.

Camera internal calibration is needed to perform the bundle adjustment and the posterior 3d reconstruction. A small checkerboard was manufactured for this purpose, considering the usual focus distance of the arthroscope and its depth of vision, thus, the checkerboard size was 2cm x 2cm. The arthroscope camera captured the checkerboard from different angles, after that, the more representative frames were chosen manually and a calibration procedure [23] was carried out using the software Matlab (Mathworks). The parameters obtained was: focal length, the principal point, radial distortion and tangential distortion.

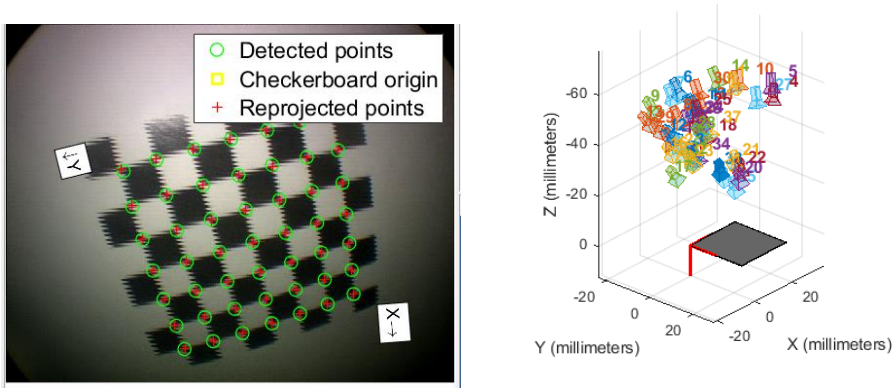

Figure 4. *Camera Calibration. Checkerboard frame with detected corners (left), camera pose of each frame used in the calibration (right).*

During the arthroscopic surgery, the video is recording and its selected the period time where the surgeon movement was done for 3d reconstruction to avoid process unusable parts. The video selected is inserted in the algorithm which will transform it in frames (25 frames/second).

2.2 images selection

Due to the framerate of the endoscope video camera, there are many frames which will not be used for photogrammetric 3d reconstruction. To obtain an accurate relative orientation and 3d reconstruction, the selection of an optimal image should be carried out. We have used ORB-SLAM[17] to compute the keyframes of the data set, but also to compute an initial camera pose and to assign a UNIX time of each keyframe. This procedure is carried out in three phases [19]: In the first, called tracking, the positions of the cameras are calculated to generate the keyframes, which will be part of the calculation process; in the second, called local mapping, keyframes are optimized and redundant keyframes are eliminated; in the last, the loop closing phase, the areas where the camera had previously passed, are detected and the trajectory is recalculated and optimized. The process generates a file with the camera pose and time UNIX for each keyframe.

Filters Applications

The keyframes and the information computed are used in the second step of the methodology: filter application. Provided to the quality of the images from the arthroscope are usually textureless or may have moved (suspension) elements, between other problems, extra filtering is necessary in this case, to remove undesired images. In some cases, if the texture is too homogeneous to obtain good enough tie points, the frames are preprocessed using the Wallis filter[25] (see figure 5).The methodology has applied 3 different filters: 1) AntiStop Filer; this filter computes the proximity between projection centres in relation to the UNIX time of each frame. If the distance between two consecutive centres is closer than a tolerance value (D_{min}) and the time difference is higher than a Time tolerance value T_{max}, those frames will be considered as the endoscope have been stopped and those frames will be deleted. 2) Self-rotation filter. This filter removes the images if the camera position has not to change more than a distance tolerance (D_{min}) but there was a rotation value higher than a R_{max} in the 3 axes (ω,φ,κ). 3) The break filter consists on detect if there are bad correlation between two images and, in this case, insert images between them. To detect the bad correlation, tie points [SIFT] are analyzed and if the number of points is less than a tie points tolerance value (Tp_{min}) and if there is a quadrant of the image with less than the 10% of the homologous points, this image will be considered with bad correlation and, in consequence, some images will be inserted between them. A new analysis will be carried out with the two old images and the new ones, and if the correlation is good enough now, the process will continue, instead, if the correlation is bad, the data set need to be divided in this point and the posterior photogrammetric process will be applied to the two different sets of images separately, losing the common reference system between the two groups of frames.

Figure 5. *Images preprocessing example to extract information from smooth areas. RGB image (left), Wallis filtered image (right)[25], [26]. The image is from the TMJ.*

2.3 Points cloud generation, mesh and texture mapping

All frames selected in the previous filters will be processing for 3D reconstruction. firstly, tie points are being computed for all the images selected using SIFT[27] descriptor and random sample consensus (RANSAC)[28] to filter homologous points and improve the correlation. In this case, the tie points computing strategy is based on find homologous points confronting all the images between themselves. Once tie points are being computed, the algorithm computes the relative orientation through direct solution [29] to obtain a first approximation to the epipolar geometry value, and then a bundle adjustment [30] is applied for a values iteration still obtain the best relative orientation values. The bundle adjustment generates a sparse point cloud together with all the camera pose in the same reference system. Finally, multiple depth maps are computed from the oriented images [28], and a unify dense points cloud is generated based on the depth map transformation and unification.

The complexity of the 3d reconstruction in the arthroscopy provided to the reasons exposes in the introduction, it can be found hanging points or outliers into the dense points cloud generated. To improve the results and remove the outliers, a statistical outliers filter [32]is applied before mesh generation. Meshing consists of an irregular triangulation of the points to generate a continuous surface; this action will help to a better interpretation of the data and a posterior texture mapping. Before meshing normal vectors are computed [33]. Then, poisson surface reconstruction [34] is applied to generate a complete mesh 3d model. In this point, the images are ortho-rectified [35] based on the camera calibration parameters, explaining in point 2.1. And finally, images and camera poses are taking into consideration, together with the normal vectors and the triangles surfaces and its positions to create the texture mapping[35] 3d model. In this phase, the images are orthoprojected on to the 3d mesh generated; the images are blended to avoid images discontinuities.

But performing a 3D reconstruction and obtaining good results in living patients requires some care and measures that must be taken while performing arthroscopy and image processing. During the arthroscopy surgery, the surgeon has to stop to introduce serum during the 3d reconstruction period. The surgeon needs to be able to don´t move the patient during this time and the movement of the arthroscope need to be slowly and well focused. In the postprocessing phase, we have to consider that, even with the surgeon cares, always there are small movements of the patient, especially when the arthroscope trajectory is long; for this reason, the VSLAM and filters images selection will detect this fact and the algorithm will create automatically small segments of images that guarantee a good relative orientation and posterior better results.

4. Results

Two arthroscopies have been processing in this section: the case 1 were done on to a simulator and the second arthroscopy were applied in a real case on to a living patient in the Hospital Infanta Cristina (Badajoz), Spain. The second arthroscopy on A real case is divided in two cases: case 2 is a colour based 3d reconstruction of one part of the TMJ adherence, and the case 3 were done using preprocessing images on to a bigger part of the same TMJ adherence. Provide to the homogeneous textures of the frames in the case 3, we have decide preprocess the images applying Wallis filter[25] [26] to extract more features of the frames and improve the 3d reconstruction in the homogeneous areas. The preprocessed images change the aspect of the images on to grayscale and, consequently, the texture aspect of the 3d model is also with the same characteristic. In this case, the texture has been sacrificed for better geometry.

TO carry out an analysis of the results of the 3d reconstruction, and to be able to observe possible deformations, as well as to do any kind of measurements, the creation of a hypsometric map and the generation of one or more sections, among other measures, IS proposed. In the hypsometric map, the height is represented by colours, thus, each colour represents a concrete height value(see figure 6). Also, as another way of representation, the normals may be activated to introduce lights and shadows in the topography details to increment the visualization details of the 3d model; this option can be seen in figure 6. All the 3d representations and geometry analysis in this section have been done using the software CloudCompare[36]. Cross-sections (see figure 6) is an effective tool to obtain the geometry of the joint concretely. A perpendicular plane is defined longitudinally onto the TMJ, to obtain topography of the joint. The cross-sections are also a simple tool that can be used to compare with other 3d models or other measurements.

The first result obtained from the photogrammetric processing is a points cloud. In table 2 can be seen the details about this procedure in the practical case. After the point cloud generation, a mesh with texture is generated; this hyperrealistic 3D model is one of the most interesting tools for 3D analysis, provided to the quality and resolution; It allows a detailed and realistic visual representation, in such a way that the human being can understand it as a real object. The mesh is formed by thousands of triangles (see table 1) and in this case, the edges have the colour textures as can be seen in figure 6.

Table 1. *3d reconstruction process information.*

	Case 1	Case 2	Case 3
Images type	RGB	RGB	Applying Wallis filter
Arthroscopy video segment (seconds)	7”	5”	6”
Total frames	175	125	150
Keyframes selected after filters	59	49	55
3d reconstruction time	250”	191”	237”
Number of Points	65.025	45.025	49.254
Number of faces	58.107	35.054	41.258

The resolution of the points cloud processed in these sections depends on the number of keyframes processed and the mean distance of the camera to the object. to determine a point to point distance, it has been determined a mean distance from the arthroscope camera to the TMJ tissues as 9mm, thus the mean point to point distance of the 3 cases is 0,07mm. In the same line, the distance that one pixel takes up in the reality was computer through the Ground Sample of Data (GSD) [20]. The GSD was defined considering the mean distance from the camera to the tissues, the arthroscope images resolution, and the field of view of the camera (see table 1). Based on those values the mean GSD value for those three cases is 0.012mm.

case 1 was done on to a simulator, on the TMJ cavity and the joint disk, and simulating the light and movements that can be done in the reality in those circumstances. The selected section of the arthroscopy video spent 6 seconds and 59 keyframes have been selected for the 3d modelling. The 3d model generated spent 4min in the 3d reconstruction shown in figure 5 represented by a hyperrealistic 3D model.

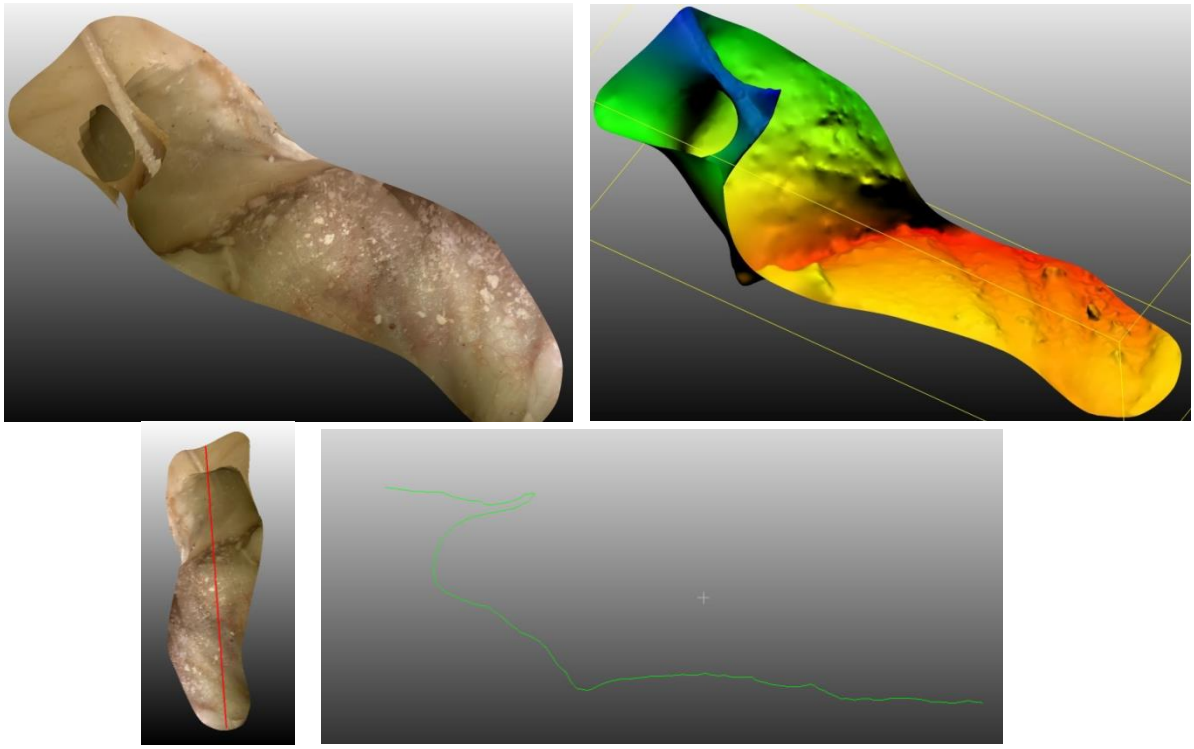

Figure 6. *ATM photorealistic 3d reconstruction of a simulator(Top left). 3D model perspective with the hypsometric map of the simulator(top right). Longitudinal Section of the ATM reconstruction(botton).*

Shown below two 3d reconstructions (case 2 and 3) have been done on the same arthroscopy on a living patient. Both are parts of the same TMJ adherence. In the case 2, (figure 7) A hyperrealistic 3D model has been generated; this kind of 3d models join and blend multiples images for texture mapping, generating high-quality textures results, in this case, 12 megapixels. A hypsometric map and a wireframe view of case 3 are shown in figure 8.

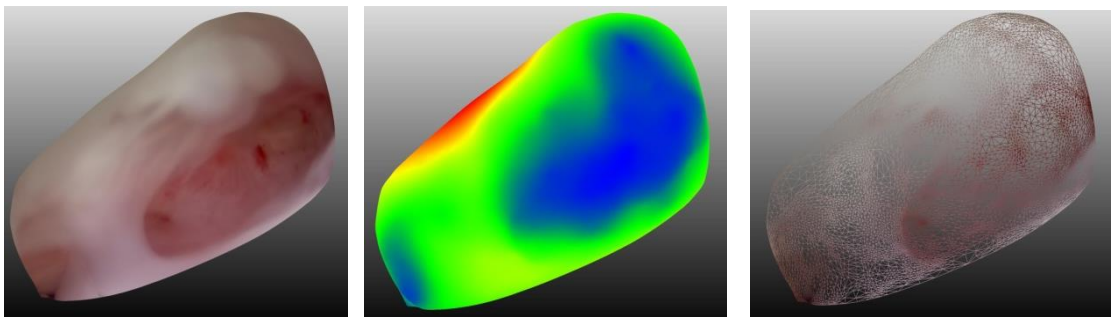

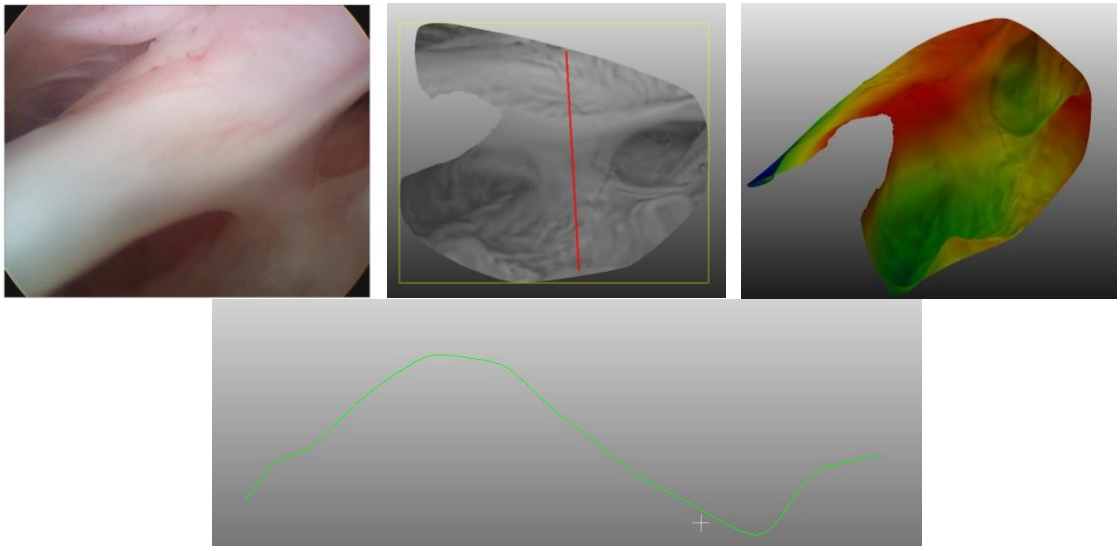

Figure 7. TMJ Adherence 3d reconstruction. photorealistic 3D model (Top left), hypsometric map (Top centre) and wireframe model (Top right). Original frame of the case 3 (Center left), Case 3 3d model of the adherence with Wallis texture mapping (Center center), Hypsometic 3D map of the Case 3 (Center right). Cross section of the case 3 (Botton).

5. Conclusions

This paper presents an approach for automatic 3d reconstruction from arthroscope videos in A temporomandibular joint environment. The methodology describes firstly the images selection used, which is based on VSLAM and filtering algorithm; and secondly, the photogrammetric procedure used and the strategies to obtain good results. Finally, the results are exposed from two arthroscopies, one from a simulator, and others were done on a living patient.

The exposed results proved a successful methodology but for small amounts of frames. The inconsistent focus of the arthroscope together with the small movements of the patients, the really small TMJ area for surgery, the necessary serum in the cavity and all the reflects and suspensions elements suppose a real problem for an optimal tie points identification and posterior 3d reconstruction. The strategy to solved those problems is based on creating small and well-selected frames using vslam techniques and filters, but also preprocess the images with concrete filters to extract features from the images. For this reason, large reconstructions are not possible in this approach, nor are they very precise, although, even so, the results obtained improve those existing in reconstructions with TMJ arthroscopies.

To improve the results in the future work is planned study methodologies to control the autofocus arthroscope camera in the surgical interventions. The autofocus is needed but have should be controlled, even fixed, during the 3D reconstruction periods; also others parameters will be checked like the diaphragm to increase the field of view. On other hand non-rigid 3d reconstruction will be studied to be implemented in this methodology, considering these algorithms only can be implemented when A small movement is detected and in the small area provide the accuracy can be affected.

5. Bibliography

[1] F. Monje, *Surgical management of temporomandibular joint: Vol .1 Arthroscopy*, Apple book. 2014.

[2] C. Wu, «3D Reconstruction of Anatomical Structures from Endoscopic Images». PhD Thesis, Tech. Report, CMU-RI-TR-10-04,Robotics Institute, Carnegie Mellon University, ene. 2010.

[3] N. Shallik, A. Moustafa, y M. Marcus, *Virtual Endoscopy and 3D Reconstruction in the Airways*. 2019.

[4] A. R. Widya, Y. Monno, M. Okutomi, S. Suzuki, T. Gotoda, y K. Miki, «Whole Stomach 3D Reconstruction and Frame Localization From Monocular Endoscope Video», *IEEE J. Transl. Eng. Health Med.*, vol. 7, pp. 1-10, 2019, doi: 10.1109/JTEHM.2019.2946802.

[5] M. J. Ali, «Three-Dimensional (3D) Endoscopy», en *Atlas of Lacrimal Drainage Disorders*, Singapore: Springer Singapore, 2018, pp. 141-144.

[6] A. Marmol, A. Banach, y T. Peynot, «Dense-ArthroSLAM: Dense Intra-Articular 3-D Reconstruction With Robust Localization Prior for Arthroscopy», *IEEE Robot. Autom. Lett.*, vol. 4, n.º 2, pp. 918-925, abr. 2019, doi: 10.1109/LRA.2019.2892199.

[7] T. Okatani y K. Deguchi, «Shape Reconstruction from an Endoscope Image by Shape from Shading Technique for a Point Light Source at the Projection Center», *Computer Vision and Image Understanding*, vol. 66, n.º 2, pp. 119-131, may 1997, doi: 10.1006/cviu.1997.0613.

[8] S. Y. Yeung, H. T. Tsui, y A. Yim, «Global Shape from Shading for an Endoscope Image», en *Medical Image Computing and Computer-Assisted Intervention – MICCAI'99*, vol. 1679, C. Taylor y A. Colchester, Eds. Berlin, Heidelberg: Springer Berlin Heidelberg, 1999, pp. 318-327.

[9] C. H. Quartucci Forster y C. L. Tozzi, «Towards 3D reconstruction of endoscope images using shape from shading», en *Proceedings 13th Brazilian Symposium on Computer Graphics and Image Processing (Cat. No.PR00878)*, Gramado, Brazil, 2000, pp. 90-96, doi: 10.1109/SIBGRA.2000.883900.

[10] F. Mourgues, F. Devemay, y E. Coste-Maniere, «3D reconstruction of the operating field for image overlay in 3D-endoscopic surgery», en *Proceedings IEEE and ACM International Symposium on Augmented Reality*, New York, NY, USA, 2001, pp. 191-192, doi: 10.1109/ISAR.2001.970537.

[11] D. Burschka, Ming Li, R. Taylor, y G. D. Hager, «Scale-invariant registration of monocular stereo images to 3D surface models», en *2004 IEEE/RSJ International Conference on Intelligent Robots and Systems (IROS) (IEEE Cat. No.04CH37566)*, Sendai, Japan, 2004, vol. 3, pp. 2581-2586, doi: 10.1109/IROS.2004.1389797.

[12] D. Stoyanov, A. Darzi, y G. Z. Yang, «A practical approach towards accurate dense 3D depth recovery for robotic laparoscopic surgery», *Computer Aided Surgery*, vol. 10, n.º 4, pp. 199-208, ene. 2005, doi: 10.3109/10929080500230379.

[13] J. Park *et al.*, «Recent Development of Computer Vision Technology to Improve Capsule Endoscopy», *Clin Endosc*, vol. 52, n.º 4, pp. 328-333, jul. 2019, doi: 10.5946/ce.2018.172.

[14] D. T. Kim, C.-H. Cheng, D.-G. Liu, K. C. J. Liu, y W. S. W. Huang, «Designing a New Endoscope for Panoramic-View with Focus-Area 3D-Vision in Minimally Invasive Surgery», *J. Med. Biol. Eng.*, vol. 40, n.º 2, pp. 204-219, abr. 2020, doi: 10.1007/s40846-019-00503-9.

[15] K. Murakami, «Rationale of arthroscopic surgery of the temporomandibular joint», *Journal of Oral Biology and Craniofacial Research*, vol. 3, n.º 3, pp. 126-134, sep. 2013, doi: 10.1016/j.jobcr.2013.07.002.

[16] Dorian Gálvez-López, Marta salas, y Juan D tardós, «Real-time monocular object SLAM», *Robotics and Autonomous Systems*.

[17] Raúl Mur-Artal, J. M. M. Montiel, y Juan D. Tardós, «ORB-SLAM: A Versatile and Accurate Monocular SLAM System», *IEEE Transactions on Robotics*, vol. 31, n.º 5, pp. 1255-1262, 2017.

[18] P. Ortiz-Coder y A. Sánchez-Rios, «A Self-Assembly Portable Mobile Mapping System for Archeological Reconstruction Based on VSLAM-Photogrammetric Algorithm», *Sensors*, vol. 19, n.º 18, p. 3952, sep. 2019, doi: 10.3390/s19183952.

[19] P. Ortiz-Coder y A. Sánchez-Ríos, «An Integrated Solution for 3D Heritage Modeling Based on Videogrammetry and V-SLAM Technology», *Remote Sensing*, vol. 12, n.º 9, p. 1529, may 2020, doi: 10.3390/rs12091529.

[20] T. Luhmann, S. Robson, S. Kyle, y I. Harley, *Close Range Photogrammetry: Principles, Techniques and Applications*. 2006.

[21] B. Kendra, C. Wells, A. Sinclair, H. Tenenbaum, B. Freeman, y C. Spry, *Interventions for Temporomandibular Joint Disorder: An Overview of Systematic Reviews*. Ottawa(ON): CADTH Rapid Response Reports., 2018.

[22] «Arthroscopy instrument website: https://www.stryker.com/us/en/portfolios/medical-surgical-equipment/surgical-visualization/arthroscopy.html Revised at 1, June, 2020.» .

[23] F. Monje Gil, C. Hernandez Vila, J. L. Moyano Cuevas, M. Lyra, J. B. Pagador, y F. M. Sanchez Margallo, «Validation of a simulator for temporomandibular joint arthroscopy», *International Journal of Oral and Maxillofacial Surgery*, vol. 45, n.º 7, pp. 836-841, jul. 2016, doi: 10.1016/j.ijom.2016.01.010.

[24] Z. Zhang, «A flexible new technique for camera calibration», *IEEE Transactions on Pattern Analysis and Machine Intelligence*, vol. 22, n.º 11, pp. 1330-1334, nov. 2000, doi: 10.1109/34.888718.

[25] C. Solomon y T. Breckon, *Fundamentals of Digital Image Processing: A Practical Approach with Examples in Matlab*. Chichester, UK: John Wiley & Sons, Ltd, 2010.

[26] D. Tan, «Image Enhancement Based on Adaptive Median Filter and Wallis Filter», presentado en 2015 4th National Conference on Electrical, Electronics and Computer Engineering, Xi'an, China, 2016, doi: 10.2991/nceece-15.2016.142.

[27] D. G. Lowe, «Distinctive Image Features from Scale-Invariant Keypoints», *International Journal of Computer Vision*, vol. 60, n.º 2, pp. 91-110, nov. 2004, doi: 10.1023/B:VISI.0000029664.99615.94.

[28] L.-R. Dung, C.-M. Huang, y Y.-Y. Wu, «Implementation of RANSAC Algorithm for Feature-Based Image Registration», *JCC*, vol. 01, n.º 06, pp. 46-50, 2013, doi: 10.4236/jcc.2013.16009.

[29] Pierrot-Deseilligny y M, Clery, «Apero, an open source bundle adjustment software for automatic calibration and orientation of set of images», vol. 38, n.º 5, pp. 269–76.

[30] B. Triggs, P. Mclauchlan, R. Hartley, y A. Fitzgibbon, «Bundle adjustment - A modern synthesis», *ICCV '99 Proceedings of the International Workshop on Vision Algorithms: Theory and Practice*, pp. 198-372, 2000.

[31] M. Pierrot Deseilligny y I. Clery, «APERO, AN OPEN SOURCE BUNDLE ADJUSMENT SOFTWARE FOR AUTOMATIC CALIBRATION AND ORIENTATION OF SET OF IMAGES», *ISPRS - International Archives of the Photogrammetry, Remote Sensing and Spatial Information Sciences*, vol. XXXVIII-5/W16, pp. 269-276, sep. 2012, doi: 10.5194/isprsarchives-XXXVIII-5-W16-269-2011.

[32] G. Bradski y A. Kaehler, *Learning OpenCV: Computer Vision in C++ with the OpenCV Library*, 2nd ed. O'Reilly Media, Inc., 2013.

[33] P. Cignoni, M. Callieri, M. Corsini, M. Dellepiane, F. Ganovelli, y G. Ranzuglia, «MeshLab: an Open-Source Mesh Processing Tool», *Eurographics Italian Chapter Conference*, p. 8 pages, 2008, doi: 10.2312/LOCALCHAPTEREVENTS/ITALCHAP/ITALIANCHAPCONF2008/129-136.

[34] H. Hoppe, «Poisson surface reconstruction and its applications», en *Proceedings of the 2008 ACM symposium on Solid and physical modeling - SPM '08*, Stony Brook, New York, 2008, p. 10, doi: 10.1145/1364901.1364904.

[35] G. Ranzuglia, M. Callieri, M. Dellepiane, P. Cignoni, y R. Scopigno, «MeshLab as a complete tool for the integration of photos and color with high resolution 3D geometry data», *CAA 2012 Conference Proceedings*, pp. 406-416, 2013.

[36] «CloudCompare (version 2.11) [GPL software]. (2020). Retrieved from http://www.cloudcompare.org/». .

5.

Conclusiones y perspectivas futuras

5.1 Conclusiones

Esta Tesis Doctoral analiza las distintas tecnologías e instrumentos de medición en el ámbito de la ingeniería y la arquitectura. De la evolución de las técnicas de medición basadas en imágenes y de una reflexión sobre los instrumentos actuales, su aplicabilidad y características propias, nace la propuesta tecnológica detallada en este proyecto y el prototipo de instrumento de medición desarrollado y evaluado pormenorizadamente, tal y como se ha mostrado a lo largo del texto.

Sobre el estudio de las distintas técnicas e instrumentos de medición.

Se ha observado una tendencia natural, en todos los nuevos desarrollos, de generar instrumentos de medición cada vez más sencillos de utilizar, con interfaces gráficos más atractivos y con posibilidades de interaccionar con otros equipos, así como de conectarse con otros profesionales y colaboradores y enviar rápidamente la información.

Por otro lado he observado un curioso efecto en las nuevas tipologías de instrumentos, muy especialmente en la última década. Esta tendencia trata de la aparición en el mercado de determinados sistemas de medición que no mejoran la precisión de los ya existentes, más bien empeoran éstos valores, pero que, a cambio, tienen más movilidad y facilidad de uso; concretamente, mencionaremos los escáneres de mano, los cuales tienen un uso más dinámico y se prescinde de postprocesos de registro de datos que podían llegar a ser tediosos. El precio no es muy diferente a los láser escáners (TLS) actuales pero están teniendo una aceptación en el mercado muy notable.

Concluimos que existe la necesidad de un instrumento sencillo en su utilización y, cuyas precisiones sean aceptables para determinadas aplicaciones. Entendemos que hay un lugar para instrumentos de menor coste pero con resultados óptimos en exteriores, edificios, yacimientos arqueológicos y obras, entre otras opciones.

Tras el análisis del procedimiento fotogramétrico y de la verificación de los requerimientos y conocimientos previos que un usuario de la fotogrametría debe saber para conseguir resultados satisfactorios, se concluye que se debe trabajar para disminuir esta ruptura y acercar la fotogrametría a usuarios sin dichos conocimientos previos.

En los desarrollos actuales en videogrametría con estos fines, se observa que se:

- Se suele realizar la selección de imágenes de una forma directa, seleccionando 1 imagen cada x *"frames"*, con los problemas que ello conlleva si se cambia de velocidad o el usuario se detiene. Esta técnica es especialmente dificultosa de aplicar con éxito en capturas largas o movimientos erráticos del usuario.
- La resolución de las cámaras de video, especialmente a través de móviles, es de mala calidad, baja resolución y/o con deformaciones importantes en la imagen por el efecto "*rolling shutter*".

- El usuario no experto en fotogrametría, no sabe moverse adecuadamente para después realizar una buena geometría de la toma.

Sobre el desarrollo de la cámara videogramétrica

Es por ello que concluímos que el sistema desarrollado debe contener los siguientes elementos: Sistema de guiado para usuarios no expertos, cámaras de alta resolución con sensores tipo "*global shutter*", que garanticen que no existen deformaciones, un sistema de selección de imágenes inteligente y adaptado a la velocidad de captura y al objeto documentado, del tipo "*3D-based*".

La cámara videogramétrica tiene una naturaleza distinta a los instrumentos de medición actuales, con elementos ventajosos como el tiempo de adquisición de imágenes, facilidad de uso e hiperrealismo en los resultados, y elementos limitantes, como la dependencia de texturas heterogéneas o la injerencia perjudicial de la luz en las cámaras, en el caso de que la posición sea frontal.

Se observó que para la realización de un sistema de localización simultánea o VisualSLAM en tiempo real, el cual realiza un ajuste de haces de los *"frames"* del video, el usuario debe limitarse en sus movimientos, evitando movimientos muy rápidos o giros sobre sí mismo muy extensos. Por ello, la aplicación de ésta técnica como elemento de guía para los usuarios, supone el primer elemento de filtrado para garantizar una reconstrucción 3D precisa y con una buena geometría de toma.

En la revisión literaria, los métodos de filtrado basados en sistemas Visual SLAM de tecnología "*3D-based*", no realizan grandes desplazamientos o trayectos muy complejos. La razón de esto, que es parte esencial de la innovación de ésta investigación, es que utilizando únicamente estos *"frames"*, no se garantiza que vaya a haber un éxito en la orientación de las imágenes. En ocasiones el salto entre imágenes es demasiado grande y, en otras ocasiones, existen *"frames"* demasiado coincidentes. Es por ello que se desarrollaron filtros para garantizar el éxito de dicho procedimiento, pudiéndose realizar ahora trayectorias de más de 30 minutos, sin riesgo a cortar la orientación u obtener geometrías imposibles. Algo que, en mi opinión, es una gran innovación en este campo.

Las evaluaciones de la cámara videogramétrica desarrolladas en este proyecto, basadas en estudios de los tiempos de captura, tiempos de procesamiento, precisiones, secciones, evaluación de texturas, etc. y de cómo los resultados del sistema propuesto se han confrontado a un software fotogramétrico comercial y a un láser escáner comercial, validan en un alto grado la eficiencia y proyección del prototipo y de su tecnología, para aplicaciones en arqueología y arquitectura.

Otra aspecto importante que podemos concluir es que, dadas las limitaciones del software fotogramétrico diseñado (por ejemplo el tiempo de procesamiento empleado es muy alto), se puede sustituir esta fase del sistema por cualquier software fotogramétrico, pudiendo mejorar los resultados y, de forma muy clara, los tiempos de procesamiento y la resolución de los modelos.

Sobre la tecnología de guiado, selección de imágenes a partir de un video y reconstrucción 3D.

La documentación a través de video y sistemas de guiado, y los algoritmos de selección de imágenes, establecen una nueva forma de documentar para la realización de fotogrametría. Esta forma de adquisición de datos permite un cambio notable de concepto metodológico en la fotogramétrica clásica. Es por ello que, tal y como ha sido confrontado en esta Tesis Doctoral, nos encontramos ante el reto de transformar la metodología clásica de adquisición de datos de la fotogrametría para transformarla en videogrametría. Y, en este transcurso, transformar la cámara fotográfica en una cámara videogramétrica.

A éste mismo respecto, la tecnología de selección de imágenes permite esquemas análogos basados en una sola cámara, tal y como ha sido detallado en el artículo de aplicación médica de reconstrucción 3D a partir de artroscopias. En mi opinión este esquema es claramente aplicable a otras tecnologías, como se verá en el apartado siguiente.

Se debe mencionar en este punto que dicha tecnología ha tenido un éxito notable en su aplicación sobre reconstrucciones 3D a partir de videos de artroscopias, incluso eliminando imágenes que pudieran registrar algún pequeño movimiento del paciente y garantizando grupos de imágenes con garantía de éxito en su orientación relativa. También se debe mencionar la utilidad de preprocesar las imágenes a través del filtro de Wallis para extraer características de las imágenes provenientes de las artroscopias que, ocasionalmente y debido a su naturaleza, pueden carecer de una textura heterogénea.

5.2 Perspectivas futuras

El reto de la transformación de la fotogrametría en videogrametría y su integración con otras tecnologías.

El sistema de guiado propuesto, más la selección de imágenes y reconstrucción 3D permitiría prescindir de la fotogrametría en algunos casos, de forma muy especial, cuando el usuario no tiene muchos conocimientos fotogramétricos y/o la zona a levantar es amplia y/o la toma de fotos una a una, puede ser un trabajo muy tedioso. El hecho de transformar la tecnología fotogramétrica en un escáner 3D abre el campo a un mayor número de aplicaciones y resalta la importancia del hardware que, en este caso sería la cámara videogramétrica, pudiéndose confrontar a otro tipo de escáneres 3D con otra tipología de sensores. Posiblemente las aplicaciones del escáner videogramétrico sean más restringidas que las basadas en laser, pero a su vez, puede desempeñar un papel igual o más interesante en otros ámbitos, como por ejemplo en arqueología, construcción, geología o minería, dadas las tipologías de las texturas en estos ámbitos.

Una posibilidad muy cercana, a mi modo de ver, es la integración de la cámara videogramétrica con otros sensores como los sistemas globales de navegación por satélite (*Global Navigation Satellite System*, GNSS) o sensores de medición inercial (*Inertial Measurement Unit*, IMU), que pueden asistir a la fotogrametría para escalar y georreferenciar, así como, asistir en la orientación a través de los valores del sistema inercial. Pero también, la integración con la tecnología LIDAR, en cualquiera de sus facetas, puede ayudar a construir un sistema más robusto y completo, mejorando las texturas del sistema LIDAR y complementando las nubes de puntos. Y este es el caso de los sistemas *"mobile mapping"*, donde una cámara videogramétrica o bien la

utilización de la tecnología diseñana en esta tesis y aplicada a las multicámaras de los MMS, podría guiar a éste en zonas con poca cobertura GNSS, ayudar a mejorar las texturas, a completar y mejorar las nubes de puntos, a ajustar las habituales desviaciones entre las imágenes y las nubes de puntos del escáner y, en definitiva, a mejorar sustancialmente el producto.

Entre las múltiples aplicaciones, existe una que puede ser muy interesante, se trata de emplear la tecnología de selección de imágenes para video capturado desde un "*drone*" o "*Unammed Aerial Vehicle*" (UAV). De ésta forma, aunque no se realizara ningún plan de vuelo y no se definiera el porcentaje de recubrimiento, se podría realizar fotogrametría con éxito. Esto podría ser útil en vuelos de emergencias, como incendios, explosiones o accidentes, donde el piloto del drone no tiene mucho tiempo para planificar el vuelo y donde, si faltara una imagen para poder completar la trayectoria y la orientación de todas las imágenes, podría suponer un problema importante y la imposibilidad de realizar la reconstrucción de la zona a posteriori. Es por ello que a través de esta tecnología, tendríamos varios *"frames"* por segundo, lo que garantizaría la cobertura, y el sistema de selección de imágenes se encargaría de seleccionar las mejores imágenes y asegurarse de la continuidad de la toma y del éxito de la posterior reconstrucción a partir de fotogrametría.

Referencias

[1] Raúl Mur-Artal, J. M. M. Montiel, y Juan D. Tardós, «ORB-SLAM: A Versatile and Accurate Monocular SLAM System», *IEEE Transactions on Robotics*, vol. 31, n.º 5, pp. 1255-1262, 2017.

[2] «Agisoft Metashape. Available online: https://www.agisoft.com (accesed on 28 August 2019.» .

[3] C. Fraser, «Network design considerations for non-topographic photogrammetry», *Photogrammetric Engineering & Remote Sensing*, vol. 50, 1984.

[4] F. Remondino, E. Nocerino, I. Toschi, y F. Menna, «A CRITICAL REVIEW OF AUTOMATED PHOTOGRAMMETRICPROCESSING OF LARGE DATASETS», *Int. Arch. Photogramm. Remote Sens. Spatial Inf. Sci.*, vol. XLII-2/W5, pp. 591-599, ago. 2017, doi: 10.5194/isprs-archives-XLII-2-W5-591-2017.

[5] B. Triggs, P. Mclauchlan, R. Hartley, y A. Fitzgibbon, «Bundle adjustment - A modern synthesis», *ICCV '99 Proceedings of the International Workshop on Vision Algorithms: Theory and Practice*, pp. 198-372, 2000.

[6] F. Remondino y S. El-Hakim, «Image-based 3D Modelling: A Review», *The Photogrammetric Record*, vol. 21, n.º 115, pp. 269-291, 2006, doi: 10.1111/j.1477-9730.2006.00383.x.

[7] A. Torresani y F. Remondino, «VIDEOGRAMMETRY VS PHOTOGRAMMETRY FOR HERITAGE 3D RECONSTRUCTION», *Int. Arch. Photogramm. Remote Sens. Spatial Inf. Sci.*, vol. XLII-2/W15, pp. 1157-1162, ago. 2019, doi: 10.5194/isprs-archives-XLII-2-W15-1157-2019.

[8] R. Hartley y A. Zisserman, *Multiple View Geometry in Computer Vision*, 2.ª ed. Cambridge: Cambridge University Press, 2004.

[9] B. Camburn *et al.*, «Design prototyping methods: state of the art in strategies, techniques, and guidelines», *Design Science*, vol. 3, 2017, doi: 10.1017/dsj.2017.10.

Notas

[1] Markets and Markets Journal. https://www.marketsandmarkets.com/Market-Reports/lidar-market-1261.html

[2] Point of beginning Journal https://www.pobonline.com/articles/101613-3d-trends-study-3d-imaging-market-growing-including-geospatial

Anexo I.
Otros méritos: Curriculum Vitae.

Curriculum Vitae

Pedro Ortiz Coder
edad: 40 años. 7th May 1980
Dirección: Cabo Verde 3, Mérida (Badajoz),
CP:06800.Spain
Email: portizcoder@gmail.com
Teléfono :+34-666278798

Educación

1998-2003 Ingeniería Técnica en Topografía. universidad de Extremadura. España.

2003 - Final Thesis/Proyecto Final de Grado I.T.Topografía. University of Gävle, Sweden. Title: *Texture mapping of 3D Laser scanning with digital photographs: Gävle theatre.* Coordinador: Maikel Johansson/ Stig-Goran Matterson.

2008-2010; Master "Geotecnologías Cartográficas en Ingeniería y Arquitectura". Politécnica de Ávila. Universidad de Salamanca.

2017 – Actualidad; Estudiante de Doctorado. Universidad de Extremadura (España).

Educación Adicional. Investigador Invitado.

2009 - IGP Institut für Geodäsie und Photogrammetrie DBAUG. ETH Eidgenössischen Technischen Hochschule, Zürich. Título: "Line scanner; 3D Phototexturing".Coordinador; Armin Grün. 1 June- 30 July. 2009, Zürich, Suiza.

2010 - Universita degli Stidi di Salerno. C.d.S Specialistico in "Ingegneria Edile-Architettura". Abril 2010.Coordinador: Salvatore Barba. Salerno, Italy.

Experiencias académicas y en Investigación

Proyectos de investigación.

Título:"Fotomodelado automático utilizando imágenes" Tesina Doctoral. Politécnica de Ávila. Universidad de Salamanca. Facultad de Cartografía y Geodesia. Director; D.Javier Gómez Lahoz. 2011, Ávila.

Título:"3D Cartografía automática; Un nuevo método de generación cartográfica". Empresa: Meditex S.L.L. Cofinanciado por el programa:" Programa regional para el Fomento Empresarial en I+D+i. Junta de Extremadura". 2011-2012. Posición en el proyecto: Director. Mérida.

Título: Project RITECA II. "Prospecciones arqueológicas a través de técnicas no intrusivas". Institución: Instituto Arqueológico de Mérida. CSIC (Consejo Superior de Investigaciones Científicas). Coordinator: Victorino Mayoral Herrera. 2012-2014. Mérida.

Título: "Sistema de captura 3D, navegación y replanteo topográfico". Empresa: Solventia, Toponova and e-Capture R&D. Cofinanciado por "FEDER-Innterconecta. CDTI" 2013-2015. Posición en el proyecto: Director. Mérida.

Título: "EyesCar-Mobile mapping system using advance photogrammetry".Empresa: e-Capture. Cofinanciado por: MINETUR. Acción Estratégica de Economía y Sociedad Digital. 2014-2016. posición en el proyecto: Director. Mérida.

Profesor:

Curso de Postgrado: *"Geometría y Arte:Documentación del patrimonio utilizando láser escáner"*. Universidad de Extremadura. Ingeniería en Cartografía y Geodesia. 2007. Cáceres. España.

Curso: Topografía aplicada a la arqueología y paleontología. Institution: IVEREM. Centro de estudios AulaCenter. 1-28 Marzo de 2011. Madrid. España.

Curso:*"Terrestrial Active Sensors & Cultural heritage Documentation"*. Profesor Invitado. Universita degli Stidi di Salerno. C.d.S Specialistico in "Ingegneria Edile-Architettura". Abril 2010. Salerno, Italia.

Curso de Postgrago: La Aplicación de las Tecnologías de Información Geográfica en Arqueología. Organizadores: CSIC-IAM, Incipit. Abril y Mayo 2013. Mérida. España.

I International Summer School for Cultural heritage Documentation. Pedro Ortiz Coder. Director y profesor. ISPRS (International Society of Photogrammetry and Remote Sensing) Septiembre 2009. Mérida.

II International Summer School for Cultural heritage Documentation. Pedro Ortiz Coder. Director y Profesor. ISPRS (International Society of Photogrammetry and Remote Sensing) 24-28 Septiembre 2012. Carmona, Sevilla.

Conferencias:

H.Pires, P.Ortiz. Superficie, Soluciones Geográficas. Universidad de Oporto. **Levantamiento de la Igreja de Santo Domingo de Guimaraes**. Facultad de Arquitectura de Oporto. Portugal 2006.

P.Ortiz, H.Pires. EITEC; 2º Encontro Internacional de Tecnologias Aplicadas à Museologia, Conservação e Restauro. **Os sistemas de varrimento laser no registo arqueológico. Análise morfológica e reconstituição virtual a partir de fragmentos de uma taça de cerâmica.** Universidad de Coimbra. Portugal 2006.

P.Ortiz, M.Matas. Jornadas: Innovaciones en las tecnologías de la Información aplicadas a la conservación del patrimonio, en Cáceres. Conference title: **Cartografía de la muralla de Cáceres utilizando Láser escáner 3D y Fotogrametría**. Universidad de Extremadura. Marzo 2009.

Pedro Ortiz Coder.**"Láser escáner y restitución 3d"** Curso de Postgrado de Intervención en el Patrimonio Histórico Artístico. Colegio Oficial de Aparejadores y Arquitectos Técnicos de Cáceres. Cáceres 11 Septiembre 2009.

Pedro Ortiz Coder. **"Documentación Gráfica del Patrimonio utilizando múltiples técnicas".** I Jornadas de Arqueología y Restauración del Patrimonio. La Recuperación del legado Medieval. Centro de investigación San Juan Bautista de burguillos del Cerro, Badajoz. 17 de Diciembre 2010.

Pedro Ortiz Coder "**Nuevas tecnologías en la Documentación Gráfica del patrimonio**". Conferencias-Coloquios *"Documentando el Patrimonio Cultural*" Organizado por Consorcio Monumental de Cáceres. Cáceres. 21 mayo 2015.

Contribuciones en libros:

Título: Good Practice in Archaeological Diagnostics. Non-invasive Survey of Complex archaeological Sites. Editors: Cristina Corsi, Bozidar, Frank Vermeulen; Natural Science in Archaeology. Contribución en Capítulo 13. "Creating and Analysing Digital Terrain Models for Archaeological Research". Autores: José-Ángel Martínez del Pozo, Victorino Mayoral-Herrea y Pedro Ortiz-Coder. ISBN-13: 978-3319017839 // ISBN-10: 9783319017839

Título: La gestación de los paisajes rurales entre la protohistoria y el período romano : formas de asentamiento y procesos de implantación. Editores: Ernesto Salas Tovar (coordinador científico); Rui Mataloto Victorino Mayoral Herrera, Conceição Roque. Series: Anejos de Archivo Español de Arqueología ; 60. eISBN: 978-84-00-09814-8

Artículos en revistas:

Modelo 3D con láser escáner combinando texturas de alta resolución: el teatro de Gävle (Suecia) y la puerta de Alfonso VI de Toledo. Pedro Ortiz Coder, María Angeles Marcelo Rubio, Juan Antonio Pérez Alvarez, Héctor Sánchez Santamaría. Revista internacional "Mapping". Enero 2007.

Computer vision methods and rock-art: towards a detection of pigments. (E.P) Enrique Cerrillo-Cuenca, Pedro Ortiz Coder, José Ángel Martínez del Pozo. International Journal of Archaeological and Anthropological Sciences. Ed.Springer. Junio 2013.

Nueva generación de instrumentos y tecnologías para la documentación gráfica en arqueología y arquitectura. Pedro Ortiz Coder. Revista de la Asociación de Dibujantes e Ilustradores de Arqueología (ADARQ). Vol 1/Nº0. Año 2016

P. Ortiz-Coder y A. Sánchez-Rios, «**A Self-Assembly Portable Mobile Mapping System for Archeological Reconstruction Based on VSLAM-Photogrammetric Algorithm**», Sensors, vol. 19, n.o 18, p. 3952, sep. 2019, doi: 10.3390/s19183952

P. Ortiz-Coder y A. Sánchez-Ríos, «**An Integrated Solution for 3D Heritage Modeling Based on Videogrammetry and V-SLAM Technology**», *Remote Sensing*, vol. 12, n.º 9, p. 1529, mayo 2020, doi: 10.3390/rs12091529.

Artículos en congresos:

P. Ortiz, H.Sánchez. **Analisys of the gävle theatre throught a high-resolution texture mapped and range data.** International Workshop on Vision Techniques applied to the Rehabilitation of City Centres. CIPA. Lisboa Octubre 2004

P. Ortiz, H.Sánchez. V**irtual city models combining cartography and photorealistic texture mapped range data.** International Cartography Conference. International Cartography Association, Sociedad Española de Cartografía, Fotogrametría y Teledetección. A Coruña, España. Julio, 2005

P.Ortiz, H.Sánchez. **El escáner láser para la documentación del patrimonio cultural**. VIII Congreso de Estudios Extremeños. Badajoz, España. Octubre 2006

H.Pires, P.Ortiz, P.Marques. **Novas tecnologias de documentaçao gráfica aplicadas ao registro arqueológico. Análise morfológica e reconstruçao virtual de uma taça de cerâmica**. Matosinhos, Portugal. Septiembre 2006.

P.Ortiz, H.Sanchez, H. Pires, J.A. Perez, **Experiences about fusioning 3d digitalization techniques for cultural heritage documentation.** ISPRS Commission V. Vision engineering and metrology. Dresden, Alemania. Septiembre 25-27, 2006

H.Pires, P.Ortiz, P.Marques, H.Sánchez. **3d digitalization of a ceramic pot for the virtual reconstruction close range laser scanning.** VSMM The evolution of information communication technology in Cultural Heritage. CIPA. Chipre 2006

P. Ortiz, H. Sanchez, H.Pires . **Fusión de técnicas aplicadas al levantamiento de la iglesia de santo domingo de guimaraes (portugal).** VII Semana de Geomática. Barcelona 2007.

Jesús Ángel Torrecilla Pinero, Pedro Ortiz Coder y José Juan de Sanjosé Blasco. **Aplicación de láser scanner a la obtención de modelos estructurales de construcciones históricas**. Congreso de métodos numéricos en ingeniería. CNME/CILAME. Asociación de Métodos numéricos en la ingeniería. Oporto, Portugal. Junio 2007.

Pedro Ortiz Coder, Hugo Pires, Héctor Sánchez Santamaría, Patricia Marques. **Reconstrucción virtual de cerámica a partir de fragmentos arqueológicos digitalizados mediante láser escáner.** S02 CEIG'07. XVII Congreso Español de Informática. Zaragoza, España. Septiembre 2007

Guadalupe Durán Domínguez, Pinero, Pedro Ortiz Coder, José Juan de Sanjosé Blasco. **Técnicas fotogramétricas aplicadas al Patrimonio**. III Congreso de la conservación infalible: de la teoría a la realidad. Oviedo 21-23 Noviembre 2007.

Pedro Ortiz Coder, J. J. de Sanjosé Blasco, Héctor Sánchez Santamaría. **Experiencias en la documentación del patrimonio cultural en extremadura.** Congreso Internacional de Ingeniería Geomática y Topográfica. TOP-CART. Valencia, España. Febrero 2008.

P. Ortiz, M. Matas. **Experiences about fusioning 3d digitalization techniques for cultural heritage documentation in caceres wall (Spain).** 3D-ARCH'2009 3D Virtual Reconstruction and Visualization of Complex Architectures International Archives of Photogrammetry, Remote Sensing and Spatial Information Sciences Volume XXXVIII-5/W1 ISSN 1682-1777. Trento, Italia. Febrero 2009.

Andrea Menéndez Menéndez1, Victor M. Gibello Bravo1 y Pedro Ortiz Coder **San juan bautista (burguillos del cerro, Badajoz), un ejemplo de documentación del patrimonio con nuevas tecnologías.** Arqueológica 2.0 II Congreso internacional de Arqueología e informática Gráfica; Patrimonio e Innovación. Sevilla 16-19. Junio 2010.

S. Barba, F. Fiorillo, P. Ortiz Coder, S. D'Auria, E. De Feo. **An application for cultural heritage in erasmus placement. Surveys and 3d cataloging archaeological finds in Mérida (Spain)** Volume XXXVIII-5/W16, 2011 ISPRS Workshop 3D-ARCH 2011 "3D Virtual Reconstruction and Visualization of Complex Architectures". Trento, Italia. 2-4 Marzo 2011

P.Ortiz Coder , S.Barba, F.Fiorillo, F.Pugliese. **Archaeological plan restitution with cloud computing** Workshop "LOW COST 3D: sensori, algoritmi e applicazioni" Trento, Italia. 8-9 ,Marzo 2012.

Pedro Ortiz-Coder. **Técnicas no intrusivas en la prospección arqueológica:geophisic and archaeology.** II Reunión científica. Los paisajes agrarios de la romanización: fortines y ocupación del territorio (siglos II a.C. - I d.C.)

Organizan: Instituto de Arqueología de Mérida, Cámara Municipal de Redondo-Alandroal. Redondo-Alandroal (Alentejo), Portugal. 24 -25 Mayo 2012.

Beatriz del Pino Espinosa, Pedro Ortiz Códer. **Evolución de la documentación gráfica del patrimonio a través del Templo de Diana (Mérida).** Encuentro de arqueología del Suroeste Peninsular. Villafranca de los Barros(Badajoz), España. 4-6 de Octubre, 2012

Jorge Blanco, Francisco Galea, Raquel Liceras, José Ángel Martínez, Pedro Mateos, Maribel Mota, Pedro Ortiz, Francisco Pérez, Antonio Pizzo, Luis Sevillano, Pau de Soto, Jose María Terrón y Victorino Mayoral. **Aplicación e integración de técnicas no destructivas al estudio arqueológico de la ciudad romana de Contributa Iulia y su entorno.** Encuentro de arqueología del Suroeste Peninsular. Villafranca de los Barros(Badajoz), España. 4-6 de Octubre, 2013.

Álvaro Corrales Álvarez y Pedro Ortiz Códer. **La Casa del Teatro (Mérida): Análisis a través de la digitalización fotogramétrica**. Encuentro de arqueología del Suroeste Peninsular. Villafranca de los Barros(Badajoz), España. 4-6 Octubre 2013.

Pedro Ortiz Códer, José Ángel Martínez, Raquel Liceras, Pedro Mateos, Antonio Pizzo, Pau de Soto y Victorino Mayoral. **Analizando el paisaje urbano de Contributa Iulia (Medina de las Torres) a partir de fotografía aérea de baja altitud**. Encuentro de arqueología del Suroeste Peninsular. Villafranca de los Barros(Badajoz), Spain. 4-6 Octubre 2013.

Pedro Ortiz Coder. **Documentación del patrimonio arqueológico utilizando fotogrametría automática.** Arqueologica 2.0. Sevilla 20-22 de Junio 2013.

Pedro Ortiz Coder, Beatriz del Pino Espinosa. **Digitalización 3D automática con Láser fotogrametría, videogrametría y láser escáner**. El caso práctico del Templo de Diana (Mérida). Arqueologica 2.0. Sevilla. 20-22 de Junio de 2013.

Otros méritos académicos

Revisor habitual de las revistas internacionales:

- Remote Sensing, MDPI; *(indexed by the Science Citation Index Expanded (Web of Science), Scopus (2019 CiteScore: 6.1), Ei Compendex, and other databases.) Impact Factor: 4.118 (2018) ; 5-Year Impact Factor: 4.740 (2018)*

- Applied Science, MDPI; *(Indexed by the Science Citation Index Expanded (Web of Science) [search for "Applied Sciences-Basel"], Scopus, Inspec (IET) and other databases.); CiteScore (2019 Scopus data): 2.40, which equals rank 85/299 (Q2) in "General Engineering"; SJR: 0.418 (Q1 in Engineering [miscellaneous]). Impact Factor: 2.217 (2018) ; 5-Year Impact Factor: 2.287 (2018)*

Experiencia Laboral:

Empresas / Instituciones:

Gavle. www.gavle.es 2004- 2010

Negocio Propio. Misión empresarial: Documentación del patrimonio cultural a través de laser escáner, fotogrametría y otras técnicas de medición.

4e Software. www.4-e.es 2010 – 2012

Negocio propio junto a la empresa Meditex. Misión: Investigación y desarrollo del software fotogramétrico 4E..

CSIC-IAM. 2012-2013. Consejo Superior de Investigaciones Científicas - Instituto de Arqueología de Mérida. Misión: Investigación en técnicas no intrusivas en arqueología.

e-Capture Research and Development S.L. 2013 – 2017 . Director Técnico o CTO. Chief Technical Officer y Socio fundador. Misión: Investigación y Desarrollo de instrumentos de medición.

Consultor en Geoslam(Nottingham). 2017-2019. Investigación sobre texturizer datos provenientes del Laser escáner de mano.

Proyectos Laborales:
2005. Febrero - Junio. Levantamiento arquitectónico con escáner 3d y fotogrametría de la iglesia de Santo Domingo de Guimaraes. Portugal. Empresa contratista: Geosuperficie.lda

2005. Sept-Nov. Levantamiento arquitectónico del retablo de la Iglesia de santa María de Bouro utilizando Láser escáner y fotogrametría. Empresa contratista: Geosuperficie.lda

2005. Oct-Nov. Escaneado 3d del Santuario de Panoias. Vila real, Portugal. Company Contractor: Geosuperficie.lda. Empresa contratista: Geosuperficie.lda.

2006. Oct-Nov.Escaneado 3D de la "Ribera de Oporto", Portugal. Empresa contratista: Geosuperficie.lda.

2006. Febrero-Marzo. Levantamiento arquitectónico de la iglesia de San Dinis., Vila Real, Portugal. Empresa contratista: Geosuperficie.lda.

2008. Marzo- Julio. Levantamiento arquitectónico de la Muralla de Cáceres. Contratista: Arq.Miguel Matas Cascos

2008. Oct. Levantamiento arqueológico del interior del Castillo de Montanchez, Cáceres. Empresa Contratista: Arquepec.S.L

Dic 2008-April 2009. Levantamiento arquitectónico de la muralla del alcazaba de Mérida. Empresa Contratista: Resgal S.L

2009 Abril-Junio.Levantamiento arquitectónico del Alcazaba of Reina (Badajoz). Institución Contratista: Junta de Extremadura.

Junio 2009 – Abril 2010. Levantamiento arquitectónico del Castillo de Montanchez, Magacela y Barcarrota utilizando multiples técnicas.Contratista: Junta de Extremadura

2010 Abril - Junio. Levantamiento arquitectónico de la Iglesia de burguillos del cerro, Badajoz. Contratista: Arqveocheck. SLU.

2010 Sept - Dic. Escaneo 3d del teatro romano de Medellín en diferentes fases.Contratista: Junta de Extremadura

2011 Enero-Marzo. Escaneado de Puerta Palma, Badajoz. Contratista: Servicios Inmobiliarios Extremeños Urbe Badajoz.

2011 Junio -Agosto. Levantamiento arqueológico del yacimiento en Villalba de los Barros, Badajoz. Contratista: TERA.SL

2011 Octubre-Noviembre. Levantamiento arqueológico de restos romanos en "Las Cardosas" , Rincón de Ballesteros, Cáceres. Contratista: EAPH.

2013 Enero - Marzo. Levantamiento arquitectónico del Teatro Romano y Anfiteatro Romano de Mérida utilizando UAV, Laser scanner y fotogrametría terrestre. CSIC-IAM

Premios:
"From students to businessman" Win of the 3ºBest Project "De universitario a empresario" from the *Fomento de emprendedores en Extremadura* between 400 projects. March 2008.

Photography award "Mérida en tus Ojos" Institution: Junta de Extremadura. 2009.

"Navegantes de Hoy". 3º Best Start Up between 48 projects. Institution: Diario Hoy. Febrary. 2013. Empresa e-capture.

"Mejor Proyecto tecnológico de inversión ". Keiretsu Forum. Evento Fundecyt. Badajoz. 2014. Empresa e-capture.

Anexo II.
Certificados de las publicaciones.

Certificado de publicación del artículo I (Sección I): "A Self-Assembly Portable Mobile Mapping System for Archeological Reconstruction Based on VSLAM-Photogrammetric Algorithm", por la revista Sensors:

sensors

an Open Access Journal by MDPI

Indexed in: PubMed | Indexed in: Ei Compendex | CITESCORE 3.72 SCOPUS | IMPACT FACTOR 3.031

CERTIFICATE OF PUBLICATION

Certificate of publication for the article titled:

A Self-Assembly Portable Mobile Mapping System for Archeological Reconstruction Based on VSLAM-Photogrammetric Algorithm

Authored by:

Pedro Ortiz-Coder; Alonso Sánchez-Ríos

Published in:

Sensors **2019**, Volume 19, Issue 18, 3952

MDPI Academic Open Access Publishing since 1996

Basel, June 2020

Certificado de publicación del artículo II (Sección II):"An Integrated Solution for 3D Heritage Modeling Based on Videogrammetry and V-SLAM Technology", por la revista remote Sensing:

remote sensing

an Open Access Journal by MDPI

Indexed in: Ei Compendex | CITESCORE 4.89 SCOPUS | IMPACT FACTOR 4.118

CERTIFICATE OF PUBLICATION

Certificate of publication for the article titled:

An Integrated Solution for 3D Heritage Modeling Based on Videogrammetry and V-SLAM Technology

Authored by:

Pedro Ortiz-Coder; Alonso Sánchez-Ríos

Published in:

Remote Sens. **2020**, Volume 12, Issue 9, 1529

MDPI Academic Open Access Publishing since 1996

Basel, June 2020

Email acreditativo de Entrega del artículo III (Sección III):"Automatic 3d dense reconstruction using VSLAM and photogrammetric algorithms: approach in the temporomandibular arthroscopy case", por la revista Measurement:

23/6/2020 Gmail - Thank you for your submission to Measurement

Gmail

Pedro Ortiz Coder <portizcoder@gmail.com>

Thank you for your submission to Measurement

Measurement <em@editorialmanager.com> 23 de junio de 2020, 18:33

Responder a: Measurement <measurement@elsevier.com>; Para:Pedro Ortiz-Coder portizcoder@gmail.com;

Dear Mr Ortiz-Coder,

Thank you for sending your manuscript Automatic 3d dense reconstruction using VSLAM and photogrammetric algorithms: approach in the temporomandibular arthroscopy case. for consideration to Measurement. Please accept this message as confirmation of your submission.

When should I expect to receive the Editor's decision?
We publicly share the average editorial times for Measurement to give you an indication of when you can expect to receive the Editor's decision. These can viewed here:
http://journalinsights.elsevier.com/journals/0263- 2241/review_speed

What happens next?
Here are the steps that you can expect as your manuscript progresses through the editorial process in the Editorial Manager (EM).

1. First, your manuscript will be assigned to an Editor and you will be sent a unique reference number that you can use to track it throughout the process. During this stage, the status in EM will be "With Editor".

2. If your manuscript matches the scope and satisfies the criteria of Measurement, the Editor will identify and contact reviewers who are acknowledged experts in the field. Since peer-review is a voluntary service, it can take some time but please be assured that the Editor will regularly remind reviewers if they do not reply in a timely manner. During this stage, the status will appear as "Under Review".

Once the Editor has received the minimum number of expert reviews, the status will change to "Required Reviews Complete".

3. It is also possible that the Editor may decide that your manuscript does not meet the journal criteria or scope and that it should not be considered further. In this case, the Editor will immediately notify you that the manuscript has been rejected and may recommend a more suitable journal.

For a more detailed description of the editorial process, please see Paper Lifecycle from Submission to

Publication: http://help.elsevier.com/app/answers/detail/a_id/160/p/8045/

How can I track the progress of my submission?
You can track the status of your submission at any time at http://ees.elsevier.com/MEAS

Once there, simply:

1. Enter your username: Your username is: portizcoder@gmail.com

If you need to retrieve password details, please go to: http://ees.elsevier.com/MEAS/automail_query.asp

2. Click on [Author Login]. This will take you to the Author MainMenu
3. Click on [Submissions Being Processed]

Many thanks again for your

interest in Measurement. Kind

regards,
Measurement

If you require further assistance, you are welcome to contact our Researcher Support team 24/7 by live chat and email or 24/5 by phone: http://support.elsevier.com

---

Agradecimientos

Dr. Alonso Sánchez Ríos

Dr. Ángel Manuel Felicísimo Pérez

Dra. María Eugenia Polo

Dr. Florencio Monje Gil

Consorcio Ciudad monumental de Mérida; Especialmente a Felix Palma y Dra.Mary Paz Chivite.

Marcel Goyvaert

Dr.Thomas Fischer

Daniel Frisch

Dr.Rubén Cabecera Soriano

Antonio De Esteban

Jairo Benitez

Manuel Donoso

José Carlos Pozo

Alejandro Tebas

Ric Durrant